Blades, bladelets or blade(let)s? Investigating early Upper Palaeolithic technology and taxonomical considerations

Klingen, Lamellen oder beides? Untersuchungen zur früh-jungpaläolithischen Technologie und taxonomische Überlegungen

Jacopo Gennai[1]*, Marco Peresani[2,3] & Jürgen Richter[1]

[1] University of Cologne, Institute of Prehistoric Archaeology, Weyertal, 125, 50931 Cologne, Germany;
ORCID: 0000-0003-2662-2855; email: jacopo.gennai@hotmail.it
[2] University of Ferrara, Department of Humanities, Prehistoric and Anthropological Sciences Unit, Corso Ercole I d'Este, 32, 44100 Ferrara, Italy;
[3] National Research Council, Institue of Environmental Geology and Geoengineering, Stratigraphy, Vegetation, Climate and Man Research Group, Piazza della Scienza 1, 20126 Milano, Italy;
Marco Peresani; ORCID: 0000-0001-6562-6336
Jürgen Richter; ORCID: 0000-0003-2793-7867

Abstract - The early Upper Palaeolithic marks a technological turning point in Western Eurasia, evidenced by the increased spread of bladelet production. The two main technocomplexes, the Aurignacian and the Ahmarian, have long histories of research and have always formed part of the debate on the *Homo sapiens* dispersal into Europe, with changing interpretations. A large aspect of the debate surrounding the recognition of different technocomplexes revolves around the question of whether or not bladelet production is independent of blade production. Here we present a first-hand analysis of three early Upper Palaeolithic assemblages in Europe and the Levant, conventionally attributed to different technocomplexes: Al-Ansab 1, Românești-Dumbrăvița I GH3, Grotta di Fumane A1-A2. Results show that the lithic technologies at the three sites display almost identical knapping concepts, geared around bladelet production. These results and other recent reassessments support a revision of the early Upper Palaeolithic technological and taxonomical models.

Zusammenfassung - *Das frühe Jungpaläolithikum markiert einen technologischen Wendepunkt in Westeurasien, der durch die Ausbreitung der Lamellen-Produktion gekennzeichnet ist. Die beiden wichtigsten anerkannten Technokomplexe, das Aurignacien und das Ahmarien, haben eine lange Forschungsgeschichte und waren immer Teil der Debatte über die Ausbreitung des Homo sapiens in Europa, mit wechselnden Interpretationen. Ein großer Teil der Debatte um die Anerkennung verschiedener Technokomplexe dreht sich um die Frage, ob die Herstellung von Lamellen unabhängig von der Herstellung von Klingen ist oder nicht. Hier präsentieren wir eine Analyse aus erster Hand von drei früh-jungpaläolithischen Inventaren aus Europa und der Levante, die konventionell zu unterschiedlichen Technokomplexen gestellt werden: Al-Ansab 1, Românești-Dumbrăvița I GH3, Grotta di Fumane A1-A2. Die Ergebnisse zeigen, dass die lithischen Technologien an den drei Fundorten fast identische Konzepte aufweisen, die auf die Herstellung von Lamellen ausgerichtet sind. Diese Ergebnisse und andere neuere Bewertungen unterstützen eine Revision der technologischen und taxonomischen Modelle des frühen Jungpaläolithikums.*

Keywords - Homo sapiens dispersal, lithic artefact, Aurignacian, Ahmarian, Europe, Levant
Homo sapiens Ausbreitung, Steinartefakt, Aurignacien, Ahmarien, Europa, Levante

Introduction

The debate on the early Upper Palaeolithic (eUP) is closely linked to the understanding of the dispersal of *Homo sapiens*. Our species' origins lie firmly in the African continent (Scerri et al. 2019), but *Homo sapiens* has expanded its range several times throughout the millennia (Hershkovitz et al. 2018). The number of *Homo sapiens* human remains located outside of the African continent increases during the Marine Isotope Stage 3 (MIS 3 – 60–30 ka) and are associated, directly or indirectly, to the Initial Upper Palaeolithic (IUP), the Uluzzian and finally the eUP technological traditions (Benazzi et al. 2011, 2015; Fu et al. 2014, 2015; Hublin 2015; Hublin et al. 2020; Prüfer et al. 2021; Boaretto et al. 2021). While the IUP coincides with an expansion

*corresponding author

This article contains supporting information online at: https://journals.ub.uni-heidelberg.de/index.php/qu/issue/archive

including the Near East, Southeastern Europe and Central-Northern Asia (Zwyns 2021), Uluzzian sites are distributed along the Italian and Peloponnese peninsulas (Koumouzelis et al. 2001; Peresani et al. 2019). In contrast, the eUP, as defined in this paper, groups together the cultural manifestations that occurred after the IUP, the Uluzzian and other transitional complexes and abruptly after the Mousterian in most of Western Eurasia, with its eastern extent in Iran, stretching as far north as the Russian plains and to Portugal in the west (Fig. 1), and occurring around 43–37 ka (Tsanova 2013; Pleurdeau et al. 2016; Barshay-Szmidt et al. 2018; Dinnis et al. 2019; Haws et al. 2020; Boaretto et al. 2021). The predominant cultural marker for the eUP is the proliferation of the bladelet, a lithic artefact scarcely represented in the previous technocomplexes (Gilead 1991; Le Brun-Ricalens 2005a; Tsanova et al. 2012; Kadowaki et al. 2021). No univocal definition of bladelet is available, generally, it is meant as a smaller blade (Inizan et al. 1999), in the study area a metrical limit of 10-12 mm width is often applied (Kaufman 1986; Bar-Yosef & Belfer-Cohen 2004; Bataille et al. 2019). As a result of separate research histories, different technocomplexes have been identified in different geographical areas during the eUP: the Aurignacian in Europe (Breuil 1909, 1913; Otte 2017; Chu and Richter 2020), the Ahmarian in the Levant (Gilead 1991; Goring-Morris & Belfer-Cohen 2018) and the Baradostian in the Zagros Mountains (Tsanova 2013; contra the Baradostian and supporting multiple independent cultural entities in the Zagros see Ghasidian et al. 2017, 2019). The present paper will focus on the European and Levantine lithic technology record.

Throughout the recent decades, early Aurignacian assemblages have been divided into the Early Aurignacian (Bon 2002; Bordes & Tixier 2002) and the Protoaurignacian (Laplace 1966; Bon 2002). The division was initially developed according to typology, with Protoaurignacian assemblages containing a high percentage of marginally retouched bladelets, while Early Aurignacian assemblages were characterised by a higher number of bigger tools such as the carinated endscrapers – with lamellar retouch along the working edge – and blades with scalar retouch (Aurignacian blades). In later studies, the typological differences acquired a technological aspect. The Protoaurignacian technology was typified by a 'continuous system' for blade and bladelet production, where relatively large bladelets were struck on-axes from the same pyramidal cores as small blades; in contrast, a 'discontinuous system' was recognised among Early Aurignacian assemblages, in which large blades were removed from prismatic cores with parallel margins, and small bladelets were primarily struck from carinated endscrapers (Bon 2002). The partition in two technocomplexes seems to be backed by stratigraphical observations, since in the few sequences where the two occur together (La Viña, Santamaría Álvarez 2012; Cueva Morin; Arrizabalaga et al. 2009; Labeko-Koba, Arrizabalaga et al. 2009; Isturitz, Normand & Turq 2005; Le Piage, Bordes 2005; Les Cottés, Roussel & Soressi 2013), the Protoaurignacian precedes the Early Aurignacian.

The Ahmarian tradition can itself be divided into a Northern and a Southern facies (Goring-Morris & Davidzon 2006; Kadowaki et al. 2015; Abulafia et al.

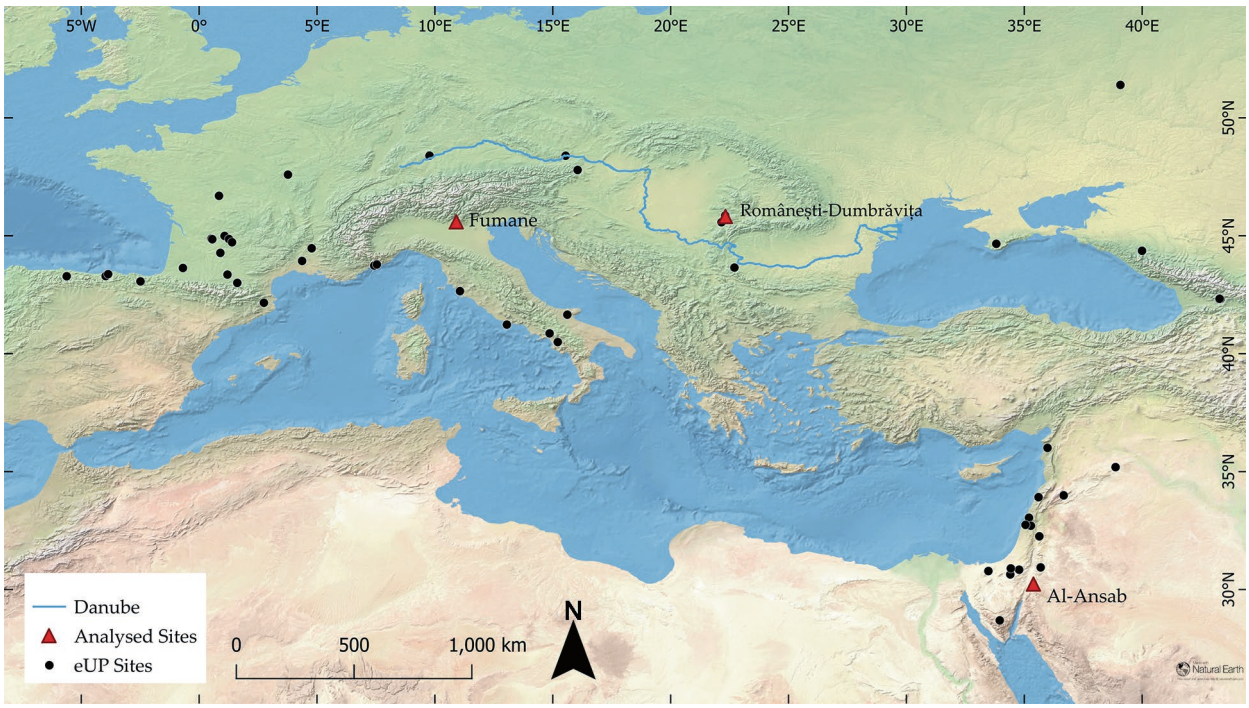

Fig. 1. The distribution of the major eUP European and Levantine sites and the analysed sites.

Abb. 1. *Die Verteilung der wichtigsten europäischen und levantinischen eUP-Standorte und die analysierten Standorte.*

2021; Richter et al. 2020). While the Northern Ahmarian is prevalently characterised by bipolar knapping of blades from narrow-fronted cores and, more rarely, from bladelet cores (Abulafia et al. 2021), the Southern Ahmarian is typified by largely unidirectional narrow-fronted cores, which were rapidly reduced to bladelet-producing sizes (Goring-Morris & Davidzon 2006). The typological hallmark of the Ahmarian, Northern and Southern alike, is the el-Wad point, mostly blades pointed through marginal retouch but displaying a variety of marginal retouch (Le Brun Ricalens et al. 2009; Bergman et al. 2017; Goring-Morris and Belfer-Cohen 2018). In the Southern Ahmarian the el-Wad point is complemented by end-scrapers and burins obtained on core-shaping products (Monigal 2003).

Explaining the different sub-technocomplexes

Various models have been built upon the eUP lithic evidence throughout the years. Most models rely on similarities among artefacts to track the dispersal of innovations along the most evident geographical corridors. The most popular hypothesis states that the large Central-Eastern European rivers, such as the Danube, would have provided the best axis for penetration into Europe from Anatolia (Conard & Bolus 2003; Floss et al. 2016). The condition of this hypothesis is the existence of a techno-typological source area in the Levant (Mellars 2011). Other dispersal routes, including through the eastern Mediterranean (Douka et al. 2011; Hauck et al. 2017; Carter et al. 2019; Çilingiroğlu & Dinçer 2021), or via the Caucasus-Black Sea (Golovanova & Doronichev 2012; Demidenko 2014; Hoffecker & Holliday 2014; Otte 2015; Cullen et al. 2021) are possible but currently lack substantial evidence in sites.

Dating is pivotal to most of the dispersal models, but while the 'geographical' models largely rely on locating the first occurrences of technologies, the chronological models attempt to illustrate the development of one sub-technocomplex into another. Within the Aurignacian, a lower stratigraphical position of Protoaurignacian assemblages compared to the Early Aurignacian ones indicates that the Protoaurignacian represents a pioneering phase, with less structuration in technology and subsistence, while the Early Aurignacian correlates to a more developed expansion into the region (Davies 2001; Anderson et al. 2015).

Finally, the Northern Ahmarian has also been hypothesised as an early manifestation within the Mediterranean biome, while the Southern Ahmarian is a later adaptation to the desert and steppe areas of the inner Levant (Richter et al. 2020). The Northern hemisphere appears to have experienced cold, dry climate conditions triggered by the Heinrich Event 4 (HE4) around 40 ka (Heinrich 1988; Rasmussen et al. 2014; Badino et al. 2020; Shao et al. 2021). The cold conditions have been suggested as a forcing factor for the introduction of the Early Aurignacian (Banks et al. 2013; Tartar 2015).

Doubts

Each of the proposed theories of eUP origin and evolution can be challenged. At a continental level, the Early Aurignacian and the Protoaurignacian seem to have a similar starting date (Higham et al. 2012; Nigst et al. 2014; Barshay-Szmidt et al. 2018). The older dates obtained on Northern Ahmarian sites (Rebollo et al. 2011; Bosch et al. 2015; Alex et al. 2017) have been questioned, on the grounds of methodological and stratigraphical uncertainties (Zilhão 2013; Douka et al. 2015). Some Protoaurignacian assemblages postdate the Campanian Ignimbrite (CI) eruption (39.3 ka calBP, Giaccio et al. 2017) and the HE4 onset, revealing greater adaptive flexibility (Palma di Cesnola 2006; Riel-Salvatore & Negrino 2018; Villa et al. 2018; Falcucci et al. 2020). Furthermore, discerning between Protoaurignacian and Early Aurignacian technology is harder than previously thought (Sitlivy et al. 2014; Falcucci et al. 2017; Bataille et al. 2018).

Research Question

Bladelets have been shown pivotal to the assessment of eUP technology. Thus, understanding the various methods of bladelets production and their relative significance within the eUP technological systems must be the basis of any behavioural model. Research evaluating eUP technology has been either focused on a single site (e.g. Ohnuma 1988; Chiotti 1999; Slimak et al. 2002; Monigal 2003; Teyssandier & Liolios 2003; Normand & Turq 2005; Goring-Morris & Davidzon 2006; Porraz et al. 2010; Roussel & Soressi 2013; Grimaldi et al. 2014; Nigst et al. 2014; Bataille 2016; Falcucci et al. 2017, 2020; Abulafia et al. 2021; Kadowaki et al. 2021), on regional clusters (e.g. Bon 2002; Bordes & Tixier 2002; Sitlivy et al. 2014; Tafelmaier 2017) or on using published data from different authors (Kadowaki et al. 2015; Bataille et al. 2018, 2020). In contrast, the current research presented here provides a first-hand, detailed, original, technological cross-comparison of eUP assemblages recovered from sites bridging the extent of the supposed eUP dispersal.

Materials & Methods

Site situations and assemblages

The analysis was conducted on assemblages recovered from three stratified sites: Al-Ansab 1 (Jordan), Românești-Dumbrăvița I (Romania) and Grotta di Fumane (Italy). Radiometric dating is constraining these assemblages to the eUP timespan. Therefore the sites are providing consistent evidence that has been previously well anchored to their technocomplex of belonging.

Al-Ansab

Al-Ansab 1 (hereafter referred to as Ansab) is found in the Lower Wadi Sabra of Jordan (30°14'2.4"N 35° 22'58.8"E; 618 m above sea level [a.s.l.]; Fig. 2) in

remnant Pleistocene sediments. During the MIS 3, the site was encompassed within the Irano-Turanian steppe biome (Miebach et al. 2019). The wadi (a seasonal water channel) that runs below the site was higher during the MIS 3 forming a more extensive floodplain. Primary chert outcrops are found in the nearby limestone ridges (Parow-Souchon et al. 2021). The site was firstly identified in 1983 during a survey of the region, and systematic excavations started in 2009. To date, an area of 24 m^2 has been excavated. The 1 m^2 basic grid unit is further subdivided into quadrants of 0.25 m^2. Deposits are excavated in arbitrary 5 cm deep spits. Finds ≥10 mm in maximum dimension have been individually piece-plotted using a total station since 2015. Finds >20 mm have two or more points plotted to record the contour. Smaller finds are identified by quadrant and spit number alongside finds retrieved by dry sieving through a 2 mm mesh. The artefacts are embedded in consolidated sandy sediments originated from fluvial and aeolian deposits, the find layer is located 2 m below the present surface and it is distinguished from other layers as a darker ashy colouration. Newer excavations have found a second occupation layer below, the lithics and data presented here refer to the upper AH I layer (Schoenenberg & Sauer 2022). Faunal remains are largely attributed to *Gazella* spp., while some marine shell fragments, probably for ornamental use, are attributed to the *Cardiidae* family (Sauer & Schoenenberg 2021). Also, the use of ochre is attested (Richter et al. 2020). The artefacts were found in horizontal and randomly oriented positions, strictly following the relief of a former occupation surface that had been consolidated by soil formation (Richter et al. 2020). The sedimentation is intersected to the West by a buried riverbed of coarse sand and gravel, while to the South-East the deposit is cut by modern erosion, a feature that allowed for the initial identification of the site. The artefacts occur as separate horizontal scatters, whose content does not vary, leading to the hypothesis they were formed during repeated visits in a residential mobility pattern (Richter et al. 2020; Schoenenberg & Sauer 2022). Optically stimulated luminescence (OSL) dating of the sediments placed the occupation layer between 45–32 ka (Klasen et al. 2013), while ^{14}C dates show high consistency between 38–37 ka calBP (Richter et al. 2020). The artefacts analysed were selected from the 2009, 2011 and 2018 excavation materials. Artefacts of the 2009–2011 excavations come from squares 165, 166, 167, 168, 156, 157, 158, 164, 174, 184. Artefacts of the 2018 excavations are from squares 193, 194, 195, 196, 197, 198, 203, 204, 205, 206, 207, 208 (Fig. 2).

Românești-Dumbrăvița I

Românești-Dumbrăvița I (hereafter Românești) is located on a river terrace overlooking the confluence of the Bega Mare and Bega Mica rivers near the Românești village, in Timiș county, in the

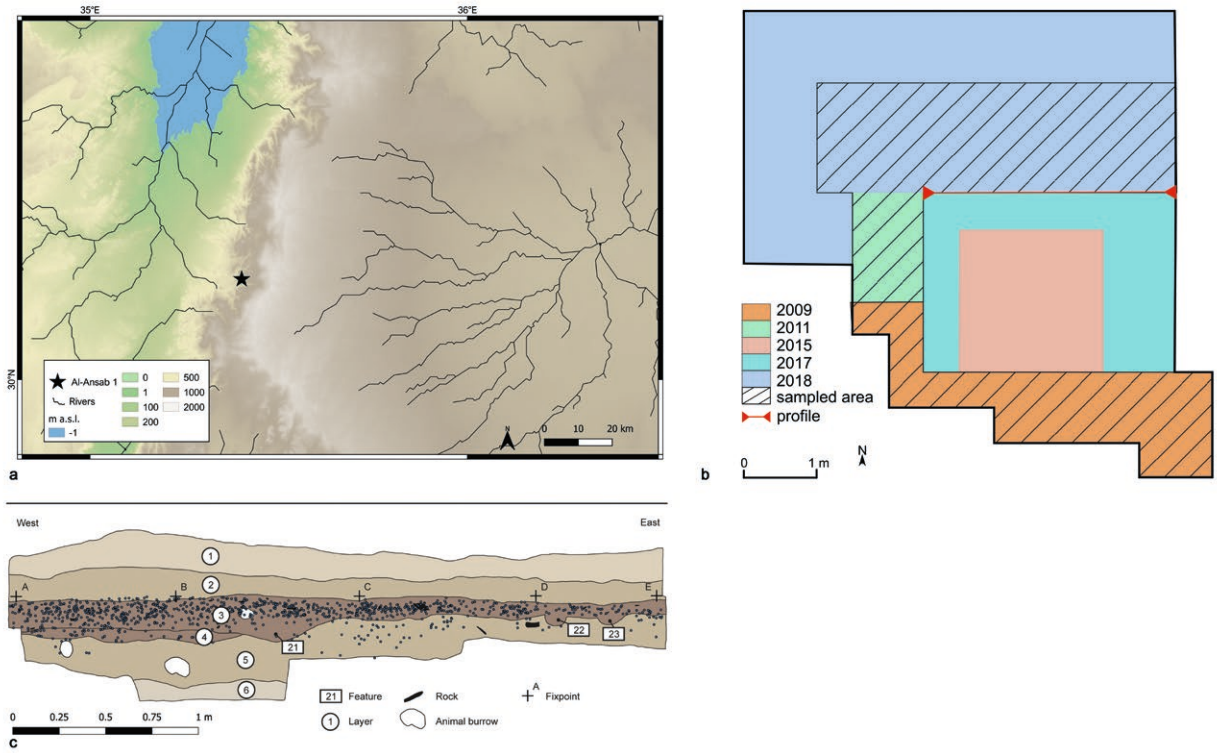

Fig. 2. Regional setting of Al-Ansab 1 (a), stratigraphy (b) (modified after Richter et al. 2020), and horizontal plan of the excavated area with sampled part for the current analysis (c).

Abb. 2. *Regionale Lage von Al-Ansab 1 (a), Stratigraphie (b) (modifiziert nach Richter et al. 2020) und Grundplan der Ausgrabungsfläche mit dem für die aktuelle Analyse beprobten Teil (c).*

Western Romania portion of the Banat (45°49′2.45″ N, 22°19′15.85″ E, 212 m a.s.l.; Fig. 3). Palaeonvironmental studies suggest the existence of a forest-steppe during the MIS 3 (Kels et al. 2014). In the same area two different archaeological locations, Românești I and II, are lying 80 m apart: Românești I is by far the most extensive (Sitlivy et al. 2012). Chert-like material, commonly called Banat flint, is widely available in primary and secondary outcrops in the site's vicinity and was extensively used in the site as well as in other regional UP assemblages (Chu et al. 2019; Ciornei et al. 2021). Faunal and organic remains, in general, are extremely rare due to the poor preservation conditions. The site was surveyed in 1959 and subject to excavations between 1960–64 and 1967–72, resulting in the discovery of large scatters of Palaeolithic lithic artefacts in the upper 1.3 m of deposits. A combined stratigraphy comprises six layers, the lowest (Layer I) being attributed to the Quartzite Palaeolithic or Mousterian and the topmost (Layer VI) to an (Epi) Gravettian period. Intervening layers, especially Layer III, have been attributed to the Aurignacian (Sitlivy et al. 2012).

In 2009–2010 test-pits were placed adjacent to previous excavation trenches to assess the stratigraphy, obtain a radiometric chronology and re-evaluate the cultural attribution. The test-pits largely confirmed the interpretations of the original excavations. Four geological horizons (GH) have been identified. The soil was classified as Albeluvisol, mostly silty and with a progressively higher content of clay in the lower GHs (Kels et al. 2014). Discrete artefact concentrations were found principally in GH2, attributed to the Epigravettian, and in GH3, attributed to the Aurignacian. In particular, the number of small finds, bladelets amongst them, increased significantly during the 2009-2010 test-pit excavations due to the adoption of wet sieving (Sitlivy et al. 2012).

Following this, excavations were performed in 2016, 2018 and 2019 in the area adjacent to the 2009 test trench. To date, a total surface area of 29 m^2 has now been excavated, down to nearly 1 m deep. The 1 m^2 basic grid unit is further subdivided into quadrants of 0.25 m^2, and digging in these later excavations have proceeded in 2 cm deep spits confined within each GH. Finds over 5 mm are spatially recorded using a total station, elongated artefacts are recorded with

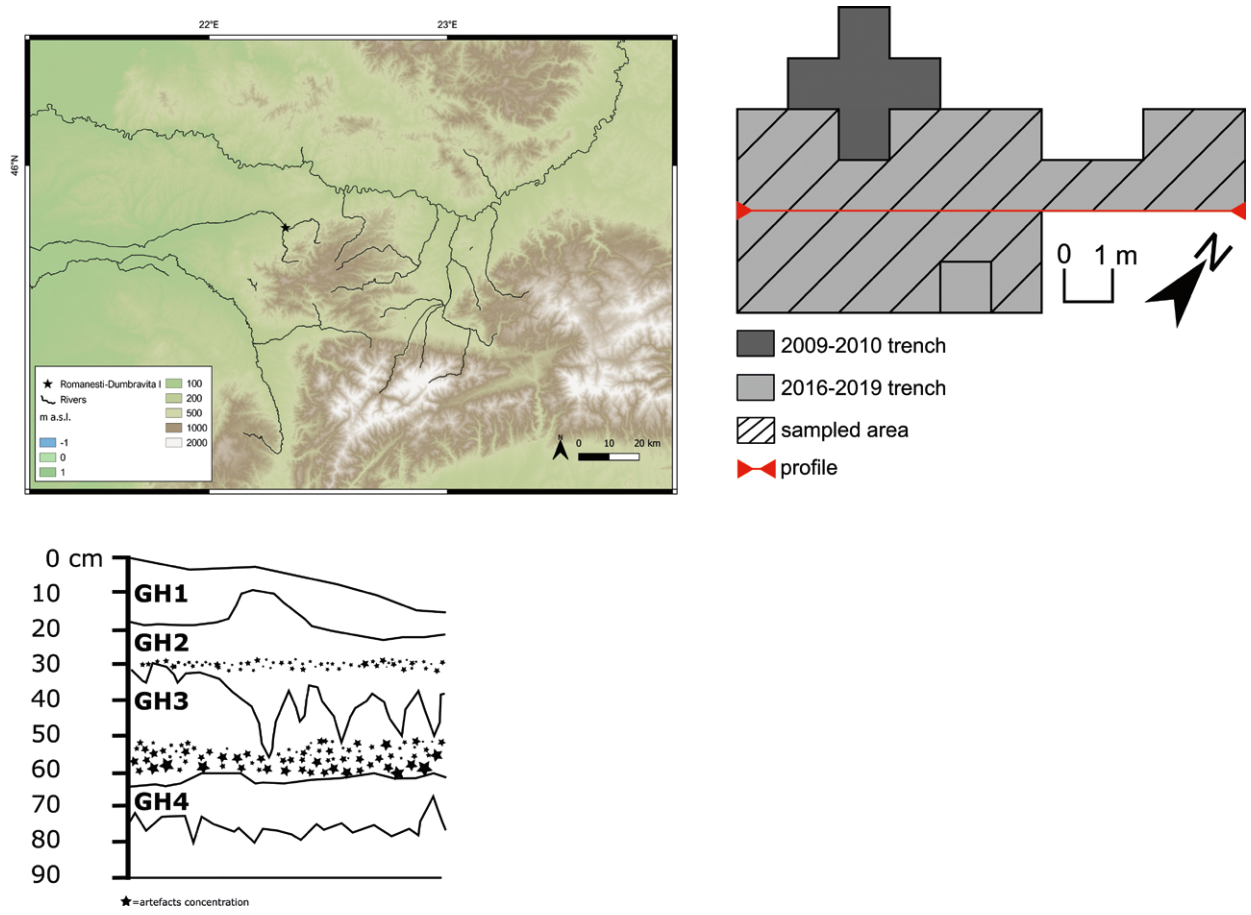

Fig. 3. Regional setting of Românești-Dumbrăvița I (a), stratigraphy (b), and horizontal plan of the excavated area with sampled part for the current analysis (c).

Abb. 3. *Regionale Lage von Românești-Dumbrăvița I (a), Stratigraphie (b), und Grundplan der Ausgrabungsfläche mit dem für die aktuelle Analyse beprobten Teil (c).*

two points at the extremities, while bulky artefacts (such as exogenous rocks) are recorded with multiple points across the contour. Excavated soil was wet sieved with a 5 mm mesh and selected sediments with a 2 mm mesh. Both OSL, on sediment, and thermoluminescence (TL), on artefacts, dates returned a mean age of 40.5 ± 1.5 ka for GH3 (Schmidt et al. 2013). The artefacts selected for analysis in the current study consist of the piece-plotted GH3 artefacts from 2016, 2018 and 2019 excavations, excluding those from square P104, as these have been kept unwashed for future analyses (Fig. 3).

Grotta di Fumane

Grotta di Fumane (hereafter referred to as Fumane) is located in one of the deep-cut valleys characterising the lower Monti Lessini Plateau of the Venetian Pre-Alps, Italy (45°35′30.52″N 10°54′18.67″E; 350 a.s.l.; Fig. 4). High-quality cherts are available throughout the plateau from various limestone formations (Delpiano et al. 2018). Environmental studies suggest the persistent presence of forests until ca. 40 ka, with progressive cooler and dryer conditions approaching the HE4 (López-García et al. 2015; Badino et al. 2020; Romandini et al. 2020). The site is a karst opening with three tunnels; one major central tunnel and two ancillary tunnels on the sides. It was sealed by the collapse of the cave roof at ca. 30 ka BP, ensuring the preservation of the fine stratigraphy. Systematic excavations started in 1988 and are still ongoing. The site has been divided into a grid of 1 m^2 squares, and further subdivided into 0.11 m^2 quadrants. This method ensured the provenance of the artefacts before the adoption of a total station in 2005. All excavated sediment is wet-sieved and screened. Artefacts then are grouped by unit, subunit, square metre, and quadrant, and divided between those that are <15 mm and >15 mm in maximum dimension. The archaeological deposit spans for over 10 m, macrounits are defined by their main paedogenic agent: D mostly consists of roof cave collapse debris; A comprises fine occupational layers; BR is characterised by breccias, and S is mostly aeolian sand. Focusing on the upper part of the sequence, in the macrounits D and A previous studies identified Gravettian in D1d (Falcucci & Peresani 2019), Aurignacian in D1c, D3, D6, A1 and A2 (Broglio et al. 2003; Falcucci et al. 2017, 2020), Uluzzian in A3 (Peresani et al. 2016), and Mousterian in A4 down to A11 (Peresani 2012). All these units are lithologically well distinguishable in

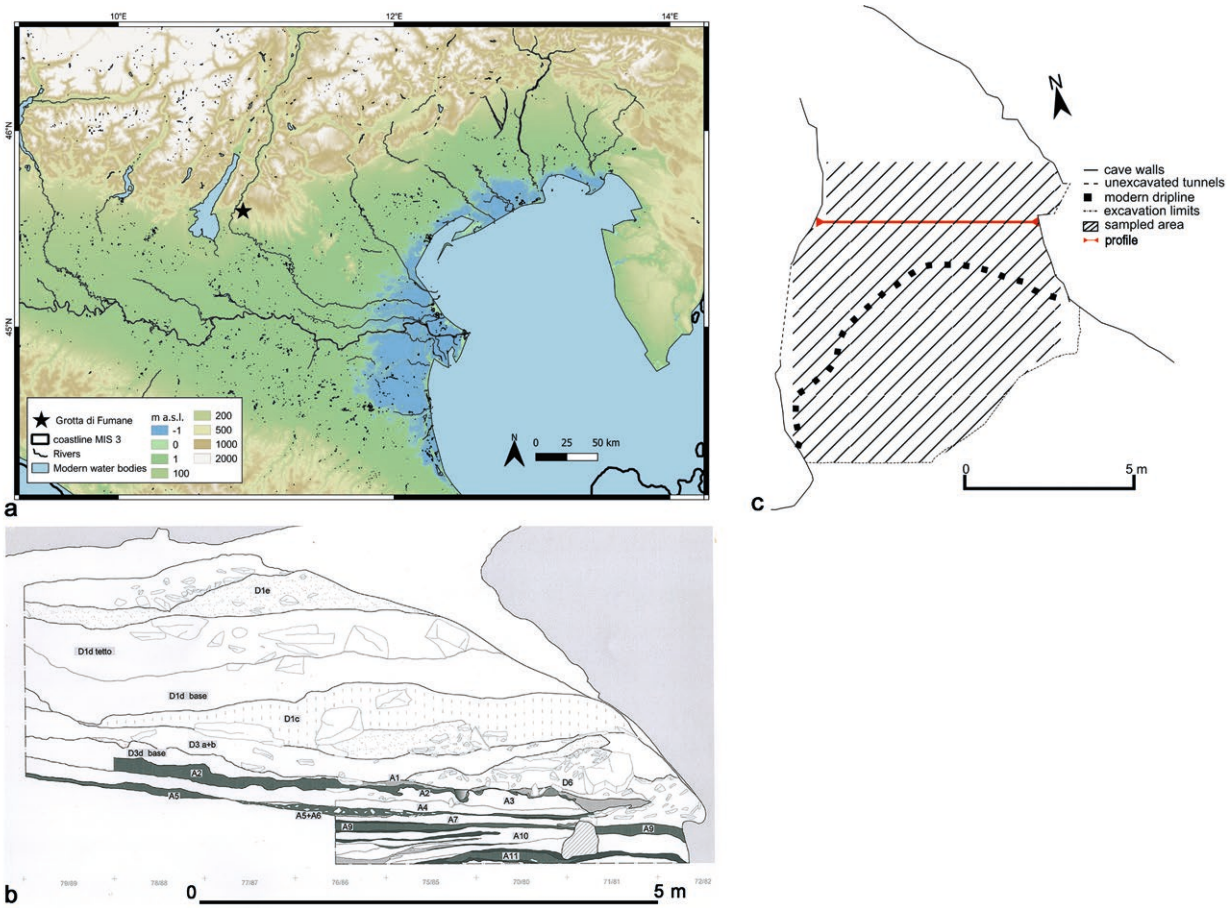

Fig. 4. Regional setting of Grotta di Fumane I (a), stratigraphy (courtesy of M.P.) (b), and horizontal plan of the excavated area with sampled area for the current analysis (c).

Abb. 4. *Regionale Lage der Grotta di Fumane (a), Stratigraphie (mit freundlicher Genehmigung von M.P.) (b), und Grundplan der Ausgrabungsfläche mit dem für die aktuelle Analyse beprobten Teil (c).*

section, especially towards the front of the cave, and the Aurignacian stands out for its red colour due to high ochre processing in A2S21 and A2R, also witnessed by painted portable stones in D3 (Broglio et al. 2009; Cavallo et al. 2017). The Aurignacian layers preserve several occupational features, as well as many perforated and non-perforated marine and fresh-water shells that were likely used for ornamental purposes (Peretto et al. 2004; Peresani et al. 2019). A1 and A2 are discrete stratigraphical units, but for technotypological purposes, they have been considered a single unit (Falcucci et al. 2017), as when taken singularly they do not differ significantly (Falcucci et al. 2020; Gennai 2021). The early Aurignacian units start between 41.9–40.2 ka calBP, at the boundary of A3/A2, and end before 38.5–37.9 ka calBP, (D3bα date (ABOx-SC¬) ^{14}C dates, with a 95 % probability; Higham et al. 2009). Artefacts were selected for analysis in the present study from among the >15 mm pieces recovered from the front section of the cave mouth (square metres lines 20–100; Fig. 4).

The studied assemblages are qualitative samples. The analysis only employed complete and semi-complete debitage products (hereafter debitage), and cores (Tab. 1). A 'semi-complete artefact' is defined as a blank where two portions (proximal, mesial, and/or distal) remain intact. This definition of semi-complete blanks is used to retrieve as much data as possible, without using shorter fragmented artefacts as these are difficult to interpret. Cores are defined as raw material pieces or large flake blanks with at least three intentional negative scars that are the result of the production of new debitage (Conard et al. 2004; Soressi & Geneste 2011).

Methods

The study methodology is a combination of chaîne opératoire (CO) reconstruction and attribute analysis (Inizan et al. 1999; Soressi & Geneste 2011; Scerri et al. 2016). CO is a common methodology applied to lithic assemblages to reconstruct the production processes. The main tool of the CO approach is the diacritical negative scars analysis scheme, which highlights the sequence of negative detachments. The analytical procedure applies mostly to cores, which preserve a bigger flaking surface than debitage. Once the diacritical scheme is understood, the debitage analysis completes the picture. Attributes related to purely technical considerations (the overhang removal in cores and laminar debitage, the bulb morphology, the flaking angle) are assessed for recognising the type of technique applied in the assemblages, in particular if it can be evaluated as tangential soft hammer direct percussion typical of volumetric laminar productions during the UP (Pelegrin 2011). The other attributes are used to integrate the analysis of the cores. Therefore, the platform type gives information about the former core striking platform; the negatives' orientation and types are compared to those found in cores; the cortical amount is proxy of reduction depth and the cortex position is proxy of the position and role of the artefact on the core volume. Standard morpho-technological attributes (longitudinal profiles, artefact silhouettes, symmetry and shape of cross-section, distal terminations) are used in comparison with the core diacritical scheme to evaluate the role of the artefact in the reduction and its position on the core volume. The debitage and core negatives can be divided into 'management' and 'ordinary'. Ordinary ones are generally taking advantage of the existing morphology of the core while management pieces are primarily shaping or maintaining the core convexities (Soressi & Geneste 2011).

For the current methodology, blades are defined as elongated debitage with sub-parallel margins which, when unbroken, are two times longer than they are wide (Inizan et al. 1999; Andrefsky 2005). Bladelets are blades that are less than 12 mm wide. This is an arbitrary threshold initially defined for Epipaleolithic North-African assemblages (Tixier 1963). This is supported by recent eUP technological analyses which suggest that the threshold is significant for separating blanks used for the specialised projectile implements from other blanks throughout the Aurignacian (Normand & Turq 2005; Roussel & Soressi 2013; Falcucci et al. 2017). Retouched implements were not subjected to a thorough analysis, because the typological framework of the three sites is well understood (Sitlivy et al. 2012; Schyle 2015; Falcucci et al. 2017, 2018; Aleo et al. 2021; Parow-Souchon et al. 2021). Nevertheless, when encountered in the sample, retouched implements have been described according to Inizan et al. (1999) and Demars and Laurent (1992). Retouched implements are ascribed to the classic eUP types encountered and described in the previous publications (marginally retouched and backed blades and bladelets, in particular (pseudo-) Dufour, dihedral burins and endscrapers). Therefore, retouch patterns are difficult to disentangle in the eUP (for a more extensive discussion see Le Brun-Ricalens et al. 2009).

The continuous data is statistically explored firstly with boxplots and violin plots. Median and inter-quartile range are preferred to mean and standard deviation because less sensitive to extreme values,

Lithics	A	R	F	Total
Blade	948	262	517	1,727
Bladelet	809	288	811	1,908
Flake	293	544	248	1,085
Cores	125	18	90	233
Total	2,175	1,112	1,666	4,953

Tab. 1. Artefacts analysed in the present study. Sites A: Ansab, R: Românești, F: Fumane.

Tab. 1. *In der vorliegenden Studie analysiert Artefakte. Fundstellen A: Ansab, R: Românești, F: Fumane.*

and then tested statistically through the nonparametric Mann-Whitney U test for two independent samples, and the nonparametric Kruskal–Wallis H test, more than two independent samples (MacFarland & Yates 2016). Categorical data is explored through frequencies and statistically tested through the nonparametric Pearson Chi-Square independence test and goodness of fit (McHugh 2013; MacFarland & Yates 2016). Analyses are performed in the open-source software R with the package "ggstatsplot", which provides an elegant and efficient combination of statistical test and graphical output. Results are reported in the text and the graphical output is accessible in the Supplementary Information (Patil 2021; R Core Team 2021).

Results

Cores

The cores were divided into different categories: semi tournant, parallel edges, narrow fronted, narrow fronted *sur tranche*, transversal carinated cores, and finally pre-cores (Tab. 2). Semi tournant cores actively involve the adjacent lateral surfaces in the main flaking surface (Falcucci & Peresani 2018). Parallel edges cores show a wide flaking surface framed by two (sub) parallel intersections with the core flanks (Bordes & Tixier 2002; Falcucci & Peresani 2018). Narrow fronted cores display a flaking surface installed on the narrower core surface and with additional core flanks shaping (Goring-Morris & Davidzon 2006). Narrow fronted *sur tranche* display a narrow flaking surface without any core flank preparation, sometimes they are referred to as burin cores as well (Normand & Turq 2005; Zwyns et al. 2012). Transversal carinated cores are also referred to as carinated endscrapers (Falcucci & Peresani 2018). Pre-cores are all those cores showing an early discard.

Dimensionally they can be divided between those having a wide flaking surface (semi-tournant, parallel cores and transversally carinated) and those having a narrow flaking surface (narrow fronted and narrow fronted *sur tranche*) as suggested by metrics (Tab. 3). The similarity of parallel edges and semi-tournant cores is supported by the Elongation values (A: p >.05; F: p >.05; SI Fig. 1). Instead, narrow fronted cores are significantly different from *sur tranche* cores with strongly diverging results (A: p <.01, r = -0.61; F: p <.01, r = -0.68; SI Fig. 2). Furthermore, the two most numerous categories of broad cores (semi-tournant) and narrow cores (narrow fronted) are significantly different from each other (A: p <.01, r = -0.52; F: p <.01, r = -0.63; SI Fig. 3). Additionally, the elongation of cores belonging to the same category is significantly similar across assemblages (SI Fig. 4).

When considering the core management operations and knapping goals, the cores are strikingly similar across categories and sites. Platform edge overhang is frequently microchipped or abraded (A: 89 % R: 50 % F: 74 %; Appendix 1: A). Of the four main core categories, only narrow fronted *sur tranche* showed minimal overhang removal (A: 25 % R: 50 % F: 50 %; Appendix 1: A). The Chi-Square independence test does not report a significant association between assemblages and overhang removal for the same core category (p >.05; SI Fig. 5). Hence, the same core categories have a similar overhang removal across assemblages. The platform angles are often less than 70° (A: 74 % R: 44 % F: 42 %; Appendix 1: B). The steepest platform angles are found on parallel edges and semi tournant cores at all three sites, and also on narrow fronted cores in Ansab. In parallel edges and *sur tranche* cores, the Chi-Square independence test reports a non-significant association between the assemblage and flaking angle (p >.05; SI Fig. 6), while semi tournant and narrow fronted cores are reporting a significant association (p <.05; SI Fig. 6). The Chi-Square goodness of fit test reveals that only in Ansab's parallel edges, semi tournant and narrow fronted cores the proportions do statistically differ from a casual distribution (p <.05; SI Fig. 6). Hence it can be suggested that <70° flaking angles are mostly associated with Ansab, while Românești and Fumane have generally acute flaking angles. Meanwhile, the shallowest platform angles are found in *sur tranche* cores (Appendix 1: B). The Chi-Square goodness of fit test reports non statistically different proportions from a casual distribution in each assemblage (p >.05; SI Fig. 6), therefore no particular flaking angle can be associated with *sur tranche* cores. In the Ansab and Fumane assemblages, the cores have been so heavily reduced that the original shape of

Sites	Pre		Pl Edges		Semi Tour		N Fronted		sur Tranche		Trans. Carinated		Frag		Others		ND		Total	
Sites	N	%	N	%	N	%	N	%	N	%	N	%	N	%	N	%	N	%	N	%
A	7	6	11	9	34	27	41	33	16	13	5	4	5	4	5	4	1	1	125	100
R	3	17	-	-	5	28	-	-	8	44	-	-	1	6	1	6	-	-	18	100
F	8	9	12	13	25	28	16	18	14	16	6	7	-	-	9	10	-	-	90	100
Total	18	8	23	10	64	27	57	24	38	16	11	5	6	3	15	6	1	<1	233	100

Tab. 2. Number and percentages of each core type identified in each assemblage. Legend Pre: Pre-Core, Semi Tour: semi tournant, N Fronted: Narrow Fronted, *sur Tranche*: Narrow Fronted sur Tranche, Trans. Carinated: Transversal Carinated, Frag: Fragment.

Tab. 2. *Anzahl und prozentualer Anteil der einzelnen Kerntypen, die in jeder Assemblage identifiziert wurden. Legende Pre: Pre-Core, Semi Tour: semi tournant, N Fronted: Narrow Fronted, sur Tranche: Narrow Fronted sur Tranche, Trans. Carinated: Transversal Carinated, Frag: Fragment.*

	Pre	Pl Edges	Semi Tour	N Fronted	sur Tranche	Trans. Carinated	Others
LENGTH							
A							
count	7	11	34	41	16	5	5
MIN	43.3	28.4	27.0	26.2	20.2	20.3	25.0
IQ	52.6	34.4	35.7	42.6	42.2	24.7	34.8
median	68.0	44.0	46.8	53.3	53.0	31.0	40.9
IIIQ	90.7	50.2	52.6	63.1	60.5	37.0	47.9
MAX	124.5	79.0	86.0	96.0	82.9	56.0	60.0
R							
count	3	-	5	-	8	-	1
MIN	23.7	-	29.8	-	41.6	-	66.6
IQ	30.0	-	34.6	-	44.3	-	66.6
median	36.4	-	47.1	-	48.3	-	66.6
IIIQ	55.9	-	55.3	-	53.5	-	66.6
MAX	75.4	-	59.9	-	57.6	-	66.6
F							
count	8	12	25	16	14	6	9
MIN	43.1	30.8	27.4	27.4	18.7	17.4	21.7
IQ	52.0	41.8	32.8	36.6	27.0	22.5	33.9
median	58.7	45.0	36.7	41.8	35.5	23.3	41.2
IIIQ	65.7	50.9	42.9	46.5	45.8	25.6	49.4
MAX	82.7	62.9	64.4	56.9	49.2	27.2	63.0
WIDTH							
A							
count	7	11	34	41	16	5	5
MIN	28.8	26.8	20.0	17.2	7.2	35.7	27.7
IQ	36.7	35.8	32.5	28.0	17.0	45.0	44.8
median	41.6	42.8	40.0	35.9	25.2	46.2	53.3
IIIQ	60.7	44.5	45.3	38.5	32.0	76.0	58.3
MAX	89.1	53.0	53.0	51.1	48.0	85.0	65.0
R							
count	3	-	5	-	8	-	1
MIN	34.2	-	32.8	-	11.4	-	46.4
IQ	35.3	-	35.3	-	15.2	-	46.4
median	36.3	-	38.3	-	16.4	-	46.4
IIIQ	55.2	-	42.1	-	26.0	-	46.4
MAX	74.0	-	42.9	-	39.5	-	46.4
F							
count	8	12	25	16	14	6	9
MIN	24.5	23.5	20.0	15.3	5.3	26.8	32.2
IQ	33.9	32.0	31.0	23.9	8.0	36.1	32.8
median	44.9	40.2	35.1	26.3	12.7	38.3	42.1
IIIQ	49.2	43.3	45.8	33.0	18.9	43.0	51.4
MAX	87.7	52.1	60.7	48.0	29.1	45.1	62.6
THICKNESS							
A							
count	7	11	34	41	16	5	5
MIN	26.3	16.9	21.0	20.4	25.0	53.0	33.6
IQ	39.6	20.8	26.7	36.2	31.5	54.8	37.6
median	43.7	24.2	31.0	46.3	37.5	55.9	52.3
IIIQ	71.2	32.3	43.6	52.9	51.9	61.0	67.7
MAX	95.1	52.0	57.4	87.0	65.1	120.0	74.0
R							
count	3	-	5	-	-	8	1
MIN	29.4	-	14.6	-	-	14.7	19.7
IQ	33.0	-	19.2	-	-	35.6	19.7
median	36.5	-	39.2	-	-	45.6	19.7
IIIQ	42.3	-	46.5	-	-	50.5	19.7
MAX	48.2	-	50.1	-	-	53.0	19.7
F							
count	8	12	25	16	14	6	9
MIN	41.5	13.4	15.3	20.8	23.4	26.8	9.9
IQ	62.8	18.6	21.9	27.2	28.0	30.7	18.8
median	68.5	23.5	25.3	32.2	36.1	37.4	29.3
IIIQ	71.0	32.7	32.8	44.7	39.3	45.6	31.5
MAX	83.2	40.7	62.3	61.5	56.8	75.2	35.2
ELONGATION							
A							
count	7	11	34	41	16	5	5
MIN	0.9	0.7	0.7	0.6	1.0	0.5	0.5
IQ	1.2	1.0	1.1	1.3	1.8	0.5	0.5
median	1.4	1.1	1.2	1.5	2.0	0.6	0.9
IIIQ	2.0	1.4	1.4	1.8	2.7	0.7	1.3
MAX	2.6	1.5	1.9	3.2	4.5	0.7	1.6

Tab. 3. Cores dimensions summary. Legend Pre: Pre-Core, Semi Tour: semi tournant, N Fronted: Narrow Fronted, *sur Tranche*: Narrow Fronted sur Tranche, Trans. Carinated: Transversal Carinated, Frag: Fragment.

Tab. 3. *Zusammenfassung der Abmessungen der Kerne. Legende Pre: Pre-Core, Semi Tour: semi tournant, N Fronted: Narrow Fronted, sur Tranche: Narrow Fronted sur Tranche, Trans. Carinated: Transversal Carinated, Frag: Fragment.*

	Pre	Pl Edges	Semi Tour	N Fronted	sur Tranche	Trans. Carinated	Others
R							
count	3	-	5	-	8	-	1
MIN	0.7	-	0.9	-	1.2	-	1.4
IQ	0.8	-	1.0	-	2.1	-	1.4
median	1.0	-	1.1	-	2.8	-	1.4
IIIQ	1.0	-	1.4	-	3.3	-	1.4
MAX	1.0	-	1.4	-	3.7	-	1.4
F							
count	8	12	25	16	14	6	9
MIN	0.6	0.9	0.7	0.8	1.2	0.5	0.7
IQ	1.2	1.1	0.9	1.2	1.9	0.6	0.8
median	1.5	1.2	1.0	1.6	2.5	0.6	0.9
IIIQ	1.8	1.4	1.2	1.9	3.6	0.7	1.0
MAX	2.1	1.8	2.2	2.4	4.2	0.7	1.7

Tab. 3. Cores dimensions summary. Legend Pre: Pre-Core, Semi Tour: semi tournant, N Fronted: Narrow Fronted, sur Tranche: Narrow Fronted sur Tranche, Trans. Carinated: Transversal Carinated, Frag: Fragment. (continued)

Tab. 3. *Zusammenfassung der Abmessungen der Kerne. Legende Pre: Pre-Core, Semi Tour: semi tournant, N Fronted: Narrow Fronted, sur Tranche: Narrow Fronted sur Tranche, Trans. Carinated: Transversal Carinated, Frag: Fragment. (Fortsetzung)*

raw material could not be determined on many of them (A: 46 % F: 39 %; Appendix 1: C), Nevertheless, it is clear that *sur tranche* cores were generally made on flake blanks (A: 50 % R: 63 % F: 79 %; Appendix 1: C). The Chi-Square independence test supports the *sur tranche* cores' blank similarity across assemblages (*p* >.05; SI Fig. 7). In most cases, only one striking platform is present on the core (A: 87 % R: 72 % F: 76 %; Appendix 1: F). The observation matches with the number of flaking surfaces that are overwhelmingly single (A: 93 %; R: 72 %, F: 80 %; Appendix 1: G). The Chi-Square independence test reports a significant association between assemblages and the number of flaking surfaces only in *sur tranche* cores and the effect size shows a strong association between variables ($p < .05$, $V_{Cramer} = 0.37$; SI Fig. 8). Multiple flaking surfaces are more common in Românești's semi-tournant cores (40 %) but the distribution of the values is statistically similar to a casual one (p>.05; SI Fig. 8). Also, Fumane's *sur tranche* cores show a higher percentage of multiple flaking surfaces (36 %; Tab.4:G) but the distribution is casual as well (p>.05; SI Fig. 8). Therefore, the association between multiple flaking surfaces and cores must be taken cautiously. The striking platform is overwhelmingly non-facetted (A: 98 % R: 100 % F: 87 %; Appendix 1: E). Within the major core categories, only Fumane shows some facetted striking platforms, nevertheless, the Chi-Square independence test reports a significant association between striking platform types and assemblages only for narrow fronted cores the association between variables is medium ($p < .05$, $V_{Cramer} = 0.28$; SI Fig. 9). Many cores are without any trace of cortex (A: 33 % R: 50 % F: 44 %; Appendix 1: E). Where present, the cortex is most often on the flanks and backs, i.e. away from the primary flaking surface. The Chi-Square independence test reports a non-significant association between assemblages and cortex position in similar core categories (p>.05; SI Fig. 10). The distributions do not differ from equal proportions in Ansab's parallel edges and narrow fronted cores, and in Românești's semi-tournant (p>.05; SI Fig. 10). Negative scars often indicate the production of bladelets (A: 76 % R: 83 % F: 79 %; Appendix 1: H) either in the framework of an independent production or intercalated with blades. A significantly similar production is shown across core categories and assemblages (p>.05; SI Fig. 11). Unidirectional reduction (A: 73 % R: 78 % F: 60 %; Appendix 1: I) or unidirectional and convergent negative scars (A: 19 % R: 6 % F: 19 %; Appendix 1: I) are the norm. The Chi-Square independence test shows a statistical similarity between the same core categories belonging to different assemblages (p>.05; SI Fig. 12). The diacritical schemes demonstrate that scars on the primary flaking surface face alternate between two key forms: convergent scars, these being struck on-axis, and typically travelling across three-quarters of the flaking surface length; these are bracketed by lateral scars, struck off-axis, extending to the far end of the flaking surface (Figs. 5 & 6).

Debitage

The technology in the three assemblages revolves around blade and bladelet production. When taken separately blades can be split almost in half between ordinary and management pieces (Figs. 7 & 8: 1-10; Tab. 4), while bladelets are mostly ordinary artefacts (Fig. 8: 11-55; Tab.5). Management pieces are mostly represented by asymmetrical blades (Fig. 7: 1-9) and bladelets, which in other contexts have been referred to as *debordant* blades (Hussain 2015) or comma-like blades (Falcucci et al. 2017). Crests (Fig. 7: 10-12) are mostly partial (one-sided and distal) and coming from later stages of the knapping (neocrest). The rest of the management pieces are divided into overshot blades (Fig. 7: 13-18), surface cleaning blades (large and robust blades removing a big part of the flaking surface) and generic maintenance blades. Most of the flakes (Fig. 9) appear to have functioned either in management roles, shaping the core flanks and flaking surfaces, shaping the core striking platforms or decorticating the core surfaces. Only the Românești assemblage shows a sizeable number of ordinary flakes (Tab. 4).

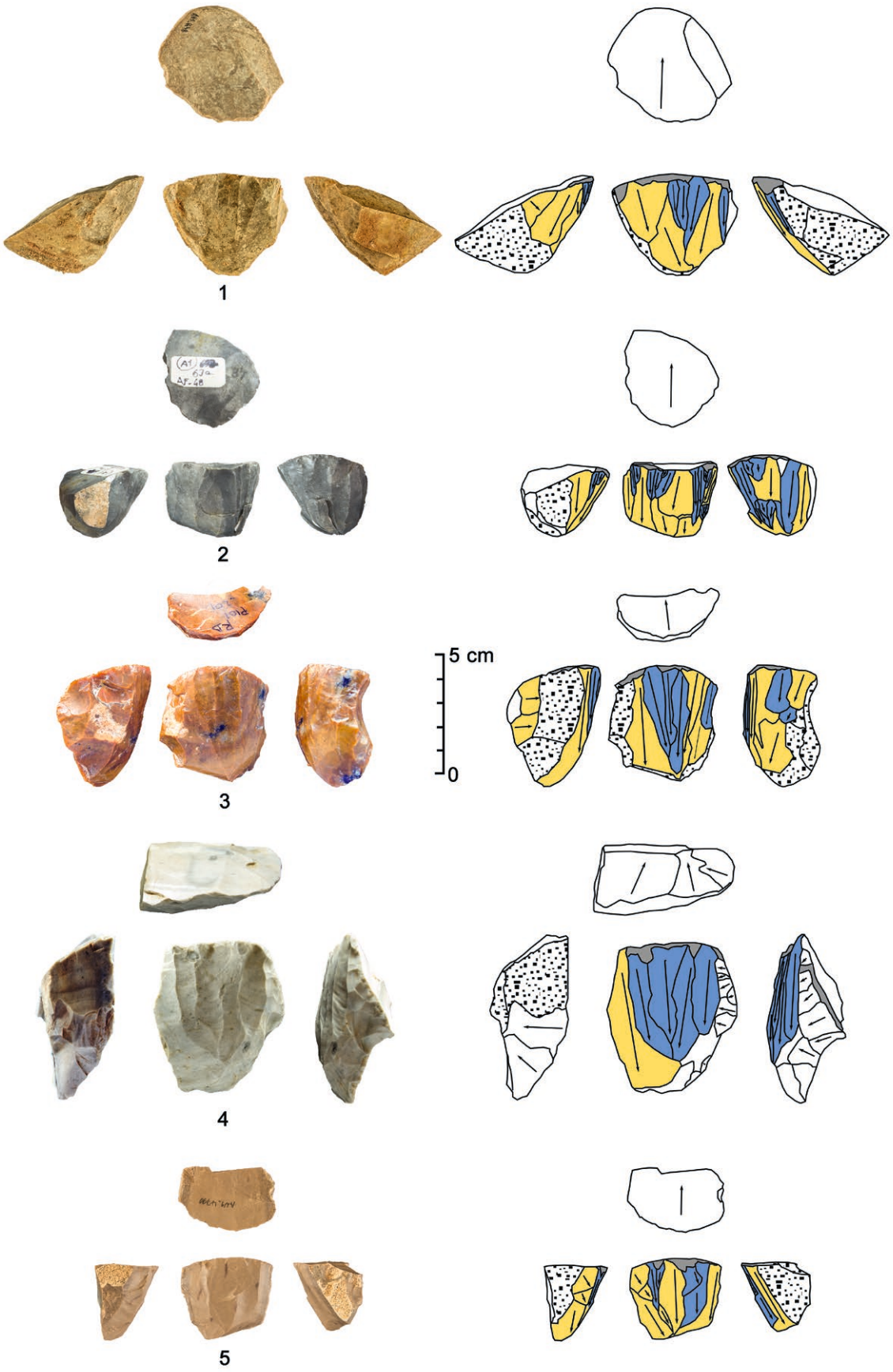

Fig. 5. Broad Cores. 1 and 5 Ansab, 2 and 4 Fumane, 3 Românești. Colour legend: blue: ordinary negatives, yellow: laminar management negatives, grey: overhang removal, dotted: natural surface. Photos and sketches: J. Gennai.

Abb. 5. *Breite Kerne. 1 und 5 Ansab, 2 und 4 Fumane, 3 Românești. Farblegende: blau: einfache Negative, gelb: Negative für laminares Management, grau: Entfernung des Überhangs, gestrichelt: natürliche Oberfläche. Fotos und Skizzen: J. Gennai.*

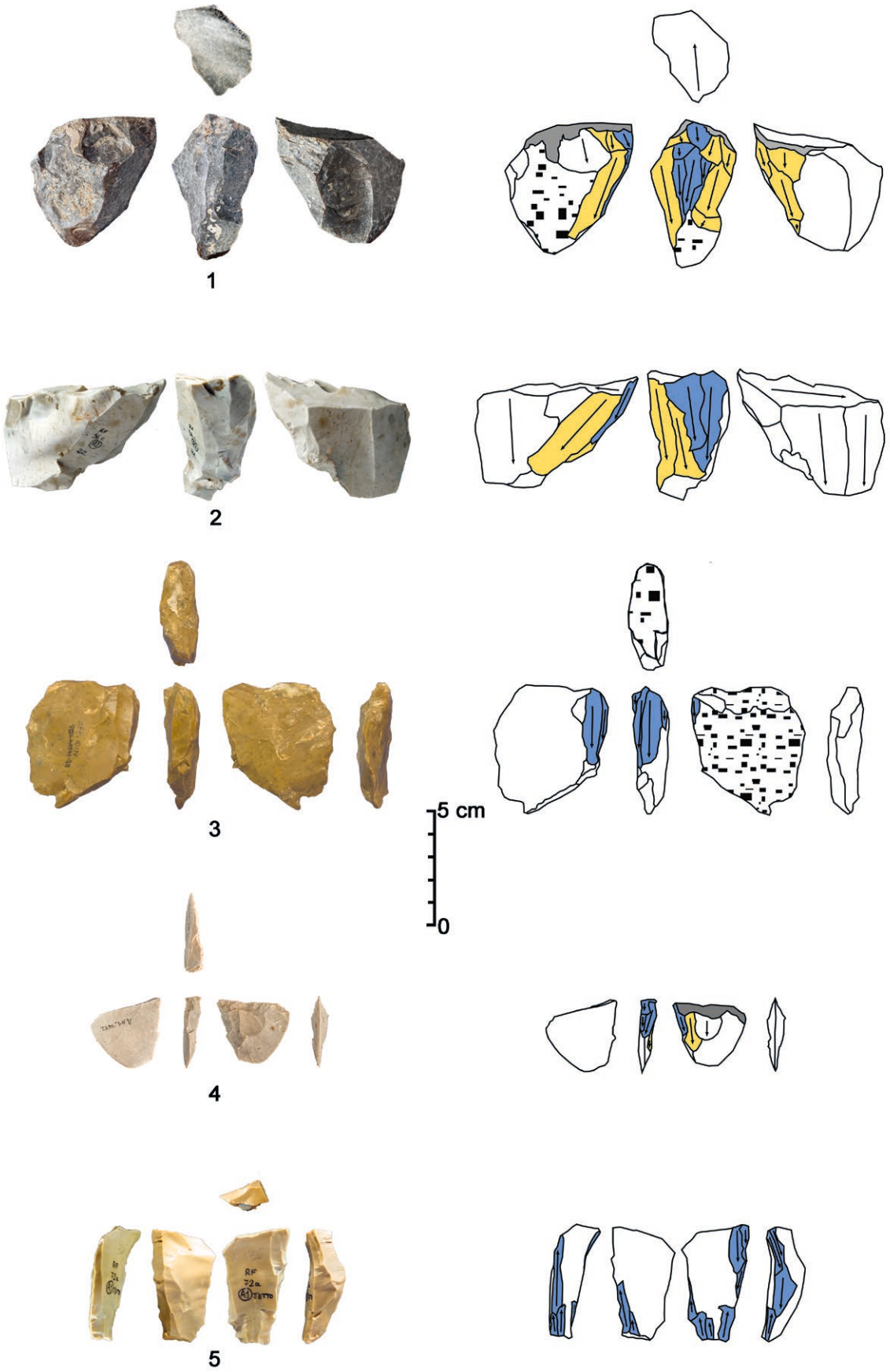

Fig. 6. Narrow Cores 1 and 4 Ansab, 2 and 5 Fumane, 3 Românești. Colour legend: blue ordinary negatives, yellow: laminar management negatives, grey: overhang removal, dotted: natural surface. Photos and sketches: J. Gennai.

Abb. 6. *Schmale Kerne 1 und 4 Ansab, 2 und 5 Fumane, 3 Românești. Farblegende: blau: einfache Negative, gelb: Negative für laminares Management, grau: Entfernung des Überhangs, gestrichelt: natürliche Oberfläche. Fotos und Skizzen: J. Gennai.*

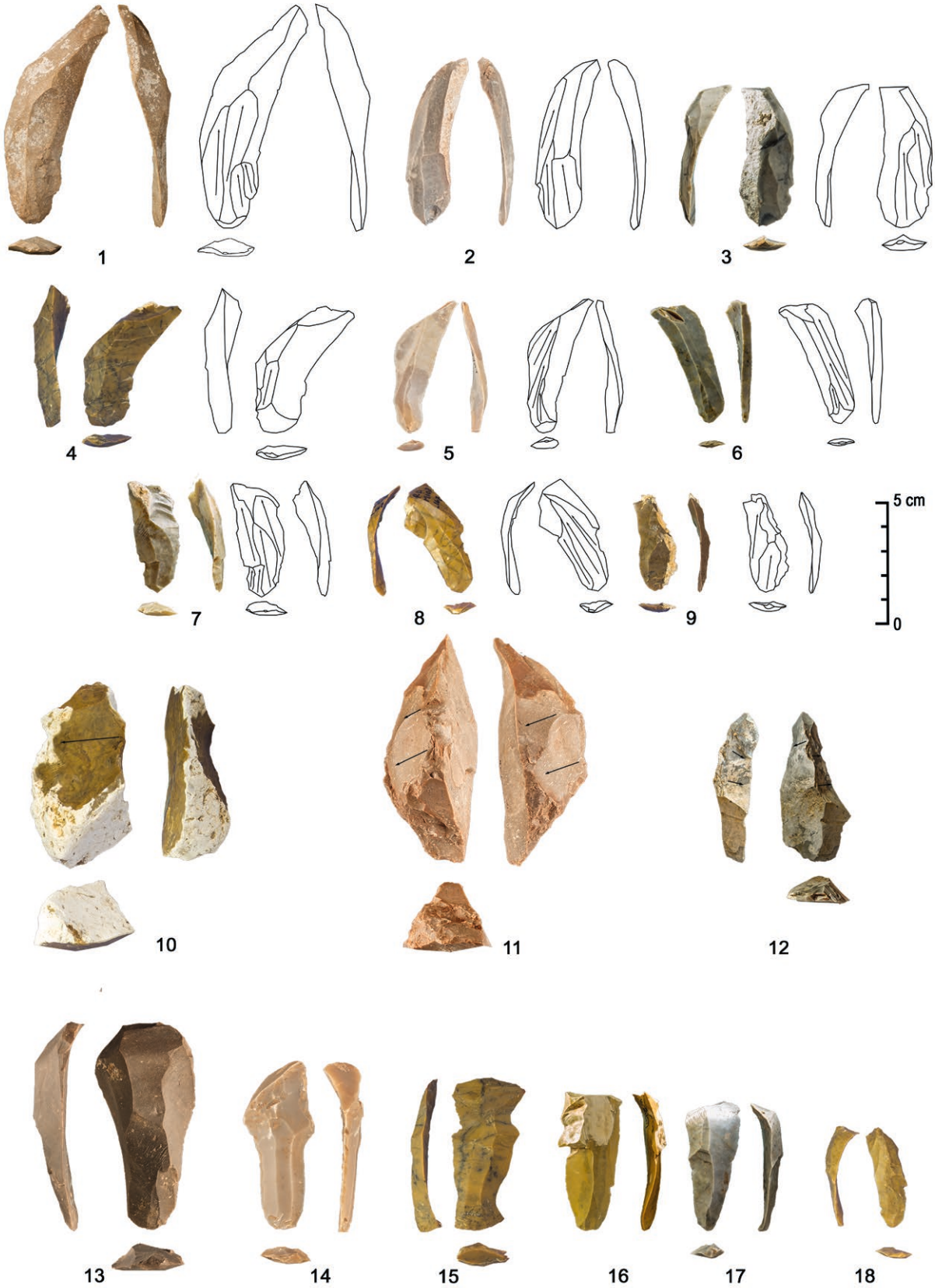

Fig. 7. Management blades. Asymmetrical Blades 1-9, Crests 10-12, Overshot Blades 13-18. 1-2,5, 11, 13-14 Ansab, 4,8-10,15, 18 Românești, 3, 6-7, 12, 16-17 Fumane. Photos and sketches: J. Gennai. Asymmetrical blades often exhibit a plunging and off-axis distal termination, and twisted profile.

Abb. 7. *Management-Klingen. Asymmetrische Klingen 1-9, Kernkantenklingen 10-12, Kernfußklingen 13-18. 1-2,5, 11, 13-14 Ansab, 4,8-10,15, 18 Românești, 3, 6-7, 12, 16-17 Fumane. Fotos und Skizzen: J. Gennai. Asymmetrische Klingen weisen oft ein gebogenes, von der Schlagachse abweichendes Distalende sowie ein verdrehtes Profil auf.*

Fig. 8. Ordinary Blades (1-11), Bladelets (11-55), Burin Spalls (56-60). 1,4,7,9, 11-17, 25-26, 29, 31, 34-36, 40, 46-47, 56, 60 Ansab, 2-3, 8, 18-19, 28, 30, 37, 39, 42, 48-55, 58-59 Romăneşti, 5-6, 10-11, 20-24, 27, 32-33, 38, 41, 43-45, 57 Fumane. Photos: J. Gennai.

Abb. 8. *Klingen (1-11), Lamellen (11-55), Stichelabfälle (56-60). 1,4,7,9, 11-17, 25-26, 29, 31, 34-36, 40, 46-47, 56, 60 Ansab, 2-3, 8, 18-19, 28, 30, 37, 39, 42, 48-55, 58-59 Românești, 5-6, 10-11, 20-24, 27, 32-33, 38, 41, 43-45, 57 Fumane. Fotos: J. Gennai.*

Debitage		A						R						F					
		Blade		Bladelet		Flake		Blade		Bladelet		Flake		Blade		Bladelet		Flake	
		N	%	N	%	N	%	N	%	N	%	N	%	N	%	N	%	N	%
O		442	47	691	85	30	10	127	48	197	68	139	26	241	47	665	82	9	4
M		505	53	108	13	162	55	132	50	57	20	267	49	276	53	129	16	111	45
	Crest	72	14	7	6	-	-	9	7	8	14	-	-	36	13	17	13	-	-
	Asymmetrical	237	47	77	71	-	-	73	55	30	53	-	-	148	54	84	65	-	-
	Overshot	141	28	19	18	-	-	19	14	6	11	-	-	58	21	19	15	-	-
	Surface	35	7	-	-	142	88	18	14	3	5	102	38	23	8	5	4	86	77
	Cleaning	-	-	-	-	-	-	-	-	-	-	-	-	-	-	-	-	-	-
	Maintenance	20	4	5	5	20	12	13	10	10	18	165	62	11	4	4	3	25	23
Sp		-	-	10	1	-	-	1	<1	29	10	-	-	-	-	17	2	-	-
I		-	-	-	-	52	18	-	-	-	-	71	13	-	-	-	-	59	24
T		1	<1	-	-	49	17	2	1	5	2	67	12	-	-	-	-	69	28
Total		948	100	809	100	293	100	262	100	288	100	544	100	517	100	811	100	248	100

Tab. 4. Debitage categories. Sites A=Ansab, R=Românești, F=Fumane. Principal categories are shown in bold (O=Ordinary, M=Management, Sp=Spall, I=Initialisation, T=Tablet), and management types are broken down into subcategories. Percentages are shown in brackets and are a portion of the total number of the relevant artefact classes. Percentages are given relative to the total of the pertaining artefact class, management subcategories of the pertaining total of management debitage.

Tab. 4. *Grundform Kategorien.Fundstellen A= Ansab, R= Românești, F= Fumane. Die Hauptkategorien sind fett gedruckt (O=Ordinary, M=Management, Sp= Spall, I=Initialisation, T=Tablet), und die Verwaltungstypen sind in Unterkategorien unterteilt Die Prozentsätze sind in Klammern angegeben und beziehen sich auf die Gesamtzahl der betreffenden Artefaktklassen. Die Prozentsätze werden im Verhältnis zur Gesamtzahl der betreffenden Artefaktklasse, der Unterkategorien der Verwaltung und der Gesamtzahl der Präparationsabfälle angegeben.*

Metrics

The summary of dimensions shows that blades have different median values than bladelets (Appendix 2).

To ascertain if the arbitrary width threshold is consistent in identifying two classes of products, the length, the thickness and the curvature of blades and bladelets in each assemblage have been tested. The Mann-Whitney test for independent samples of blades and bladelets length values returns a significant difference with strong disassociation between blades and bladelets in each site (Fig. 10). The same can be established for the thickness (Fig. 11). Blades are significantly more curved than bladelets in each assemblage even when the median is similar (Fig. 12).

Ansab's blades are significantly longer than their counterparts in Românești and Fumane (SI Fig. 13), the difference is strong in management blanks (ε^2 = .20) and moderate in ordinary blanks (ε^2 = .11). Bladelets have a significantly different length in each site, though the difference is moderate (Mgmt: ε^2 = .13 and Ordinary: ε^2 = .11): Ansab ones are the longest while Românești ones are the shortest (SI Fig. 14). Fumane's blades are significantly narrower than their counterparts in Ansab and Românești (SI Fig. 15), though the difference is weak (Mgmt: ε^2 = .03 and Ordinary: ε^2 = .02). Bladelets' widths are statistically similar across sites (SI Fig. 17). Fumane's management blades are the thinnest, though the difference is weak (ε^2 = .02; SI Fig. 18), while ordinary blades are significantly different in each site, though the difference is also rather weak (ε^2 = .05; SI Fig. 16). Management bladelets are thick alike across sites, while the ordinary ones are significantly different, though with a negligible difference (ε^2 = <.01; SI Fig. 18). Blades have a significantly different elongation, though the difference is moderate (Mgmt: ε^2 = .09 and Ordinary: ε^2 = .14; SI Fig. 20). The same applies to bladelets (Mgmt:ε^2 = .16 and Ordinary: ε^2 = .09; SI Fig. 19). Blades' curvature is significantly different across the assemblages, though with a weak difference (Mgmt: ε^2 = .03 and Ordinary: ε^2 = .02; SI Fig. 21). Management bladelets' curvature is significantly similar across assemblages, while ordinary bladelets' one is significantly different, though with a weak difference (ε^2 = .01; SI Fig. 22).

Technical attributes

Most of the debitage has a flaking angle comprised between 70°-90° in all sites (A: 54 % R: 63 % F: 80 %; Appendix 3: A). The Chi-Square independence test shows a significant association between flaking angle and assemblages, with a medium association between variables (p <.01, V_{Cramer} = .24; SI Fig. 23). Hence the higher percentage of <70° angles in Ansab could be found in a slightly different technique than the other assemblages. Nevertheless, the Chi-Square goodness of fit test shows that the prevalence of 70°-90° is significantly different from casual proportions within each assemblage (p <.01; SI Fig. 23). 70°-90° angles are the majority in each debitage category

Fig. 9. Flakes. 1-3 Cortical Flakes, 4-9 Management Flakes, 10-12 Tablets. 1,4,7,10 Ansab, 2,5,8,12 Românești, 3,6,9,11 Fumane. Photos: J. Gennai. Cortical flakes are shaping the first core convexities, Management flakes intervene later and show partial coverage of laminar negatives, tablets are slicing the core horizontally note the laminar (mostly bladelet) negatives on the flake's platform (main core flaking surface).

Abb. 9. *Abschläge. 1-3 Rindenabschläge, 4-9 Technische Abschläge, 10-12 Kernscheiben. 1,4,7,10 Ansab, 2,5,8,12 Românești, 3,6,9,11 Fumane. Fotos und Skizzen: J. Gennai. Rindenabschläge formen die ersten Kernkonvexitäten, technische Abschläge kommen später hinzu und weisen auf ihrer Dorsalfläche laminare Negative auf, Kernscheiben wurden dem Kern horizontal entnommen, deshalb zeigen sie Reste laminarer Negative auf ihrem Schlagflächenrest und auf dem anliegenden Kernkantenrest.*

of each assemblage, except in Ansab's blades. The Chi-Square independence test reveals a significant association between assemblages and flaking angle in blades, bladelet and flakes with moderate associations between variables (Blades V_{Cramer} = .24; Bladelets V_{Cramer} = .31; Flakes V_{Cramer} = .10; SI Fig. 24). However, the Chi-Square goodness of fit test shows that the prevalence of 70°-90° is statistically significant in each assemblages' category, except for Ansab's blades (SI Fig. 24). It must be noticed that undetermined angles are mostly present in bladelets (A: 27 % R: 37 % F: 34 %; Appendix 3: A).

Bulbs are mostly not marked across the three sites (A: 76 % R: 64 % F: 74 %; Appendix 3: B). The Chi-Square independence test shows a significant association between sites and bulb types with a moderate association ($p < .01$, V_{Cramer} = .11; SI Fig. 25). The Chi-Square goodness of fit test shows that bulbs values are following non-casual proportions within each assemblage ($p < .01$; SI Fig. 25). Not marked bulbs are statistically associated with blades and bladelets in each assemblage (Blade $p > .05$, Bladelet $p > .05$; SI Fig. 26), while flakes are reporting a significant association across sites ($p < .01$; SI Fig. 26). The Chi-Square

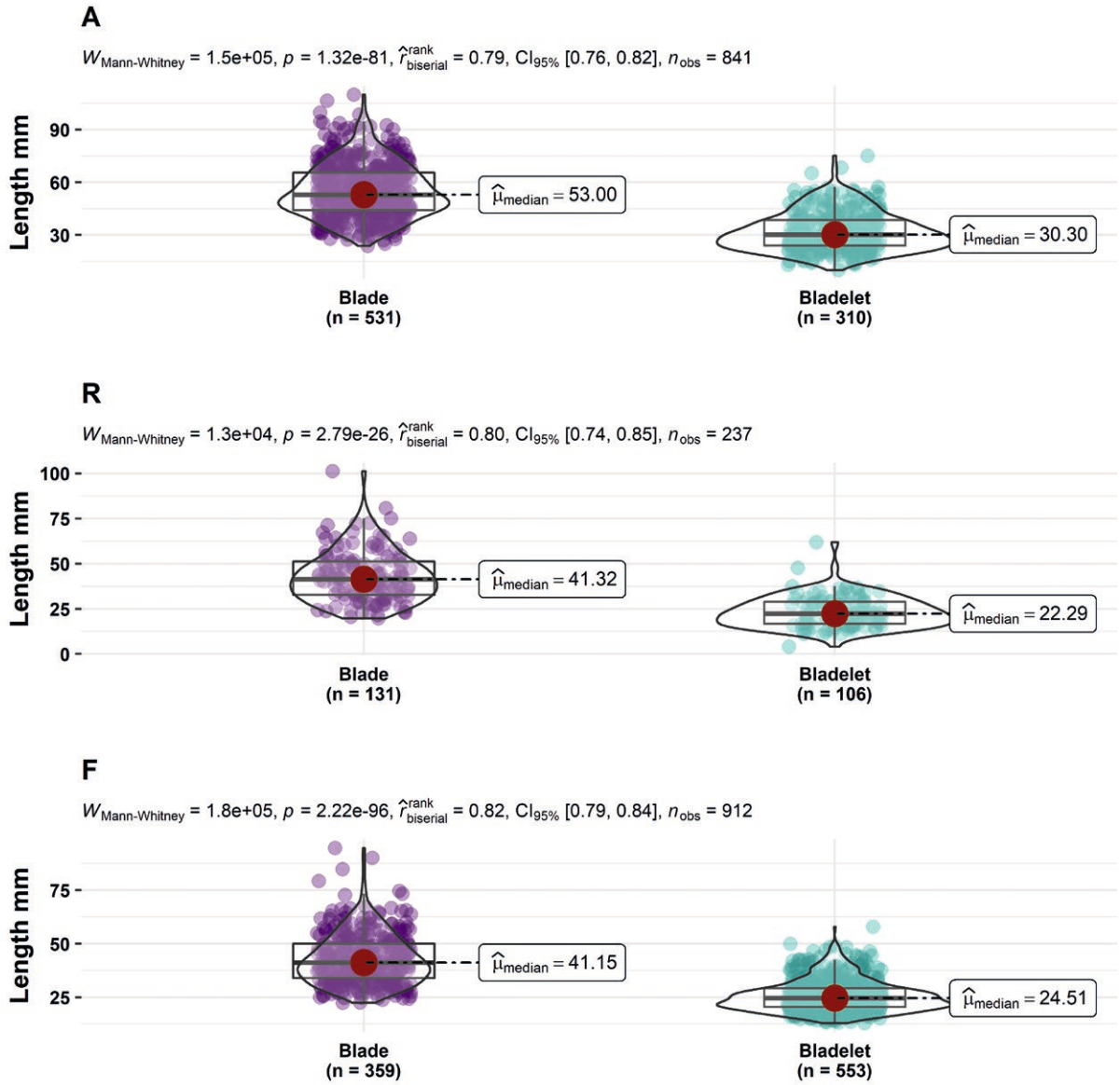

Fig. 10. Mann-Whitney U test of independence of blades and bladelets length.

Abb. 10. *Mann-Whitney-U-Test zur Unabhängigkeit der Länge von Klingen und Lamellen.*

goodness of fit test shows non-casual proportions in Fumane (p <.01; SI Fig. 26) and casual proportions in Ansab and Românești (A: p >.05; R: p >.05; SI Fig. 26). Hence, Fumane flakes are more likely to display a marked bulb.

The overhang removal occurs on most of the laminar blanks (A: 84 % R: 70 % F: 74 %; Appendix 3: C).The Chi-Square independence test reveals a significant association between assemblages and overhang removal in blades and bladelets (p <.01, V_{Cramer} = .14; SI Fig. 27). Nevertheless, the Chi-Square goodness of fit test shows that the proportions of overhang removal are non-casual in each assemblage (p <.01; SI Fig. 27). The distribution of values is similar for blades and bladelets. The higher frequencies of microchipped artefacts in the Ansab assemblage is statistically significant (Chi-Square independence test p <.01; SI Fig. 28), but microchipped artefacts are significantly prevalent in each assemblage (Chi-Square test goodness of fit p <.01; SI Fig. 28)

Non-lipped artefacts are prevalent amongst the three assemblages (A: 59 % R: 63 % F: 61 %; Appendix 3: D). No statistical difference between them is revealed (Chi-Square independence test p >.05; SI Fig. 29). Comparing the single debitage categories, there is a significant association between assemblage and lipping (Chi-Square independence test p <.01; SI Fig. 30). The proportions of values are casual only for Românești's blades (SI Fig. 30). Therefore, flakes and blades are more likely to be lipped, while bladelets are not.

Method attributes

The majority of blanks have either a non-facetted platform (A: 98 % R: 95 % F: 95 %; Appendix 4: A). The Chi-Square independence test between assemblages

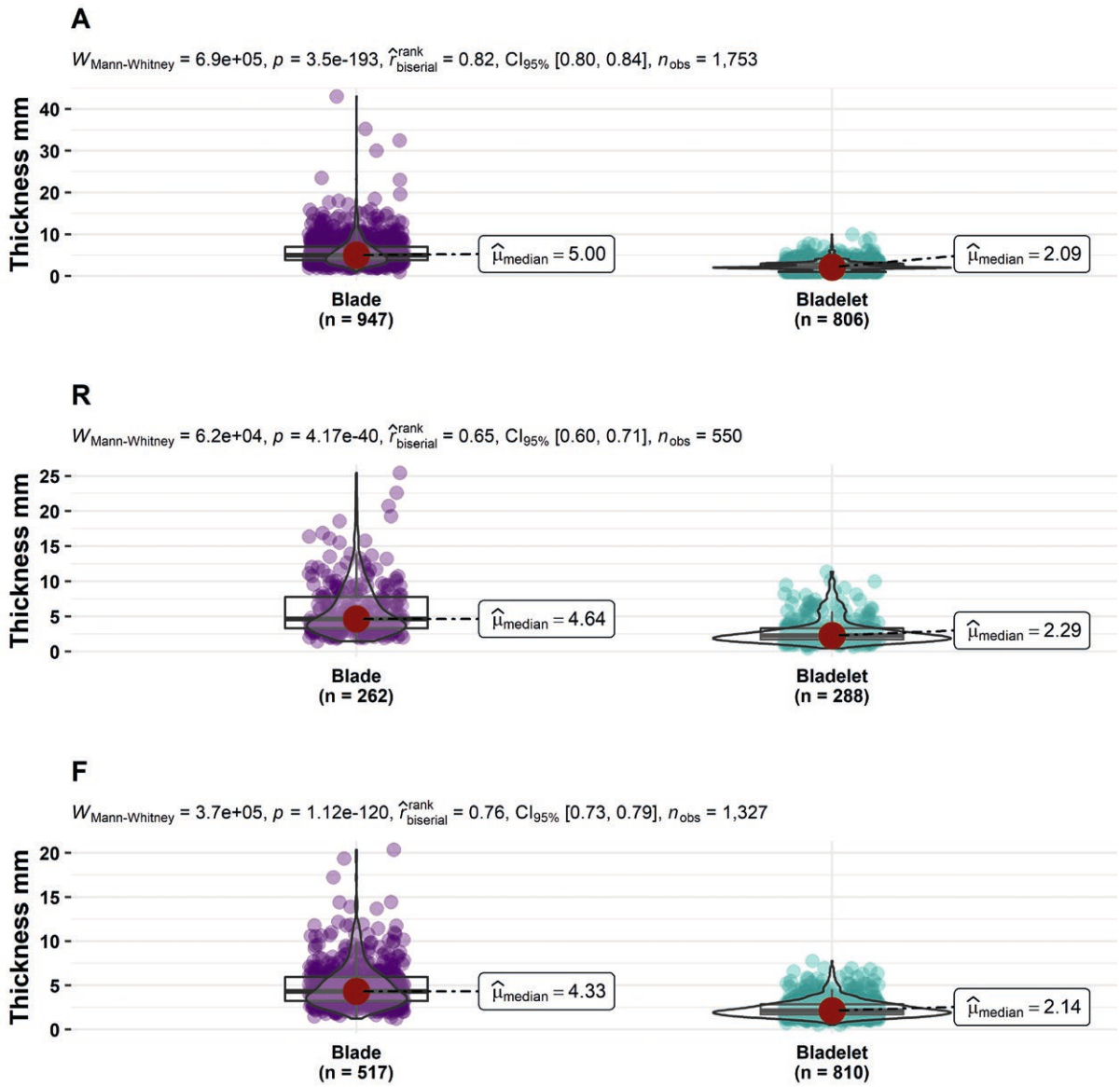

Fig. 11. Mann-Whitney U test of independence of blades and bladelets thickness.

Abb. 11. *Mann-Whitney-U-Test zur Unabhängigkeit der Dicke von Klingen und Lamellen.*

and platform types shows a significant difference and a small association (p <.01, V_{Cramer} = .05; SI Fig. 31). The Chi-Square goodness of fit test shows non-casual proportions of values in each assemblage (p <.01; SI Fig. 30). Most of the facetted platforms across sites are found in flakes (A: 11 % R: 7 % F: 16 %; Appendix 4: A), especially tablets (Fig. 9: 10-12). Bladelets are non-facetted alike across the assemblages (p >.05; SI Fig. 32), while the distribution of platform types are different across assemblages for blades and flakes (p <.01; SI Fig. 32), but equally showing non-casual proportions within each assemblage. Therefore, the prevalence of non-facetted platforms across assemblages is grounded.

Most of the debitage has non-cortical dorsal faces (A: 78 % R: 80 % F: 80 %; Appendix 4: B). Semi-cortical debitage, i.e., with cortex up to 50 % of the dorsal face, is the second most frequent (A: 18 % R: 15 % F: 15 %; Appendix 4: B). Extensively cortical debitage, i.e., with cortex more than 50 % of the dorsal face, and entames, completely covered by cortex, are rarer (Appendix 4: B). The Chi-Square independence test between assemblages and cortex presence shows a significant difference and a small association (p <.01, V_{Cramer} = .04; SI Fig. 33). The Chi-Square goodness of fit test shows non-casual proportions of values in each assemblage (p <.01; SI Fig. 33). Non-cortical artefacts are especially prevalent in bladelets (A: 94 % R: 94 % F: 93 %; Appendix 4: B) and the distribution of values is similar across assemblages (p >.05; SI Fig. 34). Cortical artefacts, especially the semi-cortical ones, are more frequent in blades (A: 26 % R: 17 % F: 24 %; Appendix 4: B) and flakes (A: 31 % R: 18 % F: 25 %; Appendix 4: B). Extensively cortical artefacts and entames are mostly found in flakes (A: combined 16 %; R: combined 10 %; F: combined 21 %; Appendix 4: B).

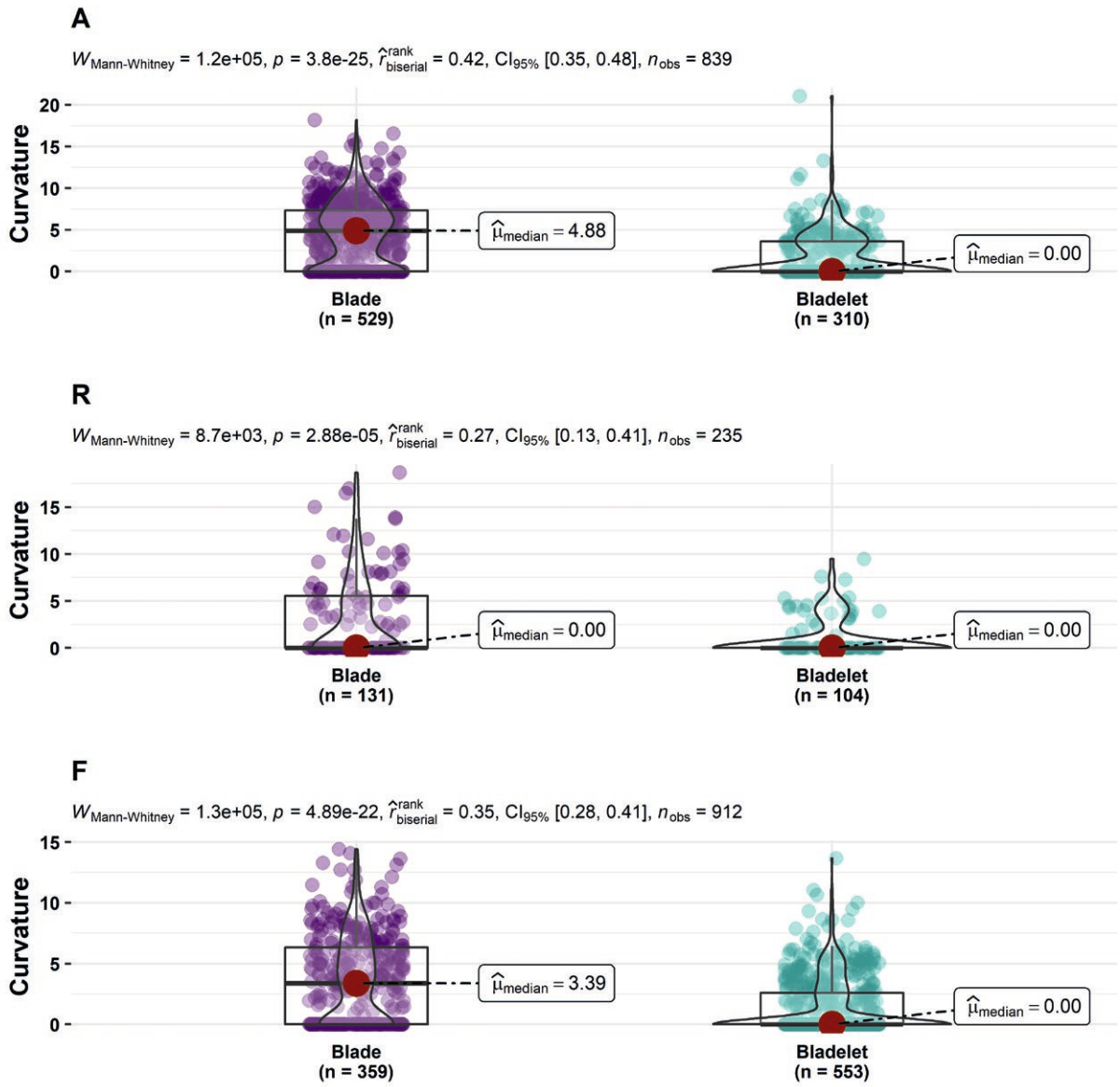

Fig. 12. Mann-Whitney U test of independence of blades and bladelets curvature.

Abb. 12. *Mann-Whitney-U-Test zur Unabhängigkeit der Krümmung von Klingen und Lamellen.*

The Chi-Square independence test between assemblages shows a significant difference and a small association in blades and flakes ($p < .05$, $V_{Cramer} = .04$; $p < .01$, $V_{Cramer} = .15$; SI Fig. 34). The Chi-Square goodness of fit test shows a non-casual values' distribution in each assemblage ($p < .01$; SI Fig. 34). Hence, while most of the debitage in each assemblage is non-cortical, flakes are showing the higher frequencies of cortical pieces and cortex amount, blades are still showing some artefacts bearing some cortex, and bladelets are almost totally devoid of cortex.

The highest frequencies for cortex position is lateral and distal in semi-cortical artefacts and dorsal in extensively cortical artefacts and entames. Cortical blades are associated with lateral and distal positions. The Chi-Square independence test between assemblages shows a significant difference and a small association for cortical positions in blades ($p < .01$, $V_{Cramer} = .14$; SI Fig. 35). The Chi-Squared test of goodness of fit shows a non-casual values' distribution in each assemblage ($p < .01$; SI Fig. 34). Cortical flakes are more associated with a dorsal position. The Chi-Squared test of independence between assemblages shows a significant difference and a small association ($p < .01$, $V_{Cramer} = .14$; SI Fig. 35). The Chi-Square goodness of fit test shows a non-casual distribution in each assemblage ($p < .01$; SI Fig. 35). Therefore, there is a clear difference in cortical positions between debitage categories.

Complete negatives scars comprising bladelets are prevalent in determinate negatives (A: 83 % R: 55 % F: 81 %; Appendix 4: C). The Chi-Square independence test between assemblages shows a significant difference and a small association ($p < .01$, $V_{Cramer} = .18$; SI Fig. 36), while the Chi-Square goodness of fit test shows a non-casual distribution in each

assemblage (p <.01; SI Fig. 36). Excluding bladelets, which are similarly associated with bladelets negatives in each assemblage (p >.05; SI Fig. 37), determined bladelets negatives are recognised in the majority of blades (A: 83 % R: 65 % F: 87 %; Appendix 4: C) and are accounting for nearly a third of the flakes (A: 37 % R: 27 % F: 27 %; Appendix 4: C). The Chi-Square independence test between assemblages shows a significant difference and a small association (p <.01, V_{Cramer} = .13; p <.01, V_{Cramer} = .15; SI Fig. 37), while the Chi-Square goodness of fit test shows a non-casual values' distribution in each assemblage (p <.01; SI Fig. 37). Indeterminate negative scars, that is when the complete width is not preserved, are frequent (A: 29 % R: 40 % F: 35 %; Appendix 4: C). Nevertheless, the picture from the determinate negatives shows that blades and bladelets are integrated into the same reduction, without the precedence of blades over bladelets in the reduction. Instead, flakes intervene more rarely on the main flaking surface where the laminar products are knapped.

Negative scars are largely unidirectional (A: 61 % R: 79 % F: 69 %; Appendix 4: D) or unidirectional and convergent (A: 16 % R: 5 % F: 16 %; Appendix 4: D). The Chi-Square independence test between assemblages shows a significant difference and a small association (p <.01, V_{Cramer} = .15; SI Fig. 38), while the Chi-Square goodness of fit test shows a non-casual distribution in each assemblage (p <.01; SI Fig. 38). Unidirectional scars are prevalent among all debitage classes, unidirectional and convergent scars have higher frequencies in blades and bladelets (Tab 8: D). The Chi-Square independence test between categories in each assemblage shows a significant difference and a small association (p <.01; SI Fig. 39), while the Chi-Square goodness of fit test shows a non-casual distribution in each assemblage (p <.01; SI Fig. 39). Therefore unidirectional knapping is the norm of each assemblage, integrated by additional orientations still coming from the same striking platform.

Morphotechnological attributes

The longitudinal profile, observed in lateral view, is largely straight or slightly curved for bladelets (A: 73 % R: 77 % F: 81 %; Appendix 5: A), and blades (A: 55 % R: 66 % F: 67 %; Appendix 5: A). Twisted profiles are slightly more frequent in blades (A: 26 % R: 24 % F: 16 %; Appendix 5: A) than in bladelets (A: 20 % R: 19 % F: 15 %; Appendix 5: A). Blades (A: 19 % R: 9 % F: 17 %; Appendix 5: A). are displaying more curved profiles than bladelets (A: 4 % R: 2 % F: 4 %; Appendix 5: A). The Chi-Square independence test between assemblages in each category shows a significant difference and a small association (p <.01, p <.05; SI Fig. 40), while the Chi-Square goodness of fit test shows a non-casual distribution in each assemblage (p <.01; SI Fig. 40). Therefore, blades are displaying a higher variety of longitudinal profiles, while bladelets are essentially non-curved.

The silhouette, as observed with the dorsal face in top view, generally has subparallel margins in blades (A: 48 % R: 57 % F: 56 %; Appendix 5: B) and bladelets (A: 33 % R: 54 % F: 49 %; Appendix 5: B). While blades`second most observed value is off-axis (A: 32 % R: 27 % F: 29 %; Appendix 5: B) that of bladelets is convergent (A: 44 % R: 27 % F: 27 %; Appendix 5: B). The Chi-Square independence test between assemblages in each category shows a significant difference and a small association (p <.01; SI Fig. 41), while the Chi-Square goodness of fit test shows a non-casual distribution in each assemblage (p <.01; SI Fig. 41). Hence, bladelets are mostly associated with regular silhouettes.

The cross-section shape in blades is mostly trapezoidal in Ansab and Fumane (A: 61 % F: 58 % Tab. 9: C) while triangular in Românești (44 %; Tab 9: C). Bladelets are mostly triangular in each assemblage (A: 52 % R: 53 % F: 49 %; Appendix 5: C). The Chi-Square independence test between blades in each assemblage shows a significant difference and a small association (p <.01, V_{Cramer} = .10; SI Fig. 42), while bladelets are statistically similar across assemblages (p >.05; SI Fig. 42). The Chi-Square goodness of fit test shows a non-casual values' distribution in most assemblages (p <.01; SI Fig. 42), except for Fumane's bladelets and Românești's blades (p >.05; SI Fig. 42). Hence, with the exclusion of Românești´s blades, triangular cross-sections are mostly associated with bladelets in each assemblage, while trapezoidal ones are associated with blades.

Blades are more asymmetrical (A: 70 % R: 62 % F: 59 %; Appendix 5: D) while bladelets tend to be more symmetrical (A: 50 % R 51 % F: 57 %; Appendix 5: D). The Chi-Square independence test between assemblages in each category shows a significant difference and a small association (p <.01; SI Fig. 43). The Chi-Square goodness of fit test shows a non-casual distribution in most assemblages (p <.01; SI Fig. 42), except for Românești's and Ansab's bladelets (p >.05; SI Fig. 43). Hence, while blades are mostly asymmetrical, bladelets could be either symmetrical or asymmetrical.

Distal terminations are largely feathered for bladelets (A: 77 % R: 74 % F: 71 %; Appendix 5: E), while blades terminations are more variable, with higher frequencies for plunging (A: 39 % R: 25 % F: 44 %; Appendix 5: E) and stepped (A: 10 % R: 19 % F: 7 %; Appendix 5: E). The Chi-Square independence test between assemblages in each category shows a significant difference and a small association (p <.01; SI Fig. 44). The Chi-Square goodness of fit test shows a non-casual distribution in each assemblage (p <.01; SI Fig. 44). Hence, bladelets are more feathered than blades in each assemblage.

Discussion

High similarity among the technologies of the three assemblages

The results are showing that the three assemblages share a comparable knapping concept within the overall technological system. Despite the categorical attributes often showing a significant difference across assemblages, the effect size is most often small,

therefore signalling a weak difference between them. In fact, within the assemblages, the distribution is more often non-casual, hence the prevalence of a certain value (i.e. unidirectional negatives) is grounded, despite not declining in a statistical similar way in each assemblage. This could be explained by the ad hoc nature of chert knapping: each knapping session is rather unique even if a similar mental template is followed. Nevertheless, the analysis protocol proved successful in identifying and substantiating the mental template leading the technological operation in each assemblage.

The technique is consistent with the soft stone hammer tangential direct percussion typical of most of the UP industries (Pelegrin 2011). Flaking angles are steeper and the overhang is more often micro-chipped at Ansab. This could account for the bigger elongation reached in comparison to the other assemblages, despite abandoned cores of the same categories having a similar elongation across assemblages. Bulbs are more marked in flakes; combined with the higher cortical coverage, it might signal a change in technique. Though, experimental analyses show that Pelegrin's observations are difficult to tie to a particular technique in a controlled environment (Roussel et al. 2009). Analyses of cores and blanks consistently revealed that laminar blanks, especially bladelets, were the sought-after product of the reduction process. Flakes were largely a by-product of the knapping stages, like shaping and striking platform preparation. In fact, flakes are outnumbered by blades and bladelets. A comparably higher number of flakes in the Românești assemblage can be linked to the physical properties of the raw material. In contrast to the good quality chert available in the vicinity of the Fumane and Ansab sites, the Banat flint available at Românești is highly prone to internal fractures, due to the original burial environment and to the sealing of these fractures with different materials, characteristic noticeable also at the macroscopic level (Ciornei et al. 2021). This property makes it difficult to extract elongated blanks from the Banat flint.

Nevertheless, cores from this assemblage strongly suggest that producing flakes was not a primary objective in Românești. The high number of ordinary flakes can be related to partial adjustments of the striking platform, an action that was erased when the main core tablet renewed the primary striking platform. These core tablets show flake removals on their dorsal faces, and coarse faceting is recorded in Fumane and was reported in previous studies on the Fumane and Românești sites (Sitlivy et al. 2012; Falcucci et al. 2017; Falcucci & Peresani 2018). Nevertheless, data from the debitage platforms points to the use of non-facetted ones, thus faceting could correspond to local adjustments of the striking platform.

The main divide between cores is the use of a narrow or a wide primary flaking face. A close examination of the diacritical schemes shows that wide flaking surfaces were not sought after *per se*, but they are the sum of adjacent and repeated narrow flaking surfaces. Such behaviour is also described in previous studies and offers a convincing explanation for the development of semi circumferential cores (Falcucci & Peresani 2018). Due to the narrowness of the used flaking surface, bladelets tend to be the most logical blank to knap and they are statistically similar in width across assemblages. Interestingly, this is not a result of decreasing core volume, as posited in pioneering studies about Protoaurignacian and Southern Ahmarian (Bon 2002; Monigal 2003; Goring-Morris & Davidzon 2006), but a goal that was pursued from the very start of the reduction process. In fact, bladelets' negatives are numerous on blades and, partially, flakes. Larger blade negatives can be observed on cores in lateral positions framing central negatives of bladelets. Blades tend to be the major blank produced from the shaping of flaking surfaces, probably because being wider they conveniently produce the desired convexities. A tendency in preferring blades as management blanks is also recorded in other recent assessments of eUP assemblages (Falcucci et al. 2017; Bataille et al. 2018). In the current analysis, this theory is supported by multiple pieces of evidence. Blades, along with flakes, show lateral or distal cortical coverage, which is consistent in their role as debitage products that are struck between the main flaking surface and the untouched, adjacent cortical faces of the core. Blades also show higher frequencies of curved and twisted profiles and are statistically more curved than bladelets. The terminations are often plunging or abrupt, travelling right to the opposite end of the flaking surface. The silhouettes tend to be more off-axis and the cross-sections are more asymmetrical as expected in blanks knapped at the intersection between flanks and flaking surface. In contrast, bladelets generally have completely non-cortical dorsal faces, are struck on-axis, have mostly a symmetrical and triangular cross-section, the silhouettes are convergent or subparallel, the longitudinal profiles are predominantly straight, and they have feathered terminations. This is consistent with features of negative scars observed in "central" locations on cores, exploiting the V-shaped volumes created by blade removals.

Context

The present results are supported by previous analyses. Falcucci and colleagues (2017) have successfully demonstrated that Protoaurignacian technology is not markedly different from the standard Early Aurignacian technology. Indeed, the difference is largely typological. The identifying tool types of the Early Aurignacian are the carinated endscraper and "Aurignacian" blades, the first of which is considered the most definitive because of its regular occurrence. Aurignacian blades have also been recognised in Protoaurignacian assemblages (Falcucci et al. 2017;

Bataille et al. 2018). On the other hand, the carinated endscraper, despite being well described (Bon 2002; Bordes & Tixier 2002; Le Brun-Ricalens 2005b; Chiotti & Cretin 2011), is still a problematic tool type/reduction method to define and shares multiple characteristics with other bladelet cores (Sitlivy et al. 2012; Tafelmaier 2017; Falcucci & Peresani 2018; Aleo et al. 2021). Like in the Early Aurignacian, blades and bladelets pursue different goals within the Protoaurignacian and the Southern Ahmarian too. Bladelets are mostly knapped from central areas of the flaking surfaces and they are transformed into marginally retouched implements, while blades are mostly coming from shaping roles and are being used for "domestic" tools like endscrapers (Davidzon & Goring-Morris 2003; Monigal 2003; Falcucci et al. 2018; Aleo et al. 2021).

The Early Aurignacian seems to be relatively elusive outside of the Aquitaine region (Falcucci et al. 2020). In the Cantabrian-Pyrenees area the transition between the Protoaurignacian and the Early Aurignacian is rather gradual (Cabrera Valdés et al. 2002; Normand & Turq 2005; Santamaría Álvarez 2012; Barshay-Szmidt et al. 2018; Bataille et al. 2018). In La Viña, the biggest difference between the Protoaurignacian (layer XIIIinferior) and the Early Aurignacian (layer XIII) is the increase of transversal carinated bladelet cores at the expenses of non-carinated ones in the latter (Santamaría Álvarez 2012: 1306). On the ground of his analysis and his comparison with Isturitz, Santamaria Álvarez suggests a gradual change as supported by the sequence of Isturitz. In El Castillo's Protoaurignacian (level 16) carinated and non-carinated cores are equally represented and bladelets are three times more frequent than blades (Cabrera Valdés et al. 2002). A recent reassessment of Labeko-Koba did not find a fundamental technological difference between the Early Aurignacian and the Protoaurignacian (Tafelmaier 2017; Bataille et al. 2018). Gatzarria cave supports a gradual change (Barshay-Szmidt et al. 2012). Also, in Isturitz the earliest Early Aurignacian (C4b1 and C4b2) shows many affinities with the lower Protoaurignacian (Barshay-Szmidt et al. 2018; Normand & Turq 2005). In Le Piage, northern Aquitaine, the Protoaurignacian (layer K) is differed from the Early Aurignacian (layer GI) mostly by the higher frequency of retouched bladelets in K (Bordes 2005). Technologically, bladelets in K are dimensionally more compatible with non-carinated cores or burin cores and an intercalated production of blades and bladelets is observed. Nevertheless, carinated cores similar to types found in Early Aurignacian sites are common as well. In Dordogne, the Abri Pataud features a long sequence starting with the Aurignacian (layer 14) and terminating with the Solutrean (layer 1) The Early Aurignacian spans layers 14–9 and it is dated between 41,3–39,6 ka calBP (95.4 % probability modelled start of layer 14) and 38,2–37,0 ka calBP (95.4 % probability modelled start of layer 8; Chiotti 1999; Higham et al. 2011). The most significant occupations, denoted by the higher amount of artefacts, are those of layers 14 and 11 (Chiotti 1999). They are connotated by the production of large blades (20-30 mm of width) and bladelets (mostly 5-12 mm width). Only a few cores are abandoned at a prismatic state and they mostly yielded blades (Chiotti 1999). The carinated end-scrapers are present in most of the layers, though the dimensions of bladelets are mostly compatible with their fronts from layer 8 onwards (Chiotti 1999). In Les Cottés, Vienne region, the researchers can discriminate between a Protoaurignacian (US 04inf.), earlier Early Aurignacian technology (US 04sup.), and a later Early Aurignacian (US 02; Roussel & Soressi 2013). The differences are mostly ascribed to typology (blade retouched implements increase from 04inf. to 02, while bladelets drastically decrease) and to dimensions (bladelets are larger in 04 inf., blades are increasingly larger and more robust in 04sup. and 02). The Early Aurignacian is practically absent in Southern-Eastern France, except La Salpetrière, while the remainder of eUP sites are attributed to the Protoaurignacian, even though most of the time they display an independent bladelet production or a blade-bladelet intercalated production (Slimak et al. 2002; Porraz et al. 2010; Barshay-Szmidt et al. 2020).

In the Italian peninsula, the transition to the Early Aurignacian is marked by higher instances of antler working and more carinated endscrapers in Mochi, but this pattern is not found in the nearby Riparo Bombrini, which instead shows a prolonged occurrence of Protoaurignacian technology (Douka et al. 2012; Tejero & Grimaldi 2015; Riel-Salvatore & Negrino 2018). In Grotta del Fossellone, the Early Aurignacian designation is supported by a large number of carinated endscrapers (Degano et al. 2019). But the Pontinian area of Italy, where Grotta del Fossellone is situated, is famed for its peculiar source of raw material, which occurs in small pebbles, and utilising this resource lead to particular ways of exploitation being adopted throughout the Palaeolithic, eUP included (D'Angelo & Mussi 2005). The other eUP Italian sites which display Protoaurignacian assemblages have been variously dated to before and after the CI and HE4 (Accorsi et al. 1979; Gambassini 1997; Palma di Cesnola 2006; Dini et al. 2012; Falcucci et al. 2020). On the northern side of the Alps, the Early Aurignacian is well recognisable in Geißenklösterle's AH II-III (Teyssandier & Liolios 2003), but only a few kilometres away from the site of Hohle Fels, layer AH IV shows a completely different technological behaviour in the same time frame (Bataille & Conard 2018). In the light of recent discoveries, the attribution of Willendorf II's AH 3 to the Early Aurignacian, based largely on a disassociated production of blades and bladelets, is rather tenuous (Nigst et al. 2014).

Protoaurignacian links are claimed for most of the Eastern and Balkan Europe (Sitlivy et al. 2012; Tsanova et al. 2012; Bataille 2016; Dinnis et al. 2019). Even if Kostenki 17/II is not classified as Protoaurignacian, the technological behaviour represented in its lithic

assemblage is not comparable to the Early Aurignacian (Bataille et al. 2020; Dinnis et al. 2020). A similarity between the Southern Ahmarian and the Protoaurignacian has long been claimed (Teyssandier et al. 2010; Kadowaki et al. 2015). At present, however, no other comprehensive technological comparison has been carried out to assess this. Here we show that the assemblages attributed to the Southern Ahmarian and the Protoaurignacian are technologically similar. Furthermore, existing literature shows that narrow fronted cores are not a reduction method peculiar to the Southern Ahmarian, as other European assemblages also show such a reduction approach done either *sur tranche* or on narrow faces (Slimak et al. 2002; Normand & Turq 2005; Ortega Cobos et al. 2005; Porraz et al. 2010; Santamaría Álvarez 2012; Sitlivy et al. 2014). The laterally twisted blades (debordant Hussain 2015) are similar to the lateral 'comma-like' blades described by some authors (Monigal 2003; Falcucci et al. 2017).

The significance of an updated lithic technology framework for the understanding of human dispersal

Abandoning the existing taxonomical picture may have a profound impact on how we consider the eUP and the dispersal of *Homo sapiens* into Europe. It has been argued that the division between Protoaurignacian and Early Aurignacian is only slight, largely linked to local adaptive expressions of a common technological package, namely the Aurignacian (Bataille et al. 2018). Recent reanalysis of the youngest Aurignacian unit in Fumane has shown a pattern of slow change rooted in the previous technology of units A2-A1, and because of this, the Protoaurignacian is seen as a flexible adaptive technological set (Falcucci et al. 2020). The continuative Protoaurignacian technology into the HE4 shown by other Italian sites may be explained by the isolation formed by the Alps during colder and drier conditions (Shao et al. 2021).

The results of this analysis further stress the similarity between eUP assemblages attributed to different technocomplexes. An example of such technological similarity over thousands of kilometres and several millennia is offered by the IUP of Eastern Asia: here the similarities in blade technology are linked to a demic expansion of populations (Zwyns 2021). The Protoaurignacian, the Early Aurignacian and the Southern Ahmarian start at roughly the same time of 43–42 ka (Barshay-Szmidt et al. 2018; Boaretto et al. 2021), so it is not completely fanciful to suggest that a successful technological package would withstand the different environments and the millennia, especially if we assume a low but constant sharing of information. It has been established that networks in eUP could be hundreds of kilometres long (e.g. Normand et al. 2008; Grimaldi et al. 2014; Peresani et al. 2019; Vaissié et al. 2021). A certain degree of connectivity between the Levant and Europe is also hypothesised for the development of the Levantine Aurignacian at the end of the eUP, though caution should be used (Goring-Morris & Belfer-Cohen 2006). Ornaments or symbolic objects are probably better indicators for arguing more precise divisions within the populations (Bataille et al. 2018). Nevertheless, pioneering work on Aurignacian ornaments shows a level of connectivity between the macrosets of sites (Vanhaeren & d'Errico 2006).

Conclusions

Following this analysis, involving a comparison of published assemblages and recent reassessments, it can be argued that eUP coincides with a homogeneous technical phenomenon, contrary to previous taxonomical classifications. The analysis showed that bladelets are a primary technological goal and that they are obtained from narrow faces of the core. Blades, on the other hand, are chiefly the product of installing or renewing the convexities of the core flaking surface. The dynamics of technological dispersal still need to be fully understood, especially given the lower density of sites in Southeastern Europe and the total absence to date of eUP sites in Anatolia. Despite this, a recent model confirms the likelihood that fluvial and coastal corridors acted as major routes for movement into Europe during the eUP (Shao et al. 2021). Following the results obtained from IUP dispersal models (Hublin et al. 2020; Zwyns 2021) it is conceivable that a technical tradition could disperse and survive through space and time. The present analysis is a first attempt to bridge different technocomplexes using a technological approach devoid of preconceptions that may otherwise bias the interpretations. In the wake of a recent revive of the taxonomical debate (Reynolds & Riede 2019b, 2019a; Riede et al. 2020), new data – and most important shared data – are pivotal to understand technological and cultural variability in the Palaeolithic, and, in particular, in the early Upper Palaeolithic.

Funding: J.G.'s Ph.D. research and research at Al-Ansab 1 and Românești-Dumbrăviță I was funded by the Deutsche Forschungsgemeinschaft (DFG, German Research Foundation) – Projektnummer 57444011 – SFB 806. Research at Fumane is coordinated by the Ferrara University (M.P.) and the project is supported by several bodies including the Italian Ministry of Culture—Veneto Archaeological Superintendence, by public institutions (the Lessinia Mountain Community—Regional Natural Park, Fumane Municipality, BIMAdige), the Leakey Foundation (spring 2015 round), and private associations and companies.

Acknowledgements: We thank all the team members that have excavated, recorded, and organised the assemblages. J.G. is particularly grateful to Prof. Marco Peresani and Dr. Armando Falcucci for granting access to the Grotta di Fumane material and to Dr. Adrian Doboș and Dr. Alexandru Ciornei for their valuable assistance. Thanks to Yinika Perston for helping improve the English manuscript. We thank the three anonymous reviewers that helped improve the paper.

Contributor roles: Jacopo Gennai: Methodology, Investigation, Conceptualisation, Writing-Original Draft, Writing-Review and Editing, Visualisation. Marco Peresani: Resources, Conceptualisation, Writing-Original Draft, Writing-Review and Editing, Visualisation. Jürgen Richter: Funding Acquisition, Resources, Supervision, Methodology, Conceptualisation, Writing-Original Draft, Writing-Review and Editing, Visualisation.

	Pre		Pl Edges		Semi Tour		N Fronted		sur Tranche		Trans. Carinated		Frag		Others		ND		Total	
	N	%	N	%	N	%	N	%	N	%	N	%	N	%	N	%	N	%		
A) Overhang																				
A																				
Yes	5	71	11	100	33	97	40	98	12	75	5	100	2	40	3	60	-	-	111	89
No	2	29			1	3	1	2	4	25			3	60	2	40	1	100	14	11
Total	7	100	11	100	34	100	41	100	16	100	5	100	5	100	5	100	1	100	125	100
R																				
Yes	-	-	-	-	4	80	-	-	4	50	-	-	-	-	1	100	-	-	9	50
No	3	100	-	-	1	20	-	-	4	50	-	-	1	100	-	-	-	-	9	50
Total	3	100	-	-	5	100	-	-	8	100	-	-	1	100	1	100	-	-	18	100
F																				
Yes	2	25	11	92	25	100	14	88	7	50	6	100	-	-	2	22	-	-	67	74
No	6	75	1	8			2	13	7	50	-	-	-	-	7	78	-	-	23	26
Total	8	100	12	100	25	100	16	100	14	100	6	100	-	-	9	100	-	-	90	100
B) Flaking Angle																				
A																				
<70°	2	29	9	82	28	82	34	83	9	56	4	80	1	20	5	100	-	-	92	74
70°-90°	3	43	2	18	3	9	7	17	6	38	1	20	1	20	-	-	-	-	23	18
ND	1	14	-	-	3	9	-	-	1	6	-	-	3	60	-	-	1	100	9	7
>90°	1	14	-	-	-	-	-	-	-	-	-	-	-	-	-	-	-	-	1	1
Total	7	100	11	100	34	100	41	100	16	100	5	100	5	100	5	100	1	100	125	100
R																				
70°-90°	2	67	-	-	1	20	-	-	5	63	-	-	-	-	1	100	-	-	9	50
<70°	1	33	-	-	3	60	-	-	3	38	-	-	1	100	-	-	-	-	8	44
ND	-	-	-	-	1	20	-	-	-	-	-	-	-	-	-	-	-	-	1	6
Total	3	100	-	-	5	100	-	-	8	100	-	-	1	100	1	100	-	-	18	100
F																				
70°-90°	4	50	3	25	12	48	9	56	9	64	4	67	-	-	6	67	-	-	47	52
<70°	2	25	8	67	13	52	7	44	4	29	2	33	-	-	2	22	-	-	38	42
>90°	2	25	-	-	-	-	-	-	1	7	-	-	-	-	-	-	-	-	3	3
ND	-	-	1	8	-	-	-	-	-	-	-	-	-	-	1	11	-	-	2	2
Total	8	100	12	100	25	100	16	100	14	100	6	100	-	-	9	100	-	-	90	100
C) Core Blank																				
A																				
Indeterminate	1	14	4	36	19	56	19	46	5	31	2	40	4	80	3	60	-	-	57	46
Cobble	1	14	3	27	9	26	11	27	-	-	-	-	1	20	-	-	1	100	26	21
Nodule	2	29	3	27	3	9	7	17	1	6	1	20	-	-	1	20	-	-	18	14
Blank	3	43	-	-	-	-	1	2	8	50	2	40	-	-	1	20	-	-	15	12
Squared Chunk	-	-	1	9	3	9	2	5	-	-	-	-	-	-	-	-	-	-	6	5
Slab	-	-	-	-	-	-	1	2	2	13	-	-	-	-	-	-	-	-	3	2
Total	7	100	11	100	34	100	41	100	16	100	5	100	5	100	5	100	1	100	125	100
R																				
Blank	-	-	-	-	1	20	-	-	5	63	-	-	-	-	1	100	-	-	7	39
Nodule	2	67	-	-	3	60	-	-	-	-	-	-	-	-	-	-	-	-	5	28
Squared Chunk	1	33	-	-	-	-	-	-	1	13	-	-	-	-	-	-	-	-	2	11
Slab	-	-	-	-	-	-	-	-	2	25	-	-	-	-	-	-	-	-	2	11
Indeterminate	-	-	-	-	-	-	-	-	-	-	-	-	1	100	-	-	-	-	1	6
Cobble	-	-	-	-	1	20	-	-	-	-	-	-	-	-	-	-	-	-	1	6
Total	3	100	-	-	5	100	-	-	8	100	-	-	1	100	1	100	-	-	18	100
F																				
Indeterminate	-	-	10	83	13	52	7	44	2	14	-	-	-	-	3	33	-	-	35	39
Cobble	2	25	1	8	10	40	4	25	-	-	1	17	-	-	4	44	-	-	22	24

Appendix 1. Cores Attributes. Sites A: Ansab, R: Românești, F: Fumane. Pre: Pre-Core, Semi Tour: semi tournant, N Fronted: Narrow Fronted, sur Tranche: Narrow Fronted sur Tranche, Trans. Carinated: Transversal Carinated, Frag: Fragment.

Appendix 1. *Merkmale der Kerne. Fundstellen A: Ansab, R: Românești, F: Fumane. Legende Pre: Pre-Core, Semi Tour: semi tournant, N Fronted: Narrow Fronted, sur Tranche: Narrow Fronted sur Tranche, Trans. Carinated: Transversal Carinated, Frag: Fragment.*

	Pre		Pl Edges		Semi Tour		N Fronted		sur Tranche		Trans. Carinated		Frag		Others		ND		Total	
	N	%	N	%	N	%	N	%	N	%	N	%	N	%	N	%	N	%		
Blank	-	-	-	-	-	-	1	6	11	79	3	50	-	-	1	11	-	-	16	18
Squared Chunk	1	13	-	-	-	-	2	13	-	-	2	33	-	-	1	11	-	-	6	7
Slab	4	50	-	-	1	4	-	-	1	7	-	-	-	-	-	-	-	-	6	7
Nodule	1	13	1	8	1	4	2	13	-	-	-	-	-	-	-	-	-	-	5	6
Total	8	100	12	100	25	100	16	100	14	100	6	100	-	-	9	100	-	-	90	100
D) Striking platform																				
A																				
Non-Facetted	7	100	11	100	34	100	41	100	16	100	5	100	3	60	5	100	1	100	123	98
Plain	7	100	11	100	33	97	38	93	16	100	5	100	3	100	5	100	1	100	119	97
Natural	-	-	-	-	1	3	3	7	-	-	-	-	-	-	-	-	-	-	4	3
ND	-	-	-	-	-	-	-	-	-	-	-	-	2	40	-	-	-	-	2	2
Total	7	100	11	100	34	100	41	100	16	100	5	100	5	100	5	100	1	100	125	100
R																				
Non-Facetted	3	100	-	-	5	100	-	-	8	100	-	-	1	100	1	100	-	-	18	100
Plain	3	100	-	-	5	100	-	-	6	75	-	-	1	100	1	100	-	-	16	89
Natural	-	-	-	-	-	-	-	-	2	25	-	-	-	-	-	-	-	-	2	11
Total	3	100	-	-	5	100	-	-	8	100	-	-	1	100	1	100	-	-	18	100
F																				
Non-Facetted	7	88	10	83	23	92	14	88	14	100	6	100	-	-	4	44	-	-	78	87
Plain	7	100	10	100	23	100	14	100	13	93	5	83	-	-	4	100	-	-	76	97
Natural	-	-	-	-	-	-	-	-	1	7	1	17	-	-	-	-	-	-	2	3
Facetted	1	13	1	8	2	8	2	13	-	-	-	-	-	-	5	56	-	-	11	12
ND	-	-	1	8	-	-	-	-	-	-	-	-	-	-	-	-	-	-	1	1
Total	8	100	12	100	25	100	16	100	14	100	6	100	-	-	9	100	-	-	90	100
E) Cortex																				
A																				
No Cortex	2	29	-	-	12	35	10	24	7	44	4	80	4	80	2	40	-	-	41	33
Back	-	-	3	27	10	29	10	24	-	-	-	-	-	-	1	20	-	-	24	19
Lateral	2	29	4	36	1	3	5	12	3	19	-	-	1	20	1	20	-	-	17	14
Back+Lateral	-	-	1	9	3	9	6	15	2	13	-	-	-	-	-	-	-	-	12	10
Back+Base	-	-	2	18	5	15	4	10	1	6	-	-	-	-	-	-	-	-	12	10
Base	1	14	1	9	2	6	5	12	1	6	-	-	-	-	1	20	-	-	11	9
Lateral Variants	1	14	-	-	1	3	1	2	1	6	-	-	-	-	-	-	1	100	5	4
Dorsal	-	-	-	-	-	-	-	-	1	6	1	20	-	-	-	-	-	-	2	2
Base and Frontal	1	14	-	-	-	-	-	-	-	-	-	-	-	-	-	-	-	-	1	1
Total	7	100	11	100	34	100	41	100	16	100	5	100	5	100	5	100	1	100	125	100
R																				
No Cortex	1	33	-	-	2	40	-	-	4	50	-	-	1	100	1	100	-	-	9	50
Lateral	-	-	-	-	-	-	-	-	3	38	-	-	-	-	-	-	-	-	3	17
Back	1	33	-	-	-	-	-	-	1	13	-	-	-	-	-	-	-	-	2	11
Frontal	-	-	-	-	1	20	-	-	-	-	-	-	-	-	-	-	-	-	1	6
Top	1	33	-	-	-	-	-	-	-	-	-	-	-	-	-	-	-	-	1	6
Back+Base	-	-	-	-	1	20	-	-	-	-	-	-	-	-	-	-	-	-	1	6
Back+Lateral	-	-	-	-	1	20	-	-	-	-	-	-	-	-	-	-	-	-	1	6
Total	3	100	-	-	5	100	-	-	8	100	-	-	1	100	1	100	-	-	18	100
F																				
No Cortex	-	-	5	42	8	32	7	44	13	93	3	50	-	-	4	44	-	-	40	44
Back	1	13	5	42	10	40	4	25	-	-	1	17	-	-	1	11	-	-	22	24
Lateral	4	50	1	8	2	8	4	25	-	-	1	17	-	-	-	-	-	-	12	13
Base	1	13	1	8	1	4	1	6	-	-	1	17	-	-	4	44	-	-	9	10
Back+Lateral	1	13	-	-	3	12	-	-	-	-	-	-	-	-	-	-	-	-	4	4

Appendix 1. Cores Attributes. Sites A: Ansab, R: Romăneşti, F: Fumane. Pre: Pre-Core, Semi Tour: semi tournant, N Fronted: Narrow Fronted, sur Tranche: Narrow Fronted sur Tranche, Trans. Carinated: Transversal Carinated, Frag: Fragment. (continued)

Appendix 1. *Merkmale der Kerne. Fundstellen A: Ansab, R: Romănești, F: Fumane. Legende Pre: Pre-Core, Semi Tour: semi tournant, N Fronted: Narrow Fronted, sur Tranche: Narrow Fronted sur Tranche, Trans. Carinated: Transversal Carinated, Frag: Fragment. (Fortsetzung)*

	Pre		Pl Edges		Semi Tour		N Fronted		sur Tranche		Trans. Carinated		Frag		Others		ND		Total	
	N	%	N	%	N	%	N	%	N	%	N	%	N	%	N	%	N	%		
Lateral Variants	1	13	-	-	-	-	-	-	1	7	-	-	-	-	-	-	-	-	2	2
Back+Base	-	-	-	-	1	4	-	-	-	-	-	-	-	-	-	-	-	-	1	1
Total	8	100	12	100	25	100	16	100	14	100	6	100	-	-	9	100	-	-	90	100
F) STRIKING PLATFORM																				
numbers and relation																				
A																				
Single	6	86	9	82	29	85	36	88	16	100	4	80	3	75	4	80	1	100	108	87
Multiple Platforms	1	14	2	18	5	15	5	12	-	-	1	20	1	25	1	20	-	-	16	13
Opposed	1	100	1	50	3	60	1	20	-	-	-	-	1	100	-	-	-	-	7	44
Independent	-	-	1	50	1	20	2	40	-	-	-	-	-	-	1	100	-	-	5	31
Adjacent	-	-	-	-	-	-	1	20	-	-	1	100	-	-	-	-	-	-	2	13
Orthogonal auxiliary	-	-	-	-	1	20	-	-	-	-	-	-	-	-	-	-	-	-	1	6
Opposed auxiliary	-	-	-	-	-	-	1	20	-	-	-	-	-	-	-	-	-	-	1	6
Total	7	100	11	100	34	100	41	100	16	100	5	100	5	100	5	100	1	100	125	100
R																				
Single	2	67	-	-	3	60	-	-	6	75	-	-	1	100	1	100	-	-	13	72
Multiple Platforms	1	33	-	-	2	40	-	-	2	25	-	-	-	-	-	-	-	-	5	28
Opposed	-	-	-	-	1	50	-	-	1	50	-	-	-	-	-	-	-	-	2	40
Opposed auxiliary	-	-	-	-	-	-	-	-	1	50	-	-	-	-	-	-	-	-	1	20
Adjacent	-	-	-	-	1	50	-	-	-	-	-	-	-	-	-	-	-	-	1	20
Independent	1	100	-	-	-	-	-	-	-	-	-	-	-	-	-	-	-	-	1	20
Total	3	100	-	-	5	100	-	-	8	100	-	-	1	100	1	100	-	-	18	100
F																				
Single	7	88	10	83	19	76	13	81	9	64	5	83	-	-	5	56	-	-	68	76
Multiple Platforms	1	13	2	17	6	24	3	19	5	36	1	17	-	-	4	44	-	-	22	24
Opposed	-	-	2	100	3	50	2	67	1	20	-	-	-	-	-	-	-	-	8	36
Adjacent	-	-	-	-	1	17	-	-	3	60	-	-	-	-	3	75	-	-	7	32
Independent	-	-	-	-	1	17	1	33	1	20	1	100	-	-	1	25	-	-	5	23
Opposed auxiliary	1	100	-	-	1	17	-	-	-	-	-	-	-	-	-	-	-	-	2	9
Total	8	100	12	100	25	100	16	100	14	100	6	100	-	-	9	100	-	-	90	100
G) Flaking surface																				
numbers and relation																				
A																				
Single Surface	6	86	10	91	33	97	37	90	16	100	4	80	5	100	4	80	1	100	116	93
Multiple	1	14	1	9	1	3	4	10	-	-	1	20	-	-	1	20	-	-	9	7
Independent	1	100	-	-	-	-	2	50	-	-	1	100	-	-	-	-	-	-	4	44
Adjacent-Orthogonal	-	-	-	-	1	100	1	25	-	-	-	-	-	-	1	100	-	-	3	33
Orthogonal	-	-	-	-	-	-	1	25	-	-	-	-	-	-	-	-	-	-	1	11
Opposed	-	-	1	100	-	-	-	-	-	-	-	-	-	-	-	-	-	-	1	11
Total	7	100	11	100	34	100	41	100	16	100	5	100	5	100	5	100	1	100	125	100
R																				
Single Surface	2	67	-	-	3	60	-	-	7	88	-	-	1	100	-	-	-	-	13	72
Multiple	1	33	-	-	2	40	-	-	1	13	-	-	-	-	1	100	-	-	5	28
Adjacent-Orthogonal	-	-	-	-	-	-	-	-	1	100	-	-	-	-	1	100	-	-	2	40
Independent	1	100	-	-	1	50	-	-	-	-	-	-	-	-	-	-	-	-	2	40
Subsequent	-	-	-	-	1	50	-	-	-	-	-	-	-	-	-	-	-	-	1	20
Total	3	100	-	-	5	100	-	-	8	100	-	-	1	100	1	100	-	-	18	100
F																				
Single Surface	8	100	12	100	20	80	13	81	9	64	5	83	-	-	5	56	-	-	72	80
Multiple	-	-	-	-	5	20	3	19	5	36	1	17	-	-	4	44	-	-	18	20
Adjacent-Orthogonal	-	-	-	-	2	40	1	33	3	60	-	-	-	-	3	75	-	-	9	50

Appendix 1. Cores Attributes. Sites A: Ansab, R: Românești, F: Fumane. Pre: Pre-Core, Semi Tour: semi tournant, N Fronted: Narrow Fronted, sur Tranche: Narrow Fronted sur Tranche, Trans. Carinated: Transversal Carinated, Frag: Fragment. (continued)

Appendix 1. *Merkmale der Kerne. Fundstellen A: Ansab, R: Românești, F: Fumane. Legende Pre: Pre-Core, Semi Tour: semi tournant, N Fronted: Narrow Fronted, sur Tranche: Narrow Fronted sur Tranche, Trans. Carinated: Transversal Carinated, Frag: Fragment. (Fortsetzung)*

	Pre		Pl Edges		Semi Tour		N Fronted		sur Tranche		Trans. Carinated		Frag		Others		ND		Total	
	N	%	N	%	N	%	N	%	N	%	N	%	N	%	N	%	N	%		
Independent	-	-	-	-	1	20	1	33	1	20	1	100	-	-	1	25	-	-	5	28
Opposed	-	-	-	-	2	40	1	33	1	20	-		-	-	-	-	-	-	4	22
Total	8	100	12	100	25	100	16	100	14	100	6	100	-	-	9	100	-	-	90	100
H) Negatives types																				
A																				
Determinate																				
With Bladelets																				
Blades & Bladelets	2	100	4	44	14	47	18	53	8	57	1	50	1	33	-	-	-	-	48	51
Bladelets	-	-	3	33	12	40	14	41	6	43	1	50	2	67	-	-	-	-	38	40
Blades & Bladelets & Flakes	-	-	-	-	3	10	2	6	-	-	-	-	-	-	-	-	-	-	5	5
Bladelets & Flakes	-	-	2	22	1	3	-	-	-	-	-	-	-	-	1	100	-	-	4	4
Blades	1	17	2	18	3	9	7	17	1	6	1	20	1	20	1	20	1	100	18	15
Flakes	2	33	-	-	-	-	-	-	-	-	1	20	1	20	3	60	-	-	7	6
Blades & Flakes	1	17	-	-	1	3	-	-	1	6	1	20	-	-	-	-	-	-	4	3
no negatives	1	14	-	-	-	-	-	-	-	-	-	-	-	-	-	-	-	-	1	1
Total	7	100	11	100	34	100	41	100	16	100	5	100	5	100	5	100	1	100	125	100
R																				
Determinate																				
With Bladelets																				
Bladelets	1	100	-	-	1	20	-	-	5	71	-	-	-	-	-	-	-	-	7	47
Blades & Bladelets	-	-	-	-	4	80	-	-	2	29	-	-	1	100	-	-	-	-	7	47
Blades & Bladelets & Flakes	-	-	-	-	-	-	-	-	-	-	-	-	-	-	1	100	-	-	1	7
Blades	1	50	-	-	-	-	-	-	-	-	-	-	-	-	-	-	-	-	1	6
Indeterminate	-	-	-	-	-	-	-	-	1	13	-	-	-	-	-	-	-	-	1	6
no negatives	1	33	-	-	-	-	-	-	-	-	-	-	-	-	-	-	-	-	1	6
Total	3	100	-	-	5	100	-	-	8	100	-	-	1	100	1	100	-	-	18	100
F																				
Determinate																				
With Bladelets																				
Bladelets	-	-	5	50	13	52	8	53	12	92	5	83	-	-	-	-	-	-	43	62
Blades & Bladelets	-	-	5	50	11	44	7	47	1	8	-	-	-	-	-	-	-	-	24	35
Blades & Bladelets & Flakes	-	-	-	-	-	-	-	-	-	-	1	17	-	-	-	-	-	-	1	1
Bladelets & Flakes	-	-	-	-	1	4	-	-	-	-	-	-	-	-	-	-	-	-	1	1
Flakes	3	43	1	8	-	-	-	-	-	-	-	-	-	-	9	100	-	-	13	15
Blades	1	14	1	8	-	-	1	6	1	7	-	-	-	-	-	-	-	-	4	4
Blades & Flakes	3	43	-	-	-	-	-	-	-	-	-	-	-	-	-	-	-	-	3	3
no negatives	1	13	-	-	-	-	-	-	-	-	-	-	-	-	-	-	-	-	1	1
Total	8	100	12	100	25	100	16	100	14	100	6	100	-	-	9	100	-	-	90	100
I) Negatives Orientation																				
A																				
Unidirectional	5	71	10	91	25	74	28	68	11	69	4	80	3	60	4	80	1	100	91	73
Unidirectional+Convergent	1	14	-	-	6	18	12	29	3	19	1	20	-	-	1	20	-	-	24	19
Bidirectional	-	-	1	9	2	6	-	-	2	13	-	-	1	20	-	-	-	-	6	5
Unidirectional Variants	-	-	-	-	1	3	1	2	-	-	-	-	-	-	-	-	-	-	2	2
Convergent	-	-	-	-	-	-	-	-	-	-	-	-	1	20	-	-	-	-	1	1
no negatives	1	14	-	-	-	-	-	-	-	-	-	-	-	-	-	-	-	-	1	1
Total	7	100	11	100	34	100	41	100	16	100	5	100	5	100	5	100	1	100	125	100
R																				
Unidirectional	2	67	-	-	3	60	-	-	8	100	-	-	1	100	-	-	-	-	14	78
Unidirectional+Convergent	-	-	-	-	1	20	-	-	-	-	-	-	-	-	-	-	-	-	1	6
Convergent	-	-	-	-	-	-	-	-	-	-	-	-	-	-	1	100	-	-	1	6

Appendix 1. Cores Attributes. Sites A: Ansab, R: Românești, F: Fumane. Pre: Pre-Core, Semi Tour: semi tournant, N Fronted: Narrow Fronted, sur Tranche: Narrow Fronted sur Tranche, Trans. Carinated: Transversal Carinated, Frag: Fragment. (continued)

Appendix 1. *Merkmale der Kerne. Fundstellen A: Ansab, R: Românești, F: Fumane. Legende Pre: Pre-Core, Semi Tour: semi tournant, N Fronted: Narrow Fronted, sur Tranche: Narrow Fronted sur Tranche, Trans. Carinated: Transversal Carinated, Frag: Fragment. (Fortsetzung)*

	Pre		Pl Edges		Semi Tour		N Fronted		sur Tranche		Trans. Carinated		Frag		Others		ND		Total
	N	%	N	%	N	%	N	%	N	%	N	%	N	%	N	%	N	%	
Bidirectional	-	-	-	-	1	20	-	-	-	-	-	-	-	-	-	-	-	-	1	6
no negatives	1	33	-	-	-	-	-	-	-	-	-	-	-	-	-	-	-	-	1	6
Total	3	100	-	-	5	100	-	-	8	100	-	-	1	100	1	100	-	-	18	100
F																				
Unidirectional	5	63	7	58	12	48	11	69	12	86	3	50	-	-	4	44	-	-	54	60
Unidirectional+Convergent	-	-	3	25	9	36	2	13	-	-	3	50	-	-	-	-	-	-	17	19
Bidirectional	1	13	2	17	3	12	2	13	2	14	-	-	-	-	-	-	-	-	10	11
Unidirectional Variants	1	13	-	-	1	4	1	6	-	-	-	-	-	-	2	22	-	-	5	6
Centripetal	-	-	-	-	-	-	-	-	-	-	-	-	-	-	3	33	-	-	3	3
no negatives	1	13	-	-	-	-	-	-	-	-	-	-	-	-	-	-	-	-	1	1
Total	8	100	12	100	25	100	16	100	14	100	6	100	-	-	9	100	-	-	90	100

Appendix 1. Cores Attributes. Sites A: Ansab, R: Românești, F: Fumane. Pre: Pre-Core, Semi Tour: semi tournant, N Fronted: Narrow Fronted, sur Tranche: Narrow Fronted sur Tranche, Trans. Carinated: Transversal Carinated, Frag: Fragment. (continued)

Appendix 1. *Merkmale der Kerne. Fundstellen A: Ansab, R: Românești, F: Fumane. Legende Pre: Pre-Core, Semi Tour: semi tournant, N Fronted: Narrow Fronted, sur Tranche: Narrow Fronted sur Tranche, Trans. Carinated: Transversal Carinated, Frag: Fragment. (Fortsetzung)*

	Blade				Bladelet				Blade and Bladelet				Flake				LCN Deb	LCN Core
	O	M	Sp	T	O	M	Sp	T	O	M	Sp	T	S	M	T	I		
Length																		
A																		
count	186	344	-	1	248	57	6	-	434	401	6	1	26	151	47	45	226	60
min	23.7	25.0	-	65.0	10.0	18.0	29.0	-	10.0	18.0	29.0	65.0	20.2	20.0	19.2	21.7	9.0	13.0
IQ	38.4	46.9	-	65.0	22.7	30.0	33.1	-	26.8	44.0	33.1	65.0	31.8	38.7	40.6	35.6	20.0	22.1
median	48.0	57.0	-	65.0	28.4	37.0	38.3	-	35.6	53.0	38.3	65.0	38.7	44.4	53.6	41.8	26.6	31.2
IIIQ	58.4	68.0	-	65.0	36.6	44.5	47.6	-	48.3	66.6	47.6	65.0	43.8	51.5	65.5	55.0	37.0	38.5
max	99.8	109.9	-	65.0	75.1	68.3	51.7	-	99.8	109.9	51.7	65.0	61.9	85.0	108.0	114.5	73.0	73.0
R																		
count	48	80	1	2	71	19	11	5	119	99	12	7	128	226	62	65	50	9
min	19.8	20.5	54.5	49.6	10.3	13.4	16.9	4.0	10.3	13.4	16.9	4.0	8.9	8.8	13.8	13.4	7.0	12.3
IQ	30.0	33.0	54.5	53.5	15.7	20.4	23.6	26.8	18.4	30.0	23.8	30.4	14.6	21.2	26.2	28.7	18.2	22.5
median	39.2	43.0	54.5	57.4	20.0	27.5	28.0	34.0	25.0	37.4	28.7	35.3	18.5	29.3	35.1	42.1	20.8	27.4
IIIQ	47.1	51.9	54.5	61.3	24.8	31.2	34.8	35.3	36.8	50.8	35.3	42.8	27.0	38.3	44.8	53.9	28.7	34.6
max	67.7	101.1	54.5	65.2	36.9	61.8	47.7	36.1	67.7	101.1	54.5	65.2	54.3	76.5	62.9	71.6	51.8	55.1
F																		
count	138	221	-	-	443	95	15	-	581	316	15	-	8	106	68	57	11	55
min	23.8	22.4	-	-	12.8	15.2	19.2	-	12.8	15.2	19.2	-	20.5	13.5	15.7	20.1	19.4	10.3
IQ	31.7	36.1	-	-	19.9	24.9	21.8	-	21.1	30.8	21.8	-	28.8	31.2	25.5	33.5	21.3	18.5
median	37.7	43.2	-	-	23.2	29.2	26.7	-	26.0	38.9	26.7	-	30.7	36.1	31.0	41.1	25.3	22.9
IIIQ	45.0	52.5	-	-	28.0	35.3	28.6	-	33.4	48.7	28.6	-	36.1	41.5	36.0	47.2	29.5	30.6
max	74.5	94.7	-	-	49.9	57.9	37.8	-	74.5	94.7	37.8	-	56.4	74.0	80.9	83.6	42.9	48.1
Width																		
A																		
count	442	505	-	1	691	108	10	-	1133	613	10	1	30	162	49	52	941	125
min	12.0	12.0	-	35.0	3.0	5.1	2.9	-	3.0	5.1	2.9	35.0	19.8	17.0	8.4	21.9	2.0	3.0
IQ	13.2	15.7	-	35.0	7.0	8.2	4.3	-	8.0	13.0	4.3	35.0	28.6	27.2	29.2	32.7	4.9	7.2
median	15.0	19.5	-	35.0	8.7	9.3	5.6	-	10.6	18.0	5.6	35.0	32.2	33.2	35.5	40.4	6.2	9.7
IIIQ	18.3	24.7	-	35.0	10.0	10.9	7.1	-	14.0	23.2	7.1	35.0	38.7	40.0	48.7	50.7	8.5	15.1
max	30.4	49.9	-	35.0	12.0	12.0	9.1	-	30.4	49.9	9.1	35.0	58.0	72.4	86.1	79.0	30.0	44.2
R																		
count	127	132	1	2	197	57	29	5	324	189	30	7	139	267	67	71	248	18
min	12.0	12.1	14.6	16.3	2.7	5.7	2.6	7.8	2.7	5.7	2.6	7.8	7.3	8.7	11.6	12.8	2.4	5.0
IQ	13.3	15.3	14.6	21.4	6.5	8.2	4.4	8.8	8.1	11.4	4.4	9.4	14.6	18.9	27.4	28.8	5.5	6.0
median	15.6	18.5	14.6	26.5	8.6	9.7	5.0	10.0	10.8	16.0	5.0	10.2	19.3	25.7	35.2	40.5	7.4	7.7
IIIQ	19.7	23.1	14.6	31.6	10.3	10.9	6.2	10.2	14.1	20.5	6.6	13.4	25.7	34.1	43.2	52.3	12.0	11.1
max	34.2	46.8	14.6	36.7	12.0	11.9	10.2	10.4	34.2	46.8	14.6	36.7	68.4	86.0	95.9	80.1	31.5	16.2
F																		
count	241	276	-	-	665	129	17	-	906	405	17	-	9	111	69	59	707	90
min	12.0	12.0	-	-	3.1	5.4	2.5	-	3.1	5.4	2.5	-	14.6	14.6	13.4	17.2	2.0	3.6
IQ	12.9	14.5	-	-	7.1	8.2	3.4	-	7.6	11.0	3.4	-	25.1	24.3	24.5	28.2	4.4	6.2
median	14.4	17.2	-	-	8.5	9.5	5.1	-	9.7	14.6	5.1	-	28.7	28.5	29.7	34.0	5.5	8.6
IIIQ	16.6	21.3	-	-	10.2	10.7	5.6	-	12.2	19.2	5.6	-	41.6	34.4	33.5	46.2	7.4	11.2
max	28.6	34.6	-	-	12.0	11.9	6.3	-	28.6	34.6	6.3	-	44.3	73.8	52.4	87.2	22.7	29.6
Thickness																		
A																		
count	442	505	-	1	691	108	10	-	1133	613	10	1	30	162	49	52	-	-
min	1.0	2.0	-	11.0	1.0	1.0	2.0	-	1.0	1.0	2.0	11.0	2.8	3.0	3.2	2.9	-	-
IQ	3.0	4.9	-	11.0	1.8	2.9	3.5	-	2.0	4.0	3.5	11.0	4.0	5.3	8.0	7.1	-	-
median	4.0	6.2	-	11.0	2.0	3.0	5.4	-	3.0	5.8	5.4	11.0	5.5	7.0	12.2	9.3	-	-
IIIQ	5.1	8.3	-	11.0	3.0	4.3	6.0	-	3.9	7.9	6.0	11.0	9.3	9.6	15.0	14.8	-	-

Appendix 2. Summary of metrical values. Sites A= Ansab, R= Românești, F= Fumane. O=Ordinary, M= Management, T=Tablet, Sp=Spall, I=Initialisation.

Appendix 2. *Zusammenfassung der Abmessungen der Debitage. Fundstellen A= Ansab, R= Românești, F= Fumane. O=Ordinary, M= Management, T=Tablet, Sp=Spall, I=Initialisation.*

	Blade				Bladelet				Blade and Bladelet				Flake				LCN Deb	LCN Core
	O	M	Sp	T	O	M	Sp	T	O	M	Sp	T	S	M	T	I		
max	11.3	43.0		11.0	6.1	10.0	8.3		11.3	43.0	8.3	11.0	15.8	36.2	30.0	31.3		
R																		
count	127	132	1	2	197	57	29	5	324	189	30	7	139	267	67	71	-	-
min	1.5	1.9	16.1	12.6	0.4	1.7	2.9	3.8	0.4	1.7	2.9	3.8	1.2	1.6	2.2	3.3	-	-
IQ	2.8	4.5	16.1	14.3	1.5	2.3	4.2	5.8	1.7	3.2	4.3	5.8	2.5	3.7	4.7	7.4	-	-
median	3.7	6.7	16.1	15.9	1.9	3.1	6.0	5.8	2.4	5.3	6.1	6.6	3.9	5.4	7.5	10.5	-	-
IIIQ	4.7	9.5	16.1	17.6	2.5	4.5	7.1	6.6	3.5	8.6	7.3	9.7	5.4	8.3	9.1	14.2	-	-
max	11.7	25.4	16.1	19.3	6.4	11.4	10.1	6.7	11.7	25.4	16.1	19.3	19.9	30.4	23.2	31.0	-	-
F																		
count	241	276	-	-	665	129	17	-	906	405	17	-	9	111	69	59	-	-
min	1.2	1.9	-	-	0.5	1.2	1.2	-	0.5	1.2	1.2	-	2.6	1.8	2.4	3.9	-	-
IQ	2.7	4.2	-	-	1.6	2.5	2.7	-	1.8	3.3	2.7	-	4.4	5.0	4.0	7.6	-	-
median	3.6	5.7	-	-	2.0	3.2	3.1	-	2.3	4.8	3.1	-	8.0	6.5	5.4	10.1	-	-
IIIQ	4.2	7.4	-	-	2.6	4.4	3.4	-	3.1	6.5	3.4	-	9.6	8.9	6.9	12.7	-	-
max	8.1	20.4	-	-	4.8	7.8	5.9	-	8.1	20.4	5.9	-	15.5	20.5	16.1	24.3	-	-
Elongation																		
A																		
count	186	344	-	1	248	57	6	-	434	401	6	1	26	151	47	45	226	60
min	1.6	1.4	-	1.9	1.9	2.1	4.2	-	1.6	1.4	4.2	1.9	0.6	0.4	0.7	0.5	1.3	0.9
IQ	2.5	2.2	-	1.9	2.8	3.4	5.3	-	2.6	2.3	5.3	1.9	0.9	1.1	0.9	0.9	3.7	2.3
median	2.9	2.7	-	1.9	3.3	4.0	7.0	-	3.2	2.8	7.0	1.9	1.1	1.4	1.4	1.2	4.5	3.0
IIIQ	3.5	3.3	-	1.9	4.1	4.8	10.0	-	3.8	3.6	10.0	1.9	1.3	1.6	1.9	1.4	5.4	4.2
max	6.1	5.5	-	1.9	7.1	6.5	11.1	-	7.1	6.5	11.1	1.9	1.6	2.3	6.3	2.0	9.5	7.0
R																		
count	48	80	1	2	71	19	11	5	119	99	12	7	128	62	65	226	50	9
min	0.7	1.4	3.7	1.8	1.5	1.5	3.9	0.5	0.7	1.4	3.7	0.5	0.4	0.4	0.5	0.5	0.7	1.9
IQ	1.9	1.8	3.7	2.1	2.3	2.1	4.5	2.6	2.0	1.8	4.1	2.2	0.8	0.8	0.8	0.9	1.4	2.8
median	2.2	2.1	3.7	2.4	2.6	2.4	6.6	3.5	2.5	2.2	5.9	3.1	1.0	1.0	1.0	1.2	2.7	3.4
IIIQ	2.8	2.5	3.7	2.7	3.0	3.4	7.5	3.6	2.9	2.7	7.3	3.5	1.2	1.2	1.3	1.4	3.8	3.8
max	3.7	3.4	3.7	3.1	5.5	5.5	8.0	4.4	5.5	5.5	8.0	4.4	2.5	2.8	2.1	2.2	5.8	6.1
F																		
count	138	221	-	-	443	95	15	-	581	316	15	-	8	106	68	57	11	55
min	1.4	1.5	-	-	1.7	2.0	3.3	-	1.4	1.5	3.3	-	0.7	0.4	0.6	0.5	1.0	0.7
IQ	2.2	2.0	-	-	2.5	2.7	3.9	-	2.4	2.1	3.9	-	0.8	1.1	0.9	1.0	2.4	2.1
median	2.5	2.4	-	-	2.8	3.1	5.9	-	2.8	2.7	5.9	-	1.3	1.3	1.1	1.2	3.2	2.8
IIIQ	2.9	2.9	-	-	3.5	3.8	8.1	-	3.4	3.1	8.1	-	1.4	1.5	1.2	1.4	3.9	3.6
max	4.4	6.1	-	-	6.9	7.0	12.0	-	6.9	7.0	12.0	-	1.5	2.3	1.9	2.0	5.6	7.4
Curvature																		
A																		
count	186	344	-	-	248	57	6	-	434	401	6	-	-	-	-	-	-	-
min	0.0	0.0	-	-	0.0	0.0	0.0	-	0.0	0.0	0.0	-	-	-	-	-	-	-
IQ	0.0	3.3	-	-	0.0	1.2	0.0	-	0.0	2.7	0.0	-	-	-	-	-	-	-
median	1.2	6.3	-	-	0.0	3.9	0.0	-	0.0	6.0	0.0	-	-	-	-	-	-	-
IIIQ	4.0	8.5	-	-	2.9	5.4	0.0	-	3.3	8.3	0.0	-	-	-	-	-	-	-
max	9.4	18.2	-	-	11.1	21.1	0.1	-	11.1	21.1	0.1	-	-	-	-	-	-	-
R																		
count	48	80	1	-	71	19	11	-	119	99	12	-	-	-	-	-	-	-
min	0.0	0.0	0.0	-	0.0	0.0	0.0	-	0.0	0.0	0.0	-	-	-	-	-	-	-
IQ	0.0	0.0	0.0	-	0.0	0.0	0.0	-	0.0	0.0	0.0	-	-	-	-	-	-	-
median	0.0	2.7	0.0	-	0.0	0.0	0.0	-	0.0	2.5	0.0	-	-	-	-	-	-	-
IIIQ	3.3	7.0	0.0	-	0.0	4.3	0.0	-	1.4	6.1	0.0	-	-	-	-	-	-	-

Appendix 2. Summary of metrical values. Sites A= Ansab, R= Românești, F= Fumane. O=Ordinary, M= Management, T=Tablet, Sp=Spall, I=Initialisation. (continued)

Appendix 2. *Zusammenfassung der Abmessungen der Debitage. Fundstellen A= Ansab, R= Românești, F= Fumane. O=Ordinary, M= Management, T=Tablet, Sp=Spall, I=Initialisation. (Fortsetzung)*

	Blade				Bladelet				Blade and Bladelet				Flake				LCN Deb	LCN Core
	O	M	Sp	T	O	M	Sp	T	O	M	Sp	T	S	M	T	I		
max	16.5	18.7	0.0		9.5	5.4	7.6		16.5	18.7	7.6							
F																		
count	138	221	-	-	443	95	15	-	581	316	15	-	-	-	-	-	-	-
min	0.0	0.0	-	-	0.0	0.0	0.0	-	0.0	0.0	0.0	-	-	-	-	-	-	-
IQ	0.0	2.2	-	-	0.0	0.0	0.0	-	0.0	0.0	0.0	-	-	-	-	-	-	-
median	0.0	5.0	-	-	0.0	4.0	0.0	-	0.0	4.6	0.0	-	-	-	-	-	-	-
IIIQ	2.6	7.8	-	-	1.6	5.4	0.6	-	1.9	6.9	0.6	-	-	-	-	-	-	-
max	8.0	14.4	-	-	11.0	13.7	6.3	-	11.0	14.4	6.3	-	-	-	-	-	-	-

Appendix 2. Summary of metrical values. Sites A= Ansab, R= Românești, F= Fumane. O=Ordinary, M= Management, T=Tablet, Sp=Spall, I=Initialisation. (continued)

Appendix 2. *Zusammenfassung der Abmessungen der Debitage. Fundstellen A= Ansab, R= Românești, F= Fumane. O=Ordinary, M= Management, T=Tablet, Sp=Spall, I=Initialisation. (Fortsetzung)*

	Blade		Bladelet		Flake		Total	
	N	%	N	%	N	%	N	%
A) Flaking Angle*								
A								
Determined								
70°-90°	29	48	262	60	139	58	680	54
<70°	307	52	172	40	97	41	576	46
>90°	-	0	-	0	3	1	3	0
ND	94	14	162	27	33	12	289	19
Total	680	100	596	100	272	100	1548	100
R								
Determined								
70°-90°	107	59	79	69	271	64	457	63
<70°	74	41	35	31	142	33	251	35
>90°	1	1	-	0	12	3	13	2
ND	23	11	68	37	80	16	171	19
Total	205	100	182	100	505	100	892	100
F								
Determined								
70°-90°	276	75	384	89	159	73	819	80
<70°	92	25	47	11	58	26	197	19
>90°	-	0	-	0	2	1	2	0
ND	66	15	224	34	24	10	314	24
Total	434	100	655	100	243	100	1332	100
B) Bulbs**								
A								
Not Marked								
Diffuse	535	99	496	92	122	100	1153	96
Not perceived	6	1	41	8	-	0	47	4
Marked								
Pronounced	113	73	53	82	115	77	281	76
Bulbar scar	41	27	12	18	35	23	88	24
ND	11	2	9	1	10	4	30	2
Crushed	4	1	3	0	-	0	7	0
Total	710	100	614	100	282	100	1606	100
R								
Not Marked								
Diffuse	158	99	166	99	233	100	557	99
Not perceived	2	1	2	1	-	0	4	1
Marked								
Pronounced	36	92	11	85	248	95	295	94
Bulbar scar	3	8	2	15	13	5	18	6
ND	10	5	7	4	27	5	44	5
Crushed	5	2	5	3	5	1	15	2
Total	214	100	193	100	526	100	933	100

Appendix 3. Technical attributes debitage. Sites A= Ansab, R= Românești, F= Fumane.* Complete and prox+mes without crushed platforms ** Complete and Prox+Mes *** Complete and prox+Mes without crushed platforms and crushed bulbs.

Appendix 3. *Technische Attribute der Debitage. Fundstellen A= Ansab, R= Românești, F= Fumane.* Vollständig und Prox+Mes ohne gebrochene Plattformen ** Vollständig und Prox+Mes *** Vollständig und Prox+Mes ohne gebrochene Plattformen und gebrochene Bulben.*

	Blade		Bladelet		Flake		Total	
	N	%	N	%	N	%	N	%
F								
Not Marked								
Diffuse	305	95	530	90	68	100	903	92
Not perceived	15	5	62	10	-	0	77	8
Marked								
Pronounced	100	85	52	88	136	80	288	83
Bulbar scar	18	15	7	12	35	20	60	17
Crushed	13	3	26	4	4	2	43	3
ND	7	2	12	2	4	2	23	2
Total	458	100	689	100	247	100	1394	100
C) Overhang Removal*								
A								
Yes	590	87	484	81	-	-	1074	84
No	89	13	112	19	-	-	201	16
Total	679	100	596	100	-	-	1275	100
R								
Yes	144	70	124	69	-	-	268	70
No	61	30	56	31	-	-	117	30
Total	205	100	180	13	-	-	385	100
F								
Yes	317	73	485	74	-	-	802	74
No	117	27	170	26	-	-	287	26
Total	434	100	655	100	-	-	1089	100
D) Lipping ***								
A								
No	296	44	500	84	114	42	910	59
Yes	383	56	94	16	158	58	635	41
Total	679	100	594	100	272	100	1545	100
R								
No	112	55	122	68	324	64	558	63
Yes	90	45	57	32	179	36	326	37
Total	202	100	179	100	503	100	884	100
F								
No	179	42	528	82	99	41	806	61
Yes	249	58	116	18	143	59	508	39
Total	428	100	644	100	242	100	1314	100

Appendix 3. Technical attributes debitage. Sites A= Ansab, R= Românești, F= Fumane.* Complete and prox+mes without crushed platforms ** Complete and Prox+Mes *** Complete and prox+Mes without crushed platforms and crushed bulbs. (continued)

Appendix 3. *Technische Attribute der Debitage. Fundstellen A= Ansab, R= Românești, F= Fumane.* Vollständig und Prox+Mes ohne gebrochene Plattformen ** Vollständig und Prox+Mes *** Vollständig und Prox+Mes ohne gebrochene Plattformen und gebrochene Bulben. (Fortsetzung)*

	Blade		Bladelet		Flake		Total	
	N	%	N	%	N	%	N	%
A) Platforms**								
A								
Determined								
Non Facetted	670	100	582	100	229	89	1481	98
Linear	303	45	281	48	55	24	639	43
Plain	234	35	119	20	145	63	498	34
Punctiform	121	18	178	31	12	5	311	21
Natural	10	1	4	1	17	7	31	2
Concave	2	<1	-	-	-	-	2	<1
Facetted	2	<1	-	-	29	11	31	2
Facetted	-	-	-	-	20	69	20	65
Dihedral	2	100	-	-	9	31	11	35
Non Determined								
Crushed	30	79	18	56	10	42	58	62
ND	8	21	14	44	14	58	36	38
Total	710	100	614	100	282	100	1606	100
R								
Determined								
Non Facetted	195	98	172	99	448	93	815	95
Plain	112	57	62	36	294	66	468	57
Linear	40	21	64	37	54	12	158	19
Punctiform	29	15	43	25	57	13	129	16
Natural	14	7	3	2	43	10	60	7
Facetted	4	2	1	1	36	7	41	5
Facetted	2	50	-	-	23	64	25	61
Dihedral	2	50	1	100	13	36	16	39
Non Determined								
Crushed	9	60	11	55	21	50	41	53
ND	6	40	9	45	21	50	36	47
Total	214	100	193	100	526	100	933	100
F								
Determined								
Non Facetted	406	95	643	99	198	84	1247	95
Linear	180	44	360	56	35	18	575	46
Plain	151	37	107	17	126	64	384	31
Punctiform	73	18	171	27	20	10	264	21
Natural	2	<1	5	1	17	9	24	2
Facetted	20	5	4	1	38	16	62	5
Facetted	19	95	3	75	34	89	56	90
Dihedral	1	100	1	100	4	100	6	100
Non Determined								
Crushed	24	75	34	81	4	36	62	73
ND	8	25	8	19	7	64	23	27
Total	458	100	689	100	247	100	1394	100
B) Cortex ****								
A								
Non Cortical	674	71	764	94	156	53	1594	78
<50%	243	26	40	5	91	31	374	18
Lateral	124	51	22	55	42	46	188	50
Distal	84	35	14	35	19	21	117	31
Dorsal	27	11	2	5	21	23	50	13
Proximal	8	3	1	3	8	9	17	5
Lateral Variants	-	-	-	-	1	1	1	<1
Proximal+Distal	-	-	1	3	-	-	1	<1

Appendix 4. Method attributes debitage. Sites A= Ansab, R= Românești, F= Fumane.** Complete and Prox+Mes **** Complete and Semi-complete artefacts.

Appendix 4. *Methodenattribute der Debitage. Fundstelle A= Ansab, R= Românești, F= Fumane.** Vollständige und Prox+Mes **** Vollständige und halbvollständige Artefakte.*

	Blade		Bladelet		Flake		Total	
	N	%	N	%	N	%	N	%
>50%	23	2	5	1	23	8	51	2
Dorsal	15	65	5	100	22	96	42	82
Lateral	8	35	-	-	-	-	8	16
Distal	-	-	-	-	1	4	1	2
100%	8	1	-	-	23	8	31	2
Dorsal	7	88	-	-	23	100	30	97
Distal	1	13	-	-	-	-	1	3
Total	948	100	809	100	293	100	2050	100
R								
Non Cortical	212	81	272	94	390	72	874	80
<50%	45	17	14	5	100	18	159	15
Lateral	20	44	3	21	23	23	46	29
Distal	12	27	6	43	22	22	40	25
Dorsal	4	9	4	29	28	28	36	23
Proximal	6	13	1	7	25	25	32	20
Lateral Variants	1	2	-	-	1	1	2	1
Proximal+Distal	2	4	-	-			2	1
ND	-	-	-	-	1	1	1	1
>50%	5	2	2	1	37	7	44	4
Dorsal	4	80	2	100	36	97	42	95
Lateral Variants	-	-	-	-	1	3	1	2
Lateral	1	20	-	-	-	-	1	2
100%	-	-	-	-	17	3	17	2
Dorsal	-	-	-	-	17	100	17	100
Total	262	100	288	100	544	100	1094	100
F								
Non Cortical	377	73	753	93	133	54	1263	80
<50%	122	24	49	6	62	25	233	15
Lateral	54	44	24	49	17	27	95	41
Distal	44	36	17	35	10	16	71	30
Dorsal	13	11	6	12	20	32	39	17
Proximal	4	3	2	4	12	19	18	8
Lateral Variants	7	6	-	-	3	5	10	4
>50%	11	2	9	1	23	9	43	3
Dorsal	7	64	7	78	23	100	37	86
Lateral	2	18	1	11	-	-	3	7
Distal	2	18	1	11	-	-	3	7
100%	7	1	-	-	30	12	37	2
Dorsal	6	86	-	-	30	100	36	97
Distal	1	14	-	-	-	-	1	3
Total	517	100	811	100	248	100	1576	100
C) Negatives type****								
A								
Determinate								
With Bladelets	602	83	471	99	61	37	1134	83
Bladelets	425	71	461	98	28	46	914	81
Blades & Bladelets	144	24	7	1	18	30	169	15
Bladelets & Flakes	24	4	3	1	10	16	37	3
Blades & Bladelets & Flakes	9	1	-	-	5	8	14	1
Blades	76	11	3	1	29	17	108	8
Flakes	30	4	3	1	68	41	101	7
Blades & Flakes	13	2	-	-	8	5	21	2
ND	211	22	293	36	85	29	589	29
No negatives	16	2	39	5	42	14	97	5
Total	948	100	809	100	293	100	2050	100

Appendix 4. Method attributes debitage. Sites A= Ansab, R= Românești, F= Fumane.** Complete and Prox+Mes **** Complete and Semi-complete artefacts. (continued)

Appendix 4. *Methodenattribute der Debitage. Fundstelle A= Ansab, R= Românești, F= Fumane.** Vollständige und Prox+Mes **** Vollständige und halbvollständige Artefakte. (Fortsetzung)*

	Blade		Bladelet		Flake		Total	
	N	%	N	%	N	%	N	%
R								
ND	117	45	153	53	173	32	443	40
Determinate								
With Bladelets	83	65	84	95	46	27	213	55
Bladelets	66	80	82	98	26	57	174	82
Blades & Bladelets	16	19	2	2	7	15	25	12
Bladelets & Flakes	1	1	-	-	11	24	12	6
Blades & Bladelets & Flakes	-	-	-	-	2	4	2	1
Flakes	7	5	3	3	100	58	110	28
Blades	36	28	1	1	12	7	49	13
Blades & Flakes	2	2			13	8	15	4
No negatives	17	6	47	16	200	37	264	24
Total	262	100	288	100	544	100	1094	100
F								
Determinate								
With Bladelets	313	87	394	98	44	27	751	81
Bladelets	255	81	386	98	15	34	656	87
Blades & Bladelets	50	16	2	1	3	7	55	7
Bladelets & Flakes	8	3	6	2	23	52	37	5
Blades & Bladelets & Flakes	-	-	-	-	3	7	3	<1
Flakes	16	4	6	1	105	64	127	14
Blades	26	7	-	-	9	5	35	4
Blades & Flakes	3	1	1	<1	6	4	10	1
ND	141	27	380	47	32	13	553	35
No negatives	18	3	30	4	52	21	100	6
Total	517	100	811	100	248	100	1576	100
D) Negatives Orientation****								
A								
Determinate								
Unidirectional	587	63	461	60	143	57	1191	61
Unidirectional+Convergent	110	12	188	24	7	3	305	16
Convergent	78	8	73	9	11	4	162	8
Unidirectional Variant	66	7	25	3	20	8	111	6
Crossed	31	3	14	2	26	10	71	4
Orthogonal	17	2	1	<1	32	13	50	3
Bidirectional	32	3	7	1	9	4	48	2
Bidirectional variant	6	1	1	<1	2	1	9	<1
Convergent+Orthogonal	3	<1	-	-	-	-	3	<1
Crossed+Orthogonal	1	<1	-	-	-	-	1	<1
No negatives	16	2	39	5	42	14	97	5
ND	1	<1	-	-	1	<1	2	<1
Total	948	100	809	100	293	100	2050	100

Appendix 4. Method attributes debitage. Sites A= Ansab, R= Romăneşti, F= Fumane.** Complete and Prox+Mes **** Complete and Semi-complete artefacts. (continued)

Appendix 4. *Methodenattribute der Debitage. Fundstelle A= Ansab, R= Romăneşti, F= Fumane.** Vollständige und Prox+Mes **** Vollständige und halbvollständige Artefakte. (Fortsetzung)*

	Blade		Bladelet		Flake		Total	
	N	%	N	%	N	%	N	%
R								
Determinate								
Unidirectional	206	84	208	87	241	70	655	79
Crossed	7	3	1	<1	34	10	42	5
Unidirectional Variant	3	1	1	<1	31	9	35	4
Unidirectional+Convergent	12	5	18	8	1	<1	31	4
Orthogonal	4	2	3	1	17	5	24	3
Bidirectional	5	2	3	1	11	3	19	2
Convergent	6	2	6	3	3	1	15	2
Crossed+Orthogonal	-	-	-	-	3	1	3	<1
Bidirectional variant	-	-	-	-	1	<1	1	<1
Convergent+Orthogonal	1	<1	-	-	-	-	1	<1
No negatives	17	6	47	16	200	37	264	24
ND	1	<1	1	<1	2	<1	4	<1
Total	262	100	288	100	544	100	1094	100
F								
Determinate								
Unidirectional	332	67	560	72	121	62	1013	69
Unidirectional+Convergent	92	18	146	19	5	3	243	16
Unidirectional Variant	31	6	21	3	24	12	76	5
Crossed	16	3	18	2	24	12	58	4
Orthogonal	11	2	7	1	11	6	29	2
Convergent	5	1	23	3	-	-	28	2
Bidirectional	10	2	5	1	8	4	23	2
Bidirectional variant	1	<1	-	-	2	1	3	<1
Convergent+Orthogonal	1	<1	-	-	-	-	1	<1
Crossed+Orthogonal	-	-	-	-	1	1	1	<1
No negatives	18	3	30	4	52	21	100	6
ND	-	-	1	<1	-	-	1	<1
Total	517	100	811	100	248	100	1576	100

Appendix 4. Method attributes debitage. Sites A= Ansab, R= Românești, F= Fumane.** Complete and Prox+Mes **** Complete and Semi-complete artefacts. (continued)

Appendix 4. *Methodenattribute der Debitage. Fundstelle A= Ansab, R= Românești, F= Fumane.** Vollständige und Prox+Mes **** Vollständige und halbvollständige Artefakte. (Fortsetzung)*

	Blade		Bladelet		Total	
	N	%	N	%	N	%
A) Profile****						
A						
Straight and slightly curved	521	55	589	73	1110	63
Straight	355	68	453	77	808	73
Slightly Curved	166	32	136	23	302	27
Twisted	243	26	164	20	407	23
Curved and very curved	176	19	33	4	209	12
Curved	139	79	31	94	170	81
Very Curved	37	21	2	6	39	19
ND	7	1	23	3	30	2
Total	947	100	809	100	1756	100
R						
Straight and slightly curved	173	66	221	77	394	72
Straight	148	86	202	91	350	89
Slightly Curved	25	14	19	9	44	11
Twisted	63	24	55	19	118	22
Curved and very curved	23	9	6	2	29	5
Curved	16	70	5	83	21	72
Very Curved	7	30	1	17	8	28
ND	3	1	4	1	7	1
Total	262	100	286	100	548	100
F						
Straight and slightly curved	346	67	655	81	1001	75
Straight	252	73	548	84	800	80
Slightly Curved	94	27	107	16	201	20
Twisted	83	16	124	15	207	16
Curved and very curved	87	17	32	4	119	9
Curved	68	78	23	72	91	76
Very Curved	19	22	9	28	28	24
ND	1	<1	-	-	1	<1
Total	517	100	811	100	1328	100
B) Silhouette *****						
A						
(sub) Parellel Edges	368	48	169	33	537	42
Convergent	152	20	222	44	374	29
Off-axis	243	32	110	22	353	28
ND	5	1	5	1	10	1
Total	768	100	506	100	1274	100
R						
(sub) Parellel Edges	102	57	107	54	209	55
Off-axis	48	27	35	18	83	22
Convergent	22	12	51	26	73	19
ND	7	4	6	3	13	3
Total	179	100	199	100	378	100

Appendix 5. Morphotechnological attributes of blades and bladelets. Sites A= Ansab, R= Românești, F= Fumane.**** Complete and Semi-complete artefacts ***** Complete and Mes+Dist.

Appendix 5. *Morphotechnologische Attribute der Klingen und Lamellen. Fundstellen A= Ansab, R= Românești, F= Fumane.**** Vollständige und halbvollständige Artefakte***** Vollständige und Mes+Dist.*

	Blade		Bladelet		Total	
	N	%	N	%	N	%
F						
(sub) Parellel Edges	232	56	328	49	560	51
Off-axis	121	29	158	23	279	26
Convergent	58	14	184	27	242	22
ND	7	2	5	1	12	1
Total	418	100	675	100	1093	100
C) Cross-section shape****						
A						
Trapezoidal	578	61	336	42	914	52
Triangular	330	35	418	52	748	43
Flat	36	4	43	5	79	4
ND	3	<1	12	1	15	1
Total	947	100	809	100	1756	100
R						
Triangular	122	47	152	53	274	50
Trapezoidal	115	44	107	37	222	41
Flat	21	8	24	8	45	8
ND	4	2	3	1	7	1
Total	262	100	286	100	548	100
F						
Trapezoidal	301	58	352	43	653	49
Triangular	172	33	395	49	567	43
Flat	40	8	60	7	100	8
ND	4	1	4	<1	8	1
Total	517	100	811	100	1328	100
D) Cross-section symmetry****						
A						
Asymmetric	637	70	375	50	1012	61
Symmetric	271	30	379	50	650	39
Total	908	100	754	100	1662	100
R						
Asymmetric	148	62	126	49	274	55
Symmetric	89	38	133	51	222	45
Total	237	100	259	100	496	100
F						
Symmetric	194	41	427	57	621	51
Asymmetric	279	59	320	43	599	49
Total	473	100	747	100	1220	100

Appendix 5. Morphotechnological attributes of blades and bladelets. Sites A= Ansab, R= Românești, F= Fumane.**** Complete and Semi-complete artefacts ***** Complete and Mes+Dist. (continued)

Appendix 5. *Morphotechnologische Attribute der Klingen und Lamellen. Fundstellen A= Ansab, R= Românești, F= Fumane.**** Vollständige und halbvollständige Artefakte***** Vollständige und Mes+Dist. (Fortsetzung)*

	Blade		Bladelet		Total	
	N	%	N	%	N	%
E) Distal Termination*****						
A						
Feathered	340	44	388	77	728	57
Plunging	298	39	67	13	365	29
Stepped	78	10	15	3	93	7
Hinged	38	5	20	4	58	5
ND	14	2	16	3	30	2
Total	768	100	506	100	1274	100
R						
Feathered	83	46	147	74	230	61
Plunging	44	25	20	10	64	17
Stepped	34	19	21	11	55	15
Hinged	13	7	6	3	19	5
ND	5	3	5	3	10	3
Total	179	100	199	100	378	100
F						
Feathered	175	42	481	71	656	60
Plunging	183	44	118	17	301	28
Stepped	30	7	38	6	68	6
Hinged	22	5	33	5	55	5
ND	8	2	5	1	13	1
Total	418	100	675	100	1093	100

Appendix 5. Morphotechnological attributes of blades and bladelets. Sites A= Ansab, R= Românești, F= Fumane.**** Complete and Semi-complete artefacts ***** Complete and Mes+Dist. (continued)

Appendix 5. *Morphotechnologische Attribute der Klingen und Lamellen. Fundstellen A= Ansab, R= Românești, F= Fumane.**** Vollständige und halbvollständige Artefakte***** Vollständige und Mes+Dist. (Fortsetzung)*

Literature cited

Abulafia, T., Goder-Goldberger, M., Berna, F., Barzilai, O. & Marder, O. (2021). A technotypological analysis of the Ahmarian and Levantine Aurignacian assemblages from Manot Cave (area C) and the interrelation with site formation processes. *Journal of Human Evolution* 160: 102707.

Accorsi, C. A., Aiello, E., Bartolini, C., Castelletti, L., Rodolfi, G. & Ronchitelli, A. (1979). Il giacimento paleolitico di Serino (Avellino), Stratigrafia, ambienti e paletnologia. *Atti Della Societa Toscana Di Scienze Naturali* 86: 435–487.

Aleo, A., Duches, R., Falcucci, A., Rots, V. & Peresani, M. (2021). Scraping hide in the early Upper Paleolithic: Insights into the life and function of the Protoaurignacian endscrapers at Fumane Cave. *Archaeological and Anthropological Sciences* 13(137): 1–27.

Alex, B., Barzilai, O., Hershkovitz, I., Marder, O., Berna, F., Caracuta, V., Abulafia, T., Davis, L., Goder-Goldberger, M., Lavi, R., Mintz, E., Regev, L., Bar-Yosef Mayer, D., Tejero, J.-M., Yeshurun, R., Ayalon, A., Bar-Matthews, M., Yasur, G., Frumkin, A., Latimer, B., Hans, M.G. & Boaretto, E. (2017). Radiocarbon chronology of Manot Cave, Israel and Upper Paleolithic dispersals. *Science Advances* 3(11): e1701450.

Anderson, L., Bon, F., Bordes, J.-G., Pasquini, A., Slimak, L. & Teyssandier, N. (2015). Relier des espaces, construire de nouveaux réseaux: aux origines du Protoaurignacien et des débuts du Paléolithique supérieur en Europe occidentale. In N. Naudinot, L. Meignen, D. Binder & G. Querré (Eds.), *Les systèmes de mobilité de la Préhistoire au Moyen Âge XXXVe rencontres internationales d'archéologie et d'histoire d'Antibes*. Éditions APDCA, Antibes, 93–109.

Andrefsky, W. (2005). *Lithics: macroscopic approaches to analysis (2nd ed)*. Cambridge University Press, Cambridge ; New York.

Arrizabalaga, A., Quirós, F., Bon, F., Iriarte-Chiapusso, M.-J., Maíllo-Fernández, J. & Normand, C. (2009). Early evidence of the Aurignacian in Cantabrian Iberia and the North Pyrenees. *In:* M. Camps M. et& C. Szmidt C. (Eds.). *The Mediterranean from 50 000 to 25 000 BP: Turning points and new directions.* Oxbow books, Oxford, 255-292 .

Badino, F., Pini, R., Ravazzi, C., Margaritora, D., Arrighi, S., Bortolini, E., Figus, C., Giaccio, B., Lugli, F., Marciani, G., Monegato, G., Moroni, A., Negrino, F., Oxilia, G., Peresani, M., Romandini, M., Ronchitelli, A., Spinapolice, E. E., Zerboni, A. & Benazzi, S. (2020). An overview of Alpine and Mediterranean palaeogeography, terrestrial ecosystems and climate history during MIS 3 with focus on the Middle to Upper Palaeolithic transition. *Quaternary International* 551: 7–28.

Banks, W. E., d'Errico, F. & Zilhão, J. (2013). Human–climate interaction during the Early Upper Paleolithic: testing the hypothesis of an adaptive shift between the Proto-Aurignacian and the Early Aurignacian. *Journal of Human Evolution* 64(1): 39–55.

Barshay-Szmidt, C., Bazile, F. & Brugal, J.-P. (2020). First AMS 14C dates on the Protoaurignacian in Mediterranean France: The site of Esquicho-Grapaou (Russan-Ste-Anastasie, Gard). *Journal of Archaeological Science: Reports* 33: 102474.

Barshay-Szmidt, C., Eizenberg, L. & Deschamps M. (2012). Radiocarbon (AMS) dating the Classic Aurignacian, Proto-Aurignacian and Vasconian Mousterian at Gatzarria Cave (Pyrénées-Atlantiques, France) . *PALEO* 23: 11-38. http://journals.openedition.org/paleo/2250

Barshay-Szmidt, C., Normand, C., Flas, D. & Soulier, M.-C. (2018). Radiocarbon dating the Aurignacian sequence at Isturitz (France): Implications for the timing and development of the Protoaurignacian and Early Aurignacian in western Europe. *Journal of Archaeological Science: Reports* 17: 809–838.

Bar-Yosef, O. & Belfer-Cohen, A. (2004). The Qafzeh Upper Paleolithic assemblages: 70 years later. *Eurasian Prehistory* 2(1): 145–180.

Bataille, G. (2016). Extracting the "Proto" from the Aurignacian. Distinct Production Sequences of Blades and Bladelets in the Lower Aurignacian Phase of Siuren I, Units H and G (Crimea). *Mitteilungen Der Gesellschaft Für Urgeschichte* 25: 49–85.

Bataille, G. & Conard, N. J. (2018). Blade and bladelet production at Hohle Fels Cave, AH IV in the Swabian Jura and its importance for characterizing the technological variability of the Aurignacian in Central Europe. *PLOS ONE* 13(4): e0194097.

Bataille, G., Falcucci, A., Tafelmaier, Y. & Conard, N. J. (2020). Technological differences between Kostenki 17/II (Spitsynskaya industry, Central Russia) and the Protoaurignacian: Reply to Dinnis et al. (2019). *Journal of Human Evolution* 146: 102685.

Bataille, G., Tafelmaier, Y. & Weniger, G.-C. (2018). Living on the edge – A comparative approach for studying the beginning of the Aurignacian. *Quaternary International* 474: 3–29.

Benazzi, S., Douka, K., Fornai, C., Bauer, C. C., Kullmer, O., Svoboda, J., Pap, I., Mallegni, F., Bayle, P., Coquerelle, M., Condemi, S., Ronchitelli, A., Harvati, K. & Weber, G. W. (2011). Early dispersal of modern humans in Europe and implications for Neanderthal behaviour. *Nature* 479(7374): 525–528.

Benazzi S., Slon V., Talamo S., Negrino F., Peresani M., Bailey S.E., Sawyer S., Panetta D., Vicino G., Starnini E., Mannino M.A., Salvadori P.A., Meyer M., Pääbo S. & Hublin J.J. (2015). The makers of the Protoaurignacian and implications for Neandertal extinction. *Science* 348(6236): 793-796.

Bergman, C., Williams, J., Douka, K. & Schyle, D. (2017). The Palaeolithic Sequence of Ksar 'Akil, Lebanon. *In:* Y. Enzel & O. Bar-Yosef (Eds.), Quaternary of the Levant: Environments, Climate Change, and Humans. Cambridge: Cambridge University Press, 267-276.

Boaretto, E., Hernandez, M., Goder-Goldberger, M., Aldeias, V., Regev, L., Caracuta, V., McPherron, S. P., Hublin, J.-J., Weiner, S. & Barzilai, O. (2021). The absolute chronology of Boker Tachtit (Israel) and implications for the Middle to Upper Paleolithic transition in the Levant. *Proceedings of the National Academy of Sciences* 118(25): e2014657118.

Bon, F. (2002). *L'Aurignacien entre mer et océan: réflexion sur l'unité des phases anciennes de l'Aurignacien dans le sud le la France*. Soc. Préhistorique Française, Paris.

Bordes, J.-G. & Tixier, J. (2002). Sur l'unité de l'Aurignacien ancien dans le Sud-Ouest de la France : la production des lames et des lamelles. *Espacio Tiempo y Forma* 15: 175–194.

Bordes, J.-G. (2005). La séquence Aurignacienne du nord de l'Aquitaine : variabilité des productions lamellaires à Caminade-est, Roc-de-Combe, Le Piage et Corbiac-Vignoble II.. *In:* F. Le Brun-Ricalens (Ed.), *Actes du XIVème congrès UISPP, Université de Liège, Belgique, 2 - 8 septembre 2001: session 6, Paléolithique supérieur ; section 6 - Upper Palaeolithic. Productions lamellaires attribuées à l'Aurignacien : Chaînes opératoires et perspectives technoculturelles (Vol. 1)*. Musée National d'Histoire et d'Art, Luxembourg, 123-154.

Bosch, M. D., Mannino, M. A., Prendergast, A. L., O'Connell, T. C., Demarchi, B., Taylor, S. M., Niven, L., van der Plicht, J. & Hublin, J.-J. (2015). New chronology for Ksâr 'Akil (Lebanon) supports Levantine route of modern human dispersal into Europe. *Proceedings of the National Academy of Sciences* 112(25): 7683–7688.

Breuil, H. (1909). L'aurignacien présolutréen : épilogue d'une controverse. *Revue préhistorique* 8–9. Vigot, Paris, 5–46.

Breuil, H. (1913). Les subdivisions du paléolithique supérieur et leur signification. *Congrès International d'anthropologie et d'archéologie Préhistoriques - Compte-Rendu de La XIVème Session*. Imprimerie Albert Kündig, Genève, 165–238.

Broglio A., Cremaschi M., Peresani M., Bertola S., Bolognesi L., De Stefani M., Fiocchi C., Gurioli F., Marini D. (2003). L'Aurignacien dans le territoire préalpin: la Grotte de Fumane. *In:* S.A. Vasil'ev, O. Soffer, J. Kozlowski (Eds.), *Perceived landscapes and built environments. The cultural geography of Late Palaeolithic Eurasia*. British Archaeological Reports, International Series 1122, 93-104.

Broglio, A., de Stefani M., Gurioli F., Pallecchi P., Giachi G., Higham T. & Brock F. (2009). L'art aurignacien dans la décoration de la Grotte de Fumane. *L'Anthropologie* 113: 753–61.

Cabrera Valdés, V., de Quirós, F. B., Maíllo Fernández, J. M., Valladas, H. & Martinez de La Riva Llorret, M. (2002). El Auriñaciense arcaico de El Castillo (Cantabria). *Espacio Tiempo y Forma* 15: 67–86.

Carter, T., Contreras, D. A., Holcomb, J., Mihailović, D. D., Karkanas, P., Guérin, G., Taffin, N., Athanasoulis, D. & Lahaye, C. (2019). Earliest occupation of the Central Aegean (Naxos), Greece: Implications for hominin and Homo sapiens' behavior and dispersals. *Science Advances* 5(10): eaax0997.

Cavallo, G., Fontana, F., Gonzato, F., Peresani, M., Riccardi, M. P. & Zorzin, R. (2017). Textural, microstructural, and compositional characteristics of Fe-based geomaterials and Upper Paleolithic ocher in the Lessini Mountains, Northeast Italy: Implications for provenance studies. *Geoarchaeology*, 32(4) : 437–455.

Chiotti, L. (1999). *Les industries lithiques des niveaux aurignaciens de l'abri Pataud, Les Eyzies-de-Tayac (Dordogne): étude technologique et typologique.* Ph.D. dissertation, Museum National d'Histoire Naturelle Laboratoire de Préhistoire, Paris.

Chiotti, L. & Cretin, C. (2011). Les mises en forme de grattoirs carénés nucléus de l'aurignacien ancien de l'abri Castanet (Sergeac, Dordogne). *PALEO Revue d'archéologie préhistorique* 22: 69–84.

Chu, W., Pötter, S., Doboş, A., Albert, T., Klasen, N., Ciornei, A., Bösken, J. J. & Schulte, P. (2019). Geoarchaeology and geochronology of the Upper Palaeolithic site of Temereşti Dealu Vinii, Banat, Romania: Site formation processes and human activity of an open-air locality. *Quartär* 66: 111–134.

Chu, W. & Richter, J. (2020). Aurignacian Cultural Unit. *In:* C. Smith (Ed.), Encyclopedia of Global Archaeology. Springer, Cham, 1-10.

Ciornei, A., Chu, W., Mariş, I. & Doboş, A. (2021). Lithic raw material procurement patterns at the Upper Palaeolithic site of Românești – Dumbrăvița I (southwestern Romania). *Dacia* 64: 67–122.

Çilingiroğlu, Ç. & Dinçer, B. (2021). Two Possible Upper Paleolithic Sites on the Karaburun Peninsula, Turkey. *Journal of Paleolithic Archaeology* 4(12): 1–11.

Conard, N. J. & Bolus, M. (2003). Radiocarbon dating the appearance of modern humans and timing of cultural innovations in Europe: new results and new challenges. *Journal of Human Evolution* 44(3): 331–371.

Conard, N. J., Soressi, M., Parkington, J. E., Wurz, S. & Yates, R. (2004). A Unified Lithic Taxonomy Based on Patterns of Core Reduction. *The South African Archaeological Bulletin* 59(179): 13–17.

Cullen, V. L., Smith, V. C., Tushabramishvili, N., Mallol, C., Dee, M., Wilkinson, K. N. & Adler, D. S. (2021). A revised AMS and tephra chronology for the Late Middle to Early Upper Paleolithic occupations of Ortvale Klde, Republic of Georgia. *Journal of Human Evolution* 151: 102908.

D'Angelo, E. & Mussi, M. (2005). Galets et lamelles de l'Aurignacien du Latium (Italie Centrale): le cas de grotta Barbara. *In:* F. Le Brun-Ricalens (Ed.), *Actes du XIVème congrès UISPP, Université de Liège, Belgique, 2 - 8 septembre 2001: session 6, Paléolithique supérieur ; section 6 - Upper Palaeolithic. Productions lamellaires attribuées à l'Aurignacien : Chaînes opératoires et perspectives technoculturelles (Vol. 1).* Musée National d'Histoire et d'Art, Luxembourg, 313-322.

Davidzon, A. & Goring-Morris, N. (2003). Sealed in Stone: The Upper Palaeolithic Early Ahmarian Knapping Method in the Light of Refitting Studies at Nahal Nizzana XIII, Western Negev, Israel. *Journal of The Israel Prehistoric Society* 33: 75–205.

Davies, W. (2001). A Very Model of a Modern Human Industry: New Perspectives on the Origins and Spread of the Aurignacian in Europe. *Proceedings of the Prehistoric Society* 67: 195–217.

Degano, I., Soriano, S., Villa, P., Pollarolo, L., Lucejko, J. J., Jacobs, Z., Douka, K., Vitagliano, S. & Tozzi, C. (2019). Hafting of Middle Paleolithic tools in Latium (central Italy): New data from Fossellone and Sant'Agostino caves. *PLOS ONE* 14(6): e0213473.

Delpiano, D., Heasley, K. & Peresani, M. (2018). Assessing Neanderthal land use and lithic raw material management in Discoid technology. *Journal of Anthropological Sciences* 96: 89–100.

Demars, P. Y. & Laurent, P. (1992). *Types d'outils lithiques du paleolithique superieur en Europe*. CNRS, Paris.

Demidenko, Y. E. (2014). The great North Black Sea region Early Upper Paleolithic and human migrations into the region from different territories. *In:* M. Otto & F. Le Brun-Ricalens (Eds.), *Modes de contacts et de déplacements au Paléolithique eurasiatique, UISPP — Liège, mai 2012 (Vol. 140).* ERAUL, Liege, 171-185.

Dini, M., Baills, H., Conforti, J. & Tozzi, C. (2012). Le Protoaurignacien de la Grotte La Fabbrica (Grosseto, Italie) dans le contexte de l'arc nord méditerranéen. *L'Anthropologie* 116(4): 550–574.

Dinnis, R., Bessudnov, A., Reynolds, N., Devièse, T., Pate, A., Sablin, M., Sinitsyn, A. & Higham, T. F. G. (2019). New data for the Early Upper Paleolithic of Kostenki (Russia). *Journal of Human Evolution* 127: 21–40.

Dinnis, R., Bessudnov, A., Reynolds, N., Pate, A., Sablin, M. & Sinitsyn, A. (2020). Response to Bataille et al.'s 'Technological differences between Kostenki 17/II (Spitsynskaya industry, Central Russia) and the Protoaurignacian: Reply to Dinnis et al. (2019)' [J. Hum. Evol. (2019), 102685]. *Journal of Human Evolution* 146: 102792.

Douka, K., Grimaldi, S., Boschian, G., del Lucchese, A. & Higham, T. F. G. (2012). A new chronostratigraphic framework for the Upper Palaeolithic of Riparo Mochi (Italy). *Journal of Human Evolution* 62(2): 286–299.

Douka, K., Higham, T. F. G. & Bergman, C. A. (2015). Statistical and archaeological errors invalidate the proposed chronology for the site of Ksar Akil. *Proceedings of the National Academy of Sciences* 112(51): E7034–E7034.

Douka, K., Perlès, C., Valladas, H., Vanhaeren, M. & Hedges, R. E. M. (2011). Franchthi Cave revisited: the age of the Aurignacian in south-eastern Europe. *Antiquity* 85(330): 1131–1150.

Falcucci, A., Conard, N. J. & Peresani, M. (2017). A critical assessment of the Protoaurignacian lithic technology at Fumane Cave and its implications for the definition of the earliest Aurignacian. *PLOS ONE* 12(12): e0189241.

Falcucci, A., Conard, N. J. & Peresani, M. (2020). Breaking through the Aquitaine frame: A re-evaluation on the significance of regional variants during the Aurignacian as seen from a key record in southern Europe. *Journal of Anthropological Sciences* 98: 1–42.

Falcucci, A. & Peresani, M. (2018). Protoaurignacian Core Reduction Procedures: Blade and Bladelet Technologies at Fumane Cave. *Lithic Technology* 43(2): 125–140.

Falcucci, A. & Peresani, M. (2019). A pre-Heinrich Event 3 assemblage at Fumane Cave and its contribution for understanding the beginning of the Gravettian in Italy. *Quartär* 66: 135-154.

Falcucci, A., Peresani, M., Roussel, M., Normand, C. & Soressi, M. (2018). What's the point? Retouched bladelet variability in the Protoaurignacian. Results from Fumane, Isturitz, and Les Cottés. *Archaeological and Anthropological Sciences* 10(3): 539–554.

Floss, H., Froehle, S. & Wettengl, S. (2016). The Aurignacian along the Danube Its Two-Fold Role as a Transalpine and Cisalpine Passageway of Early Homo Sapiens into Europe. *In:* R. Krauss & H. Floss (Eds.), *Southeast Europe Before Neolithisation. Proceedings of the International Workshop within the Collaborative Research Centres SFB 1070 "RESSOURCENKULTUREN", Schloß Hohentübingen, 9th of May 2014.* Universität Tübingen, Tübingen, 13-39.

Fu, Q., Hajdinjak, M., Moldovan, O. T., Constantin, S., Mallick, S., Skoglund, P., Patterson, N., Rohland, N., Lazaridis, I., Nickel, B., Viola, B., Prüfer, K., Meyer, M., Kelso, J., Reich, D. & Pääbo, S. (2015). An early modern human from Romania with a recent Neanderthal ancestor. *Nature* 524(7564): 216–219.

Fu, Q., Li, H., Moorjani, P., Jay, F., Slepchenko, S. M., Bondarev, A. A., Johnson, P. L. F., Aximu-Petri, A., Prüfer, K., de Filippo, C., Meyer, M., Zwyns, N., Salazar-García, D. C., Kuzmin, Y. V., Keates, S. G., Kosintsev, P. A., Razhev, D. I., Richards, M. P., Peristov, N. V., Lachmann, M., Douka, K., Higham, T. F.G., Slatkin, M., Hublin, J.-J., Reich, D., Kelso, J., Viola, B. T. & Pääbo, S. (2014). Genome sequence of a 45,000-year-old modern human from western Siberia. *Nature*, 514(7523): 445–449.

Gambassini, P. (1997). Le industrie paleolitiche di Castelcivita. *In:* P. Gambassini & G. Napoleone (Eds.), *Il Paleolitico di Castelcivita: culture e ambiente*. Electa Napoli, Napoli, 92–145.

Gennai, J. (2021). *Back to the lithics: technological comparison of early Upper Palaeolithic assemblages from Al-Ansab/ Jordan, Românești Dumbrăvița/ Romania and Fumane/ Italy.* Ph.D., dissertation, Universität zu Köln, Köln.

Ghasidian, E., Bretzke, K. & Conard, N. J. (2017). Excavations at Ghār-e Boof in the Fars Province of Iran and its bearing on models for the evolution of the Upper Palaeolithic in the Zagros Mountains. *Journal of Anthropological Archaeology* 47: 33–49.

Ghasidian, E., Heydari-Guran, S. & Mirazón Lahr, M. (2019). Upper Paleolithic cultural diversity in the Iranian Zagros Mountains and the expansion of modern humans into Eurasia. *Journal of Human Evolution* 132: 101–118.

Giaccio, B., Hajdas, I., Isaia, R., Deino, A. & Nomade, S. (2017). High-precision 14C and 40Ar/39Ar dating of the Campanian Ignimbrite (Y-5) reconciles the time-scales of climatic-cultural processes at 40 ka. *Scientific Reports* 7: 45940. DOI: 10.1038/srep45940

Gilead, I. (1991). The Upper Paleolithic period in the Levant. *Journal of World Prehistory* 5(2): 105–154.

Golovanova, L. V. & Doronichev, V. B. (2012). The Early Upper Paleolithic of the Caucasus in the West Eurasian Context. In M. Otte, S. Shidrang & D. Flas (Eds.), *L'Aurignacien de la grotte Yafteh et son contexte (fouilles 2005-2008) /The Aurignacian of Yafteh cave and its context (2005-2008 excavations) (Vol. 132).* ERAUL, Liege, 137–160.

Goring-Morris, N. & Belfer-Cohen, A. (2006). A hard look at the "Levantine Aurignacian": how real is the taxon? In O. Bar-Yosef & J. Zilhão (Eds.), *Towards a definition of the Aurignacian: proceedings of the symposium held in Lisbon, Portugal, June 25-30, 2002*. Instituto Português de Arqueologia ; American School of Prehistoric Research, Peabody Museum, Harvard University, Lisboa : [Cambridge, Mass.], 297–314.

Goring-Morris, N. & Davidzon, A. (2006). Straight to the point: Upper Paleolithic Ahmarian lithic technology in the Levant. *Anthropologie* XLIV(1): 93–111.

Goring-Morris, N. & Belfer-Cohen, A. (2018). The Ahmarian in the Context of the Earlier Upper Palaeolithic in the Near East. *In:* Y. Nishiaki & T. Akazawa (Eds.), *The Middle and Upper Paleolithic Archeology of the Levant and Beyond*. Springer Singapore, Singapore, 87–104.

Grimaldi, S., Porraz, G. & Santaniello, F. (2014). Raw material procurement and land use in the northern Mediterranean Arc: insight from the first Proto-Aurignacian of Riparo Mochi (Balzi Rossi, Italy). *Quartär* 61: 113–127.

Hauck, T. C., Ruka, R., Gjipali, I., Richter, J. & Nolde, N. (2017). The "German Albanian Palaeolithic" Programme (GAP): A status report. *In:* M. Otte (Ed.), *Vocation préhistoire Hommage à Jean-Marie Le Tensore (Vol. 148).* ERAUL, Liege, 159–173.

Haws, J. A., Benedetti, M. M., Talamo, S., Bicho, N., Cascalheira, J., Ellis, M. G., Carvalho, M. M., Friedl, L., Pereira, T. & Zinsious, B. K. (2020). The early Aurignacian dispersal of modern humans into westernmost Eurasia. *Proceedings of the National Academy of Sciences*: 202016062.

Heinrich, H. (1988). Origin and Consequences of Cyclic Ice Rafting in the Northeast Atlantic Ocean During the Past 130,000 Years. *Quaternary Research* 29(2): 142–152.

Hershkovitz, I., Weber, G. W., Quam, R., Duval, M., Grün, R., Kinsley, L., Ayalon, A., Bar-Matthews, M., Valladas, H., Mercier, N., Arsuaga, J. L., Martinón-Torres, M., Bermúdez de Castro, J. M., Fornai, C., Martín-Francés, L., Sarig, R., May, H., Krenn, V. A., Slon, V., Rodríguez, L., García, R., Lorenzo, C., Carretero, J. M:, Frumkin, A., Shahack-Gross, R., Bar-Yosef Mayer, D. E., Cui, Y., Wu, X., Peled, N., Groman-Yaroslavski, I., Weissbrod, L., Yeshurun, R., Tsatskin, A., Zaidner, Y. & Weinstein-Evron, M. (2018). The earliest modern humans outside Africa. *Science* 359(6374): 456–459.

Higham, T. F. G., Jacobi, R., Basell, L., Ramsey, C. B., Chiotti, L. & Nespoulet, R. (2011). Precision dating of the Palaeolithic: A new radiocarbon chronology for the Abri Pataud (France), a key Aurignacian sequence. *Journal of Human Evolution* 61(5): 549-563.

Higham, T. F. G., Basell, L., Jacobi, R., Wood, R., Ramsey, C. B. & Conard, N. J. (2012). Testing models for the beginnings of the Aurignacian and the advent of figurative art and music: The radiocarbon chronology of Geißenklösterle. *Journal of Human Evolution* 62(6): 664–676.

Higham, T. F. G., Brock, F., Peresani, M., Broglio, A., Wood, R. & Douka, K. (2009). Problems with radiocarbon dating the Middle to Upper Palaeolithic transition in Italy. *Quaternary Science Reviews* 28(13–14): 1257–1267.

Hoffecker, J. F. & Holliday, V. T. (2014). Landscape Archaeology and the Dispersal of Modern Humans in Eastern Europe. *In:* S. A. Vasil'ev & E. S. Tkach (Eds.), *Verkhnii Paleolit Severnoi Evrazii i Ameriki: Pamiatniki, Kul'tury, Traditsii. Peterburgskoe Vostokovedenie, Peterburgskoe Vostokovedenie*, Saint Petersburg, 140–170.

Hublin, J.-J. (2015). The modern human colonization of western Eurasia: when and where? *Quaternary Science Reviews* 118: 194–210.

Hublin, J.-J., Sirakov, N., Aldeias, V., Bailey, S. E., Bard, E., Delvigne, V., Endarova, E., Fagault, Y., Fewlass, H., Hajdinjak, M., Kromer, B., Krumov, I., Marreiros, J., Martisius, L. N., Paskulin, L., Sinet-Mathiot, V., Meyer, M., Pääbo, S., Popov, V., Rezek, Z., Sirakova, S., Skinner, M.M., Smith, M. G., Spasov, R., Talamo, S., Tuna, T., Wacker, L., Welker, F., McPherron, P. S. & Tsanova, T. (2020). Initial Upper Palaeolithic Homo sapiens from Bacho Kiro Cave, Bulgaria. *Nature* 581: 299–302.

Hussain, S. T. (2015). Betwixt seriality and sortiment: rethinking early Ahmarian blade technology in Al-Ansab 1. *In:* D. Schyle & J. Richter (Eds.), *Pleistocene archaeology of the Petra area in Jordan*. Leidorf, Rahden/Westf, 131–147.

Inizan, M.-L., Reduron-Ballinger, M., Roche, H., Tixier, J. & Féblot-Augustins, J. (Eds.). (1999). *Technology and terminology of knapped stone: followed by a multilingual vocabulary - Arabic, English, French, German,Greek, Italian, Portuguese, Spanish*. CREP, Nanterre.

Kadowaki, S., Omori, T. & Nishiaki, Y. (2015). Variability in Early Ahmarian lithic technology and its implications for the model of a Levantine origin of the Protoaurignacian. *Journal of Human Evolution* 82: 67–87.

Kadowaki, S., Suga, E. & Henry, D. O. (2021). Frequency and production technology of bladelets in Late Middle Paleolithic, Initial Upper Paleolithic, and Early Upper Paleolithic (Ahmarian) assemblages in Jebel Qalkha, Southern Jordan. *Quaternary International* 596: 4-21.

Kaufman, D. (1986). A Proposed Method for Distinguishing Between Blades and Bladelets. *Lithic Technology* 15(1): 34–40.

Kels, H., Protze, J., Sitlivy, V., Hilgers, A., Zander, A., Anghelinu, M., Bertrams, M. & Lehmkuhl, F. (2014). Genesis of loess-like sediments and soils at the foothills of the Banat Mountains, Romania – Examples from the Paleolithic sites Românești and Coșava. *Quaternary International* 351: 213–230.

Klasen, N., Hilgers, A., Schmidt, C., Bertrams, M., Schyle, D., Lehmkuhl, F., Richter, J. & Radtke, U. (2013). Optical dating of sediments in Wadi Sabra (SW Jordan). *Quaternary Geochronology* 18: 9–16.

Koumouzelis, M., Ginter, B., Kozlowski, J. K., Pawlikowski, M., Bar-Yosef, O., Albert, R. M., Litynska-Zajac, M., Stworzewicz, E., Wojtal, P., Lipecki, G., Tomek, T., Bochenski, Z. M. & Pazdur, A. (2001). The Early Upper Palaeolithic in Greece: The Excavations in Klisoura Cave. *Journal of Archaeological Science* 28(5): 515–539.

Laplace, G. (1966). *Recherches sur l'origine et l'évolution des complexes leptolithiques*. École Française de Rome, Rome.

Le Brun-Ricalens, F. (Ed.). (2005a). *Actes du XIVème congrès UISPP, Université de Liège, Belgique, 2 - 8 septembre 2001: session 6, Paléolithique supérieur ; section 6 - Upper Palaeolithic*. Musée National d'Histoire et d'Art, Luxembourg.

Le Brun-Ricalens, F. (2005b). Reconaissance d'un 'concept technoculturel' de l'Aurignacien Ancien? *In:* F. Le Brun-Ricalens (Ed.), *Actes du XIVème congrès UISPP, Université de Liège, Belgique, 2 - 8 septembre 2001: session 6, Paléolithique supérieur ; section 6 - Upper Palaeolithic. Productions lamellaires attribuées à l'Aurignacien : Chaînes opératoires et perspectives technoculturelles (Vol. 1)*. Musée National d'Histoire et d'Art, Luxembourg, 157-190.

Le Brun-Ricalens, F., Bordes, J.-G. & Eizenberg, L. (2009). A crossed-glance between southern European and Middle-Near Eastern early Upper Palaeolithic lithic technocomplexes. Existing models, new perspectives. *In:* M. Camps & C. Szmidt (Eds.). *The Mediterranean from 50 000 to 25 000 BP: Turning points and new directions*. Oxbow books, Oxford, 11-33.

López-García, J. M., dalla Valle, C., Cremaschi, M. & Peresani, M. (2015). Reconstruction of the Neanderthal and Modern Human landscape and climate from the Fumane cave sequence (Verona, Italy) using small-mammal assemblages. *Quaternary Science Reviews* 128: 1–13.

MacFarland, T. W. & Yates, J. M. (2016). Mann–Whitney U Test. *In:* T. W. MacFarland & J.M. Yates (Eds.), *Introduction to Nonparametric Statistics for the Biological Sciences Using R*. Springer International Publishing, Cham, 103-132.

McHugh, M. L. (2013). The Chi-Square independence test. *Biochemia Medica* 2013 23(2): 143–149.

Mellars, P. (2011). The earliest modern humans in Europe. *Nature* 479(7374): 483–485.

Miebach, A., Stolzenberger, S., Wacker, L., Hense, A. & Litt, T. (2019). A new Dead Sea pollen record reveals the last glacial paleoenvironment of the southern Levant. *Quaternary Science Reviews*: 214: 98–116.

Monigal, K. (2003). Technology, Economy, and Mobility at the Beginning of the Levantine Upper Palaeolithic. *In:* N. Goring-Morris & A. Belfer-Cohen (Eds.), *More than Meets the Eye: Studies on Upper Palaeolithic Diversity in the Near East.* Oxbow ; David Brown Book Co, Oxford : Oakville, CT, 118–133.

Nigst, P. R., Haesaerts, P., Damblon, F., Frank-Fellner, C., Mallol, C., Viola, B., Götzinger, M., Niven, L., Trnka, G. & Hublin, J.-J. (2014). Early modern human settlement of Europe north of the Alps occurred 43,500 years ago in a cold steppe-type environment. *Proceedings of the National Academy of Sciences* 111(40): 14394–14399.

Normand, C., O'Farrell, M. & Rios Garaizar, J. (2008). Quelle(s) utilisation(s) pour le productions lamellaires de l'Aurignacien Archaique? Quelques données et réflexions à partir des exemplaires de la grotte d'Isturitz (Pyrénées-Atlantiques; France). *In:* V. Lea (Ed.), *Recherches sur les armatures de projectiles du Paléolithique supérieur au Néolithique (actes du colloque C83, XVe congrès de l'UISPP, Lisbonne, 4-9 septembre 2006) (Vol. 1)*. Palaeoethnologie, Presses universitaires du Midi, 7-46.

Normand, C. & Turq, A. (2005). L'Aurignacien de la grotte d'Isturitz (France): la production lamellaire dans la séquence de la salle de Saint-Martin. *In:* F. Le Brun-Ricalens (Ed.), *Actes du XIVème congrès UISPP, Université de Liège, Belgique, 2 - 8 septembre 2001: session 6, Paléolithique supérieur ; section 6 - Upper Palaeolithic. Productions lamellaires attribuées à l'Aurignacien : Chaînes opératoires et perspectives technoculturelles (Vol. 1)*. Musée National d'Histoire et d'Art, Luxembourg, 375-392.

Ohnuma, K. (1988). *Ksar Akil, Lebanon: a technological study of the earlier upper palaeolithic levels of Ksar Akil ; Volume III Levels XXV-XIV*. BAR Publishing, Oxford.

Ortega Cobos, D., Soler Masferrer, N. & Maroto Genover, J. (2005). La production des lamelles pendant l'Aurignacien Archaique dans la grotte de l'Arbreda: organisation de la production, variabilité des méthodes et des objectifs. *In:* F. Le Brun-Ricalens (Ed.), *Actes du XIVème congrès UISPP, Université de Liège, Belgique, 2 - 8 septembre 2001: session 6, Paléolithique supérieur ; section 6 - Upper Palaeolithic. Productions lamellaires attribuées à l'Aurignacien : Chaînes opératoires et perspectives technoculturelles (Vol. 1)*. Musée National d'Histoire et d'Art, Luxembourg, 359-373.

Otte M. (2015). Des steppes aux déserts, à l'Aurignacien. Les hommes modernes venus d'Asie *L'Anthropologie* 119: 508–518.

Otte, M. (Ed.) (2017). *Les Aurignaciens. La culture des Hommes modernes en Europe*. Ed. Errance, Arles.

Palma di Cesnola, A. (2006). L'Aurignacien et le Gravettien ancien de la grotte Paglicci au Mont Gargano. *L'Anthropologie* 110(3): 355–370.

Parow-Souchon, H., Hussain, S. T. & Richter, J. (2021). Early Ahmarian Lithic Techno-Economy and Mobility at Al-Ansab 1, Wadi Sabra, Southern Jordan. *Journal of the Israel Prehistoric Society, 51, 6–64*.

Patil, I. (2021). Visualizations with statistical details: The 'ggstatsplot' approach. *Journal of Open Source Software, 6(61), 3167.*

Pelegrin, J. (2011). Sur les débitages laminaires du Paléolithique supérieur. *In:* F. Delpech & J. Jaubert (Eds.), *François Bordes et la Préhistoire: colloque international François Bordes, Bordeaux 22-24 Avril 2009*. Éd. du Comité des travaux historiques et scientifiques, Paris, 141-152.

Peresani, M. (2012). Fifty thousand years of flint knapping and tool shaping across the Mousterian and Uluzzian sequence of Fumane cave. *Quaternary International* 247: 125–150.

Peresani, M., Bertola, S., Delpiano, D., Benazzi, S. & Romandini, M. (2019). The Uluzzian in the north of Italy: insights around the new evidence at Riparo Broion. *Archaeological and Anthropological Sciences* 11(7): 3503–3536.

Peresani M., Cristiani E., Romandini M. (2016). The Uluzzian technology of Grotta di Fumane and its implication for reconstructing cultural dynamics in the Middle – Upper Palaeolithic transition of Western Eurasia. *Journal of Human Evolution* 91: 36-56.

Peresani, M., Forte, M., Quaggiotto, E., Colonese, A. C., Romandini, M., Cilli, C. & Giacobini, G. (2019). Marine and Freshwater Shell Exploitation in the Early Upper Paleolithic: Re-Examination of the Assemblages from Fumane Cave (NE Italy). *PaleoAnthropology* Special Issue: Personal Ornaments in Early Prehistory: 64–81.

Peretto C., Biagi P., Boschian G., Broglio A., de Stefani M., Fasani L., Fontana F., Grifoni R., Guerreschi A., Iacopini A., Minelli A., Pala F., Peresani M., Radi G., Ronchitelli A., Sarti L., Thun-Hohenstein U. & Tozzi C. (2004). Living-Floors and Structures From the Lower Palaeolithic to the Bronze Age, *In:* F. Facchini, A. Belcastro & U. Thun-Hohenstein, (Eds.), *Evolution of the Human Peopling in Italy. Paleobiology, Behavior, Subsistence Strategies. A Research Program Financed by the MIUR (Ministry of Education, University and Research)*. Collegium Antropologicum, 28 (1), 63-88.

Pleurdeau, D., Moncel, M.-H., Pinhasi, R., Yeshurun, R., Higham, T., Agapishvili, T., Bokeria, M., Muskhelishvili, A., Le Bourdonnec, F.-X., Nomade, S., Poupeau, G., Bocherens, H., Frouin, M., Genty, D., Pierre, M., Pons-Branchu, E., Lordkipanidze, D. & Tushabramishvili, N. (2016). Bondi Cave and the Middle-Upper Palaeolithic transition in western Georgia (south Caucasus). *Quaternary Science Reviews* 146 : 77–98.

Porraz, G., Simon, P. & Pasquini, A. (2010). Identité technique et comportements économiques des groupes proto-aurignaciens à la grotte de l'Observatoire (principauté de Monaco). *Gallia préhistoire* 52(1): 33–59.

Prüfer, K., Posth, C., Yu, H., Stoessel, A., Spyrou, M. A., Deviese, T., Mattonai, M., Ribechini, E., Higham, T., Velemínský, P., Brůžek, J. & Krause, J. (2021). A genome sequence from a modern human skull over 45,000 years old from Zlatý kůň in Czechia. *Nature Ecology & Evolution* 5: 820–825.

R Core Team (2021). *R: A language and environment for statistical computing*. R Foundation for Statistical Computing, Vienna, Austria.

Rasmussen, S. O., Bigler, M., Blockley, S. P., Blunier, T., Buchardt, S. L., Clausen, H. B., Cvijanovic, I., Dahl-Jensen, D., Johnsen, S. J., Fischer, H., Gkinis, V., Guillevic, M., Hoek, W. Z., Lowe, J. J., Pedro, J. B., Popp, T., Seierstad, I. K., Steffensen, J. P., Svensson, A. M., Vallelonga, P., Vinther, B.M., Walker, M. J.C., Wheatley, J.J. & Winstrup, M. (2014). A stratigraphic framework for abrupt climatic changes during the Last Glacial period based on three synchronized Greenland ice-core records: refining and extending the INTIMATE event stratigraphy. *Quaternary Science Reviews* 106: 14–28.

Rebollo, N. R., Weiner, S., Brock, F., Meignen, L., Goldberg, P., Belfer-Cohen, A., Bar-Yosef, O. & Boaretto, E. (2011). New radiocarbon dating of the transition from the Middle to the Upper Paleolithic in Kebara Cave, Israel. *Journal of Archaeological Science* 38(9): 2424–2433.

Reynolds, N. & Riede, F. (2019a). House of cards: cultural taxonomy and the study of the European Upper Palaeolithic. *Antiquity* 93(371): 1350–1358.

Reynolds, N. & Riede, F. (2019b). Reject or revive? The crisis of cultural taxonomy in the European Upper Palaeolithic and beyond. *Antiquity* 93(371): 1368–1370.

Richter, J., Litt, T., Lehmkuhl, F., Hense, A., Hauck, T. C., Leder, D. F., Miebach, A., Parow-Souchon, H., Sauer, F., Schoenenberg, J., Al-Nahar, M. & Hussain, S. T. (2020). Al-Ansab and the Dead Sea: Mid-MIS 3 archaeology and environment of the early Ahmarian population of the Levantine corridor. *PLOS ONE* 15(10): 1–36.

Riede, F., Araujo, A. G. M., Barton, M. C., Bergsvik, K. A., Groucutt, H. S., Hussain, S. T., Fernandez-Lopez de Pablo, J., Maier, A., Marwick, B., Pyne, L., Ranhorn, K., Reynolds, N., Riel-Salvatore, J., Sauer, F., Serwatka, K. & Zander, A. (2020). Cultural taxonomies in the Paleolithic—Old questions, novel perspectives. *Evolutionary Anthropology: Issues, News, and Reviews* 29(2): 49-52.

Riel-Salvatore, J. & Negrino, F. (2018). Proto-Aurignacian Lithic Technology, Mobility, and Human Niche Construction: A Case Study from Riparo Bombrini, Italy. *In:* E. Robinson & F. Sellet (Eds.), *Lithic Technological Organization and Paleoenvironmental Change (Vol. 9)*. Springer International Publishing, Cham, 163–187.

Romandini, M., Crezzini, J., Bortolini, E., Boscato, P., Boschin, F., Carrera, L., Nannini, N., Tagliacozzo, A., Terlato, G., Arrighi, S., Badino, F., Figus, C., Lugli, F., Marciani, G., Oxilia, G., Moroni, A., Negrino, F., Peresani, M., Riel-Salvatore, J., Ronchitelli, A., Spinapolice, E.E. & Benazzi, S. (2020). Macromammal and bird assemblages across the late Middle to Upper Palaeolithic transition in Italy: an extended zooarchaeological review. *Quaternary International* 551: 188–223.

Roussel, M., Bourguignon, L. & Soressi, M. (2009). Identification par l'expérimentation de la percussion au percuteur de calcaire au Paléolithique moyen : le cas du façonnage des racloirs bifaciaux Quina de Chez Pinaud (Jonzac, Charente-Maritime). *Bulletin de la Société préhistorique française* 106(2): 219–238.

Roussel, M. & Soressi, M. (2013). Une nouvelle séquence du Paléolithique supérieur ancien aux marges sud-ouest du Bassin parisien : les Cottés dans la Vienne. *In:* P. Bodu, L. Chehmana, L. Klaric, L. Mevel, S. Soriano & N. Teyssandier (Eds.), *Le Paléolithique supérieur ancien de l'Europe du Nord-ouest. Réflexions et synthèses à partir d'un projet collectif de recherches sur le Paléolithique supérieur ancien du Bassin parisien, Journées SPF, Sens, 15-18 avril (2009) (Vol. 56)*. Mémoire de la Société préhistorique française, Paris, 283-298.

Santamaría Álvarez, D. (2012). *La transición del Paleolítico medio al superior en Asturias: el abrigo de La Viña (La Manzaneda, Oviedo) y la cueva de El Sidrón (Borines, Piloña)*. Ph.D., dissertation. Universidad de Oviedo, Oviedo.

Sauer, F. & Schoenenberg, J. (2021). Gazelle Hunting Strategies in the Early Ahmarian: Close-Range Visuospatial Characteristics of Site Locations Indicate Spatially Focused Hunting Strategies on Gazella sp. During the Early Ahmarian. *Journal of Paleolithic Archaeology* 4(3): 24.

Scerri, E. M. L., Chikhi, L. & Thomas, M. G. (2019). Beyond multiregional and simple out-of-Africa models of human evolution. *Nature Ecology & Evolution*, 3(10), 1370–1372.

Scerri, E. M. L., Gravina, B., Blinkhorn, J. & Delagnes, A. (2016). Can Lithic Attribute Analyses Identify Discrete Reduction Trajectories? A Quantitative Study Using Refitted Lithic Sets. *Journal of Archaeological Method and Theory*, 23(2), 669–691.

Schmidt, C., Sitlivy, V., Anghelinu, M., Chabai, V., Kels, H., Uthmeier, T., Hauck, T., Băltean, I., Hilgers, A., Richter, J. & Radtke, U. (2013). First chronometric dates (TL and OSL) for the Aurignacian open-air site of Românești-Dumbrăviţa I, Romania. *Journal of Archaeological Science* 40(10): 3740–3753.

Schoenenberg, J. & Sauer, F. (2022). Intra-Site Structure of the Early Ahmarian Site of Al-Ansab 1, AH 1 (Jordan). *J Paleo Arch* 5, 2.

Schyle, D. (2015). The Ahmarian site of al-Ansab 1. *In:* J. Richter & D. Schyle (Eds.), *Pleistocene archaeology of the Petra area in Jordan*. Leidorf, Rahden, 91-130.

Shao, Y., Limberg, H., Klein, K., Wegener, C., Schmidt, I., Weniger, G.-C., Hense, A. & Rostami, M. (2021). Human-existence probability of the Aurignacian techno-complex under extreme climate conditions. *Quaternary Science Reviews* 263: 106995.

Sitlivy, V., Chabai, V., Anghelinu, M., Uthmeier, T., Kels, H., Hilgers, A., Schmidt, C., Niţă, L., Băltean, I., Veselsky, A. & Hauck, T. (2012). The earliest Aurignacian in Romania: New investigations at the open air site of Românești-Dumbrăviţa I (Banat). *Quartär 59*: 85–130.

Sitlivy, V., Niţă, L., Băltean, I., Anghelinu, M., Uthmeier, T., Hilger, A., Chabai, V. P., Hauck, T. & Schmidt, C. (2014). Placing the Aurignacian from Banat (Soutwestern Romania) into the European Early Upper Paleolithic context. *In:* M. Otte & F. Le Brun-Ricalens (Eds.), *Modes de contacts et de déplacements au Paléolithique eurasiatique: actes du colloque international de la Commission 8 (Paléolithique Supérieur") de l'UISPP, Université de Liège, 28 - 31 mai 2012 = Modes of contact and mobility during the Eurasian Palaeolithic (Vol. 140)*. ERAUL, Liège, 243–277.

Slimak, L., Pesesse, D. & Giraud, Y. (2002). La grotte Mandrin et les premières occupations du Paléolithique supérieur en Occitanie orientale. *Espacio Tiempo y Forma* 15: 237–259.

Soressi, M. & Geneste, J.-M. (2011). The History and Efficacy of the Chaîne Opératoire Approach to Lithic Analysis: Studying Techniques to Reveal Past Societies in an Evolutionary Perspective. *PaleoAnthropology*, 334–350.

Tafelmaier, Y. (2017). *Technological variability at the beginning of the Aurignacian in Northern Spain: Implications for the Proto- and Early Aurignacian distinction*. Neanderthal Museum, Mettmann.

Tartar, É. (2015). Origin and Development of Aurignacian Osseous Technology in Western Europe: a Review of Current Knowledge. *In:* R. White & R. Bourrillon (Eds.), *Aurignacian Genius: Art, Technology and Society of the First Modern Humans in Europe, Proceedings of the International Symposium, April 08-10 2013, New York University (Vol. 7)*. Palaeoethnologie-New York University, 33-55.

Tejero, J.-M. & Grimaldi, S. (2015). Assessing bone and antler exploitation at Riparo Mochi (Balzi Rossi, Italy): implications for the characterization of the Aurignacian in South-western Europe. *Journal of Archaeological Science* 61: 59–77.

Teyssandier, N., Bon, F. & Bordes, J.-G. (2010). Within projectile range: Some Thoughts on the Appearance of the Aurignacian in Europe. *Journal of Anthropological Research* 66(2): 209–229.

Teyssandier, N. & Liolios, D. (2003). Defining the earliest Aurignacian in the Swabian Alp: the relevance of the technological study of the Geissenklösterle (Baden-Württemberg, Germany) lithic and organic productions. *In:* J. Zilhão & F. d'Errico (Eds.), *The Chronology of the Aurignacian and of the Transitional Technocomplexes Dating, Stratigraphies, Cultural Implications. Proceedings of Symposium 6.1 of the XIVth Congress of the UISPP (University of Liège, Belgium, September 2-8, 2001) (Vol. 33)*. Instituto Português de Arqueologia, Lisboa, 179-196.

Tixier, J. (1963). *Typologie de l'épipaléolithique du Maghreb (Vol. 1–2)*. Arts et Métiers Graphiques, Paris.

Tsanova, T. (2013). The beginning of the Upper Paleolithic in the Iranian Zagros. A taphonomic approach and techno-economic comparison of Early Baradostian assemblages from Warwasi and Yafteh (Iran). *Journal of Human Evolution* 65(1): 39–64.

Tsanova, T., Zwyns, N., Eizenberg, L., Teyssandier, N., Le Brun-Ricalens, F. & Otte, M. (2012). Le plus petit dénominateur commun : réflexion sur la variabilité des ensembles lamellaires du Paléolithique supérieur ancien d'Eurasie. Un bilan autour des exemples de Kozarnika (Est des Balkans) et Yafteh (Zagros central). *L'Anthropologie* 116(4): 469–509.

Vaissié, E., Caux, S. & Faivre, J.-P. (2021). Supply distances and territories in south-west France through the Middle and Upper Palaeolithic: a petro-techno-economic approach. *Bulletin de La Societe Prehistorique Francaise* 118(1): 7–32.

Vanhaeren, M. & d'Errico, F. (2006). Aurignacian ethno-linguistic geography of Europe revealed by personal ornaments. *Journal of Archaeological Science* 33(8): 1105–1128.

Villa, P., Pollarolo, L., Conforti, J., Marra, F., Biagioni, C., Degano, I., Lucejko, J. J., Tozzi, C., Pennacchioni, M., Zanchetta, G., Nicosia, C., Martini, M., Sibilia, E. & Panzeri, L. (2018). From Neandertals to modern humans: New data on the Uluzzian. *PLOS ONE* 13(5): e0196786.

Zilhão, J. (2013). Neandertal-Modern Human Contact in Western Eurasia: Issues of Dating, Taxonomy, and Cultural Associations. *In:* T. Akazawa, Y. Nishiaki & K. Aoki (Eds.), *Dynamics of Learning in Neanderthals and Modern Humans Volume 1*. Springer Japan, Tokyo, 21–57.

Zwyns, N. (2021). The Initial Upper Paleolithic in Central and East Asia: Blade Technology, Cultural Transmission, and Implications for Human Dispersals. *Journal of Paleolithic Archaeology* 4(3): 19.

Zwyns, N., Rybin, E. P., Hublin, J.-J. & Derevianko, A. P. (2012). Burin-core technology and laminar reduction sequences in the initial Upper Paleolithic from Kara-Bom (Gorny-Altai, Siberia). *Quaternary International* 259: 33–47.